SUPPORTING CELL MEDIATED HOMEOSTASIS OF CHICK BASILAR PAPILLA FOR HAIR CELL RESTORATION

A THESIS TO BE SUBMITTED TO

THE UNIVERSITY OF TRANS-DISCIPLINARY HEALTH SCIENCES AND TECHNOLOGY

FOR THE AWARD OF THE DEGREE OF
DOCTOR OF PHILOSOPHY

BY

NISHANT SINGH

UNDER THE GUIDANCE OF

DR. RAJESH KUMAR LADHER

NATIONAL CENTRE FOR BIOLOGICAL SCIENCES, TATA INSTITUTE OF FUNDAMENTAL RESEARCH, BENGALURU-560065

MARCH 2025

SUPPORTING CELL MEDIATED HOMEOSTASIS OF CHICK BASILAR PAPILLA FOR HAIR CELL RESTORATION

A THESIS TO BE SUBMITTED TO

THE UNIVERSITY OF TRANS-DISCIPLINARY HEALTH SCIENCES AND TECHNOLOGY

FOR THE AWARD OF THE DEGREE OF
DOCTOR OF PHILOSOPHY

BY

NISHANT SINGH

UNDER THE GUIDANCE OF

DR. RAJESH KUMAR LADHER

NATIONAL CENTRE FOR BIOLOGICAL SCIENCES, TATA INSTITUTE OF FUNDAMENTAL RESEARCH, BENGALURU-560065

MARCH 2025

THE UNIVERSITY OF TRANS-DISCIPLINARY HEALTH SCIENCES AND TECHNOLOGY

Private University Established in Karnataka by ACT 35 of 2013
BENGALURU - 560064

DECLARATION BY THE CANDIDATE

I declare that this thesis entitled "**Supporting Cell Mediated Homeostasis of Chick Basilar Papilla for Hair Cell Restoration**" submitted for the award of Doctor of Philosophy to THE UNIVERSITY OF TRANS-DISCIPLINARY HEALTH SCIENCES AND TECHNOLOGY, Bengaluru, is my original work, conducted under the supervision of my guide **Dr. Rajesh Kumar Ladher**. I also wish to inform that no part of the research has been submitted for a degree or examination at any university. References, help and material obtained from other sources have been duly acknowledged.

I hereby confirm the originality of the work and that there is no plagiarism in any part of the dissertation.

Place: Bengaluru **Signature of the Candidate**

Date: 20 March 2025

Name of candidate: Nishant Singh
Reg. No.: 20318020207
(December 2021)

THE UNIVERSITY OF TRANS-DISCIPLINARY HEALTH SCIENCES AND TECHNOLOGY

Private University Established in Karnataka by ACT 35 of 2013
BENGALURU - 560064

CERTIFICATE

This is to certify that the work incorporated in this thesis **"Supporting Cell Mediated Homeostasis of Chick Basilar Papilla for Hair Cell Restoration"** submitted by **Nishant Singh** was carried out under my supervision. No part of this thesis has been submitted for a degree or examination at any university. References, help and material obtained from other sources have been duly acknowledged. I hereby confirm the originality of the work and that there is no plagiarism in any part of the dissertation.

Research Supervisor

Date: 20 March 2025

Name, designation & address details:

Dr. Rajesh Kumar Ladher

Associate Professor

National Centre for Biological Sciences, Tata Institute of Fundamental Research, Bellary Road, Bengaluru-560065, Karnataka, India

Acknowledgment

There are many people I want to thank for their love, care, and support throughout my PhD journey. First and foremost, my wife, Dr. Srishti Batra, whose immense support was crucial during this difficult project with its countless failed experiments before success. Her inspiration was a driving force behind my PhD. My parents, Mr. Prithvi Singh and Mrs. Saroj Devi, also provided tremendous support. During this journey, I achieved personal milestones as well, such as getting married and welcoming my son, Adrij.

I was the first member to join the Earlab, and I vividly remember the day I joined. The lab was more like an office space, empty and without chairs, and it was just Raj and me. From those humble beginnings, the lab has grown into a bustling hub full of students competing for space to work and sit. I feel incredibly fortunate to have had Dr. Raj Ladher as my PhD supervisor. I learned not only science but also scientific temperament from him. His approach to problem-solving is something I greatly admire. There were many times when I couldn't interpret data or find anything new, but Raj had a special knack for spotting intriguing details in the same data. His understanding of the time required for experiments is exceptional, ensuring ample time for progress before seeking updates.

The Earlab is a vibrant place with interesting people from diverse cultures. We've had a lot of fun together, enjoying parties, dancing, and getting drunk. Anubhav, with his can-do attitude, has been a great colleague. We've worked together from the beginning, standardizing many of the protocols practiced in the lab today. Raman has become a close friend, assisting extensively in the project from electroporation to imaging. I will never forget all those exciting and difficult imaging sessions we had together.

Thank you all for being a part of this incredible journey.

Dedication

The natural world thrums with a symphony of sound, a complex tapestry woven by diverse species for communication, navigation, and survival. This intricate dialogue transcends visual and olfactory cues, relying heavily on the rich and varied soundscapes that define different ecosystems. Yet, within this symphony lies a dissonance – the human auditory system lacks the remarkable ability to regenerate damaged hair cells, a process readily observed in non-mammalian vertebrates. This lost regenerative potential underlies a significant global health concern: sensorineural hearing loss (SNHL).

This thesis delves into the captivating phenomenon of hair cell regeneration within the chick basilar papilla. Utilizing genetic manipulation techniques and exploring relevant signaling pathways, this research aims to illuminate the intricate mechanisms governing cell fate determination and regeneration. By studying this non-mammalian system, we hope to decipher the secrets that unlock this lost human ability.

The widespread prevalence of SNHL, affecting millions worldwide, demands innovative solutions. This research not only seeks to understand the regenerative process but also aspires to pave the way for future therapies capable of restoring hearing in humans. By unlocking the secrets of hair cell regeneration, we aim to contribute to a future where the human auditory system can once again participate fully in the rich symphony of the natural world. Early identification and intervention are crucial in addressing sensorineural hearing loss, offering numerous benefits to those affected. This thesis explores the mechanisms underlying hair cell regeneration and seeks to contribute to the development of strategies for combating auditory dysfunction and enhancing the quality of life for individuals affected by hearing impairment.

Table of Contents

List of Tables

Chapter 2: Material and Methods

List of Figures

Chapter 1: Introduction

Chapter 2: Material and Methods

Chapter 3: Atoh1 Purification and Antibody Validation

Chapter 4: CRISPR-Cas9 Atoh1 Gene Editing

List of Acronyms

HC: Hair Cell

SC: Support Cell

IHC: Inner Hair Cell

OHC: Outer Hair Cell

THC: Tall Hair Cell

SHC: Short Hair Cell

BP: Basilar papilla

TV: Tegmentum vasculosum

TM: Tectorial membrane

BM: Basilar membrane

OP: Otic Placode

OV: Otic Vesicle

MET: Mechanoelectrical transduction

SNHL: Sensorineural Hearing Loss

E. coli: *Escherichia coli*

UTR: Untranslated region

IPTG: Isopropyl β-d-1-thiogalactopyranoside

IMAC: Immobilized metal affinity chromatography

E(day): Embryonic Day

HH: Hamburger Hamilton

DIV: Days In vitro

DMSO: Di-methyl Sulphoxide

EdU: 5-Ethynyl-2-deoxyuridine

mRNA: Messenger RNA

gRNA: Guide RNA mRNA

WT: Wildtype

Synopsis

Supporting Cell Mediated Homeostasis of Chick Basilar Papilla for Hair Cell Restoration

Nishant Singh

Supervisor: Dr. Rajesh Kumar Ladher

July 2024

Introduction

Auditory dysfunction can result from the loss of sensory hair cells (HCs) in the organ of Corti due to chronic noise exposure, ototoxic substances, and aging (Coleman, 1976; McGill and Schuknecht, 1976). Non-mammalian vertebrates, such as birds, have HC regenerative abilities, a property that has been lost in mammals (Corwin and Cotanche, 1988; Cotanche, 1987; Cruz et al., 1987; Ryals and Rubel, 1988). In birds, HC regenerate from a second cell type found in the auditory epithelium, known as supporting cells (SC). In normal physiology, SC serve diverse functions, such as mechanical and metabolic support, as well as maintaining ionic homeostasis during physiological processes (Monzack and Cunningham, 2013). In birds, SC can regenerate HC through one of two mechanisms: direct trans-differentiation or, more rarely, through asymmetric mitotic division (Shang et al., 2010; Stone and Cotanche, 2007). These events are initiated when HC are lost, however the steps involved in SC activation, and a clear dissection of the pathways that are involved in HC regeneration, have remained elusive. Parallels with HC differentiation suggest the role of various signaling pathways. Notably, the interaction between the Wnt and Notch signaling pathways, extensively studied in cochlear development and regeneration, plays a crucial role (Jacques et al., 2014; Zak et al., 2015).

In chick, hair cells become apparent from embryonic day (E)6, starting from a small circular patch at the distal end of the basilar papilla (BP) and extending proximally (Goodyear and Richardson, 1997). The number of differentiated HCs increases until E10, after which HC number stabilize and show a moderate increase until E12 (Goodyear and Richardson, 1997). HC themselves arise from a prosensory domain, a group of sensory precursors that express the transcription factor Sox2 which is necessary for HC formation (Kiernan et al., 2005b; Neves et al., 2007; Pan et al., 2013). Both Notch and Wnt signaling can impact the regulation of

expression of Sox2: Notch, through its interaction with its ligand Jag1, positively regulates Sox2 expression (Brooker et al., 2006; Daudet et al., 2007; Kiernan et al., 2006). The Wnt pathway, through its downstream effector ß-catenin, has been shown to upregulate Sox2 expression and promote proliferation (Jacques et al., 2014; Jacques et al., 2012), however more recent data suggest that this regulation depends on the exact levels of Wnt activity, with low levels of signalling necessary for Sox2 expression and high levels being inhibitory (Zak and Daudet, 2021). Wnt signalling is also thought to activate the transcription factor, Atoh1, in the prosensory region. Atoh1 is necessary and sufficient for hair cell differentiation, and initially, all cells in the prosensory region express Atoh1 (Bermingham et al., 1999; Driver et al., 2013; Stone et al., 2003). However, HC differentiation is limited to specific cells through the action of Notch, this time with its ligands Dll1 and Jag2 (Kiernan et al., 2005a; Lanford et al., 1999). This interaction releases the Notch intracellular domain (NICD), which translocates to the nucleus to activate target gene transcription. In this case, NICD activates a repressor of HC differentiation, specifying these cells as Supporting Cells (SC) and allowing neighbouring cells to develop as HC, creating a mosaic of Notch-ligand expressing HC surrounded by Notch-active SC.

While differentiation is occurring, the BP is undergoing considerable cellular rearrangements as convergence and extension movements extend the epithelium and drive the alignment of intrinsic polarity (Goodyear and Richardson, 1997; Prakash et al., 2023). On average SC lose SC neighbours as they reorganize around HC. Cell rearrangements and the increase in the apical surface area of hair cells have been proposed to account for much of these changes. However, there remains the possibility that some plasticity in cell identity exists that allows the HC-SC mosaic to be maintained in the BP, even while cellular rearrangement occurs. To understand this, we used an electroporation approach to knock-down Atoh1 mosaically, in the otocyst of the chick. We find that at E9, electroporation leads to the loss of HC. However, by E12 HC number is restored. Using inhibitor studies and by introducing reporter constructs, we find that both Wnt and Notch pathways are involved in HC restoration. We suggest that there is a second wave of HC differentiation, that occurs during BP cellular rearrangements that ensure cellular pattern is maintained.

Materials and Methods

The comprehensive description of the materials and methodologies utilized in this research can be found in the publication; Singh, N., Prakash, A., Chakravarthy, S.R., Kaushik, R., Ladher,

R.K., 2022. ‘In Ovo and Ex Ovo Methods to Study Avian Inner Ear Development. Journal of visualized experiments’ and in Singh, N., Kaushik, R., Prakash, A., Saini, S., Garg, S., Adhikary, A., Ladher, R.K., 2024. ‘Mosaic Atoh1 Deletion in the Chick Auditory Epithelium Reveals a Second Period of Differentiation to Restore Hair Cell Number. http://dx.doi.org/10.2139/ssrn.4814834’.

Results

Hair Cells are lost in Atoh1-crispant Basilar Papilla

The right otic vesicle of an E3.5-4 embryo was electroporated with either a control-gRNA or Atoh1-gRNA, (Fig. 1A & 1B) with the left otic vesicle as the internal control. Embryos were incubated until E9-E12, at which point the BP was dissected and HC development assessed.

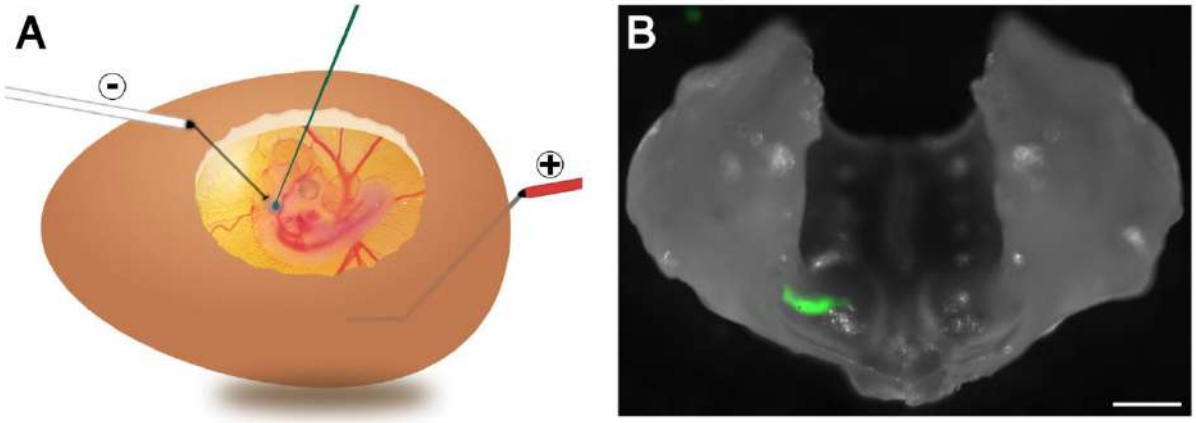

Figure 1: In Ovo Electroporation of guide RNA and Tol2-eGFP plasmids at E4. (A) Schematic illustrating the technique of in ovo microinjection and electroporation into the chick otic vesicle at embryonic day 4 (E4). (B) The left inner ear serves as an internal control. The GFP expression is observed in the E10 cochlear duct of the right inner ear, scale bar is 1.5 inches.

As the spatial arrangement of HCs and SCs varies along the length of BP from proximal to distal end as well as during development, we independently assessed the three regions (Figure 2A) for each embryonic stage (Goodyear and Richardson, 1997; Prakash et al., 2023). At E9 stage, the Atoh1-crispant BP shows a reduced number of HCs when compared to both control and control-gRNA BP (Fig. 2B-D). However, we find that, by E12, no difference in HC number was observed (Fig. 2E-G). The presence of the tracer GFP allowed us to assess the extent of electroporation. We noted that at E9, in the Atoh1-crispants, patches of missing HCs coincided with areas where GFP expression is observed (Fig. 2D). By E12, despite the presence of GFP, HC numbers had recovered (Fig. 2H-K). However, upon close inspection, we noticed that recovered HC were not GFP positive (Fig. 2G). To quantitate this, we quantified the

number of cells that co-expressed GFP and the hair cell marker, Myosin 7a. We found that when compared to control-gRNA samples, significantly fewer Myo7a/GFP double-positive cells in Atoh1-crispants (Fig. 2L).

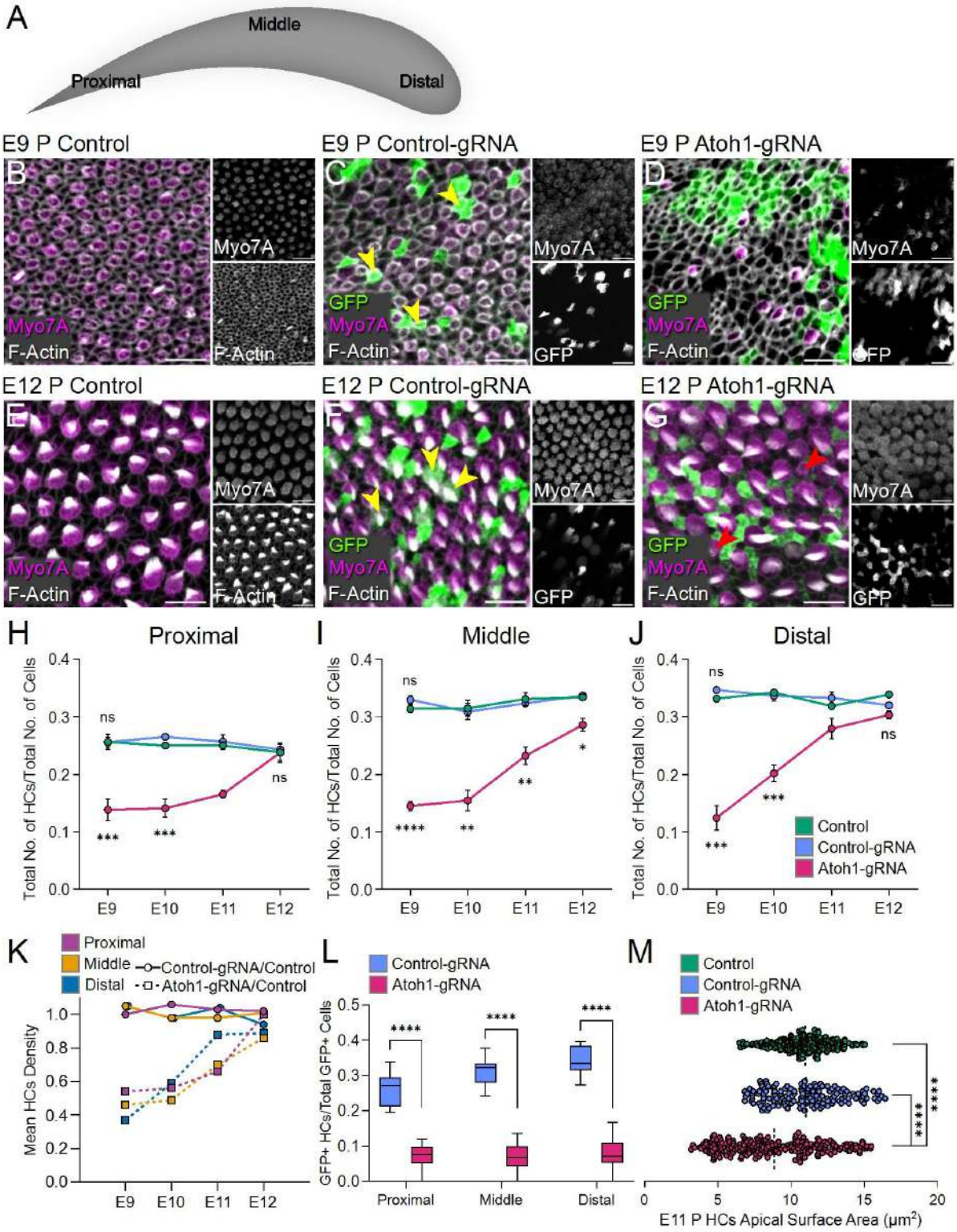

Figure 2: Mosaic Atoh1 deletion results in loss of hair cells at E9 & subsequent recovery by E12. (A) Schematic of BP divided into three regions proximal, middle and distal. Images (B-G) are obtained from the proximal region of the BP (Scale bar is 10μm). (B-D) are from chick embryo E9 and (E-G) are from chick embryo E12. (B)

*Contralateral Control E9 BP showing phalloidin-stained F-Actin (gray) and Myo7a-labeled hair cells (HCs) (magenta). (C) Control-gRNA electroporated E9 BP showing GFP electroporated cells (green), phalloidin-stained F-Actin (gray) and Myo7a-labeled hair cells (HCs) (magenta). Yellow arrowheads mark GFP-positive HCs. (D) Atoh1-gRNA electroporated E9 BP showing GFP electroporated cells (green), phalloidin-stained F-Actin (gray) and reduced Myo7a-labeled hair cells (HCs) (magenta). (E) Contralateral Control E12 BP showing phalloidin-stained F-Actin (gray) and Myo7a-labeled hair cells (HCs) (magenta). (F) Control-gRNA electroporated E12 BP showing GFP electroporated cells (green), phalloidin-stained F-Actin (gray) and Myo7a-labeled hair cells (HCs) (magenta). Yellow arrowheads mark GFP-positive HCs. (G) Atoh1-gRNA electroporated E9 BP showing GFP electroporated cells (green), phalloidin-stained F-Actin (gray) and restored Myo7a-labeled hair cells (HCs) (magenta). Red arrowheads mark new born HCs, identified based on size. (H - J) Graph showing the number of HC as a proportion of the total number of cells in contralateral control (green), Control-gRNA (blue) and Atoh1-gRNA (red), at four stages (E9, E10, E11 and E12), in the proximal (H), middle (I) and distal (J) regions of the BP. (**** P<0.0001; *** P < 0.001; ** P < 0.01 * P < 0.05; ns = non-significant). (K) Graph showing the density of HC, compared to that of the contralateral control, of Control-gRNA (solid line) and Atoh1-gRNA (dashed line) in proximal (magenta), middle (orange) and distal (blue) at E9-12. (L) The graph showing ratio of GFP-positive HCs to the total number of GFP-positive cells in different regions of the BP for Control-gRNA (blue) and Atoh1-gRNA (red). (M) The graph shows apical surface area of HCs at proximal region of E11 BP (**** P<0.0001)*

To understand the time course of hair cell restoration, we examined the BP of embryos at E9, 10, 11 and 12. We found that the rate of hair cell restoration appears distally first followed by more proximal regions, mirroring the natural process of hair cell differentiation in the BP (Fig. 2K). At E12, Atoh1-crispants show restored hair cell and support cell arrangement resembling that of both the control and control-gRNA groups. In Atoh1-crispants, GFP is predominantly confined to supporting cells. (Fig. 2G). Moreover, the apical surface area of the restored hair cells is smaller compared to those in the control basilar papilla (Fig. 2M), with some lacking hair bundles but, nonetheless, expressing Myo7a.

Neighbourhood Analysis

HC and SC are mosaically organized in the BP. HC contact SC (HC-SC contact), but very rarely another HC (HC-HC contact) (Goodyear and Richardson, 1997; Prakash et al., 2023). SC can contact HC (SC-HC contact) and SC (SC-SC contact) (Fig. 3A). To understand whether HC restoration is accompanied by a restoration in the mosaic pattern of the BP, we conducted neighbour number analysis for both HC and SC between E9 and E12.

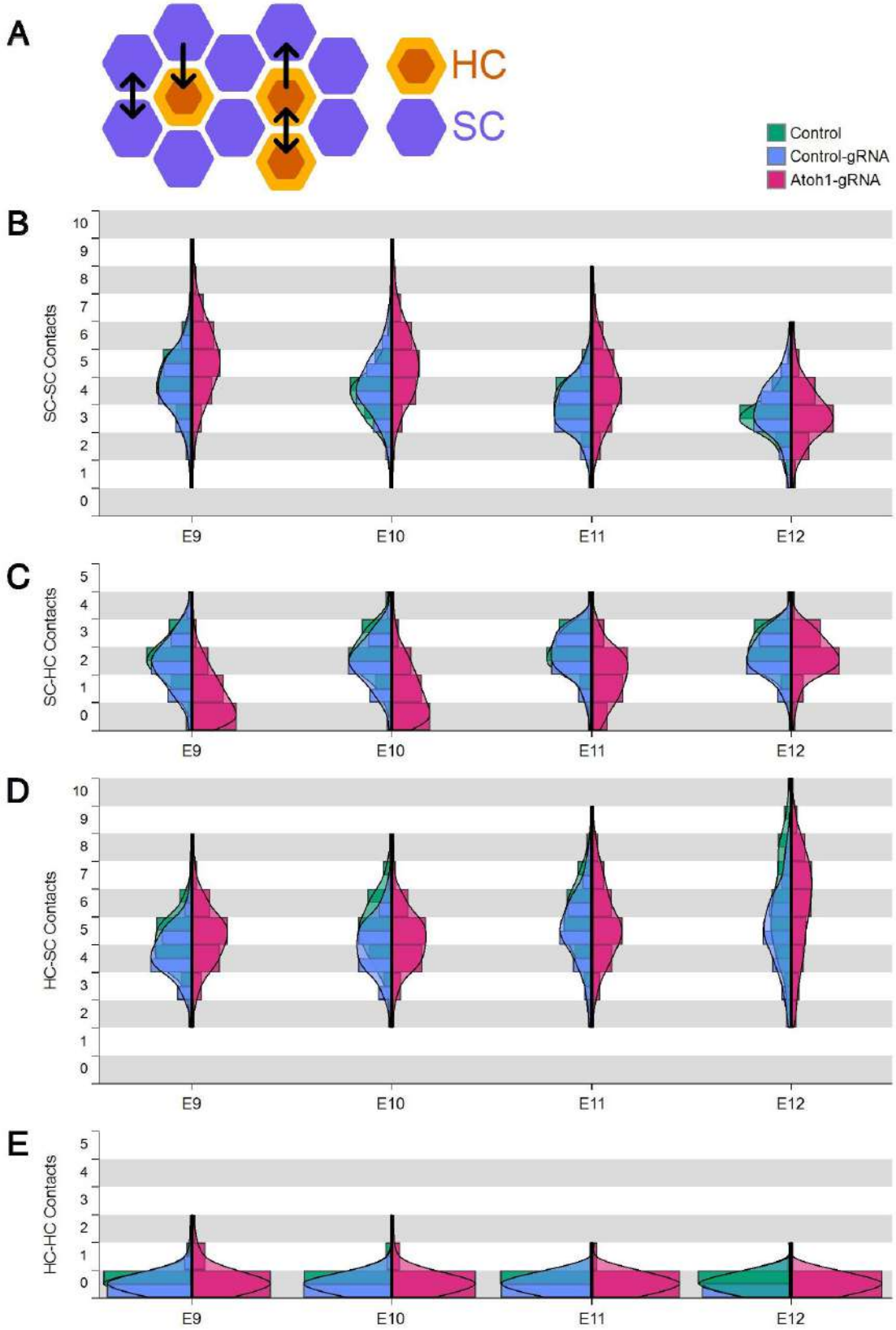

Figure 3: Neighborhood connections: HC and SC interaction analysis. (A) The type of interactions between HCs and SCs. The arrows symbolise four types of connections between these two cell types: SC-SC, SC-HC, HC-SC,

and HC-HC. (B-E) The split-histograms show the number of neighboring cells for each cell type in contralateral control (green), control-gRNA (blue), and Atoh1-gRNA (red) at four embryonic stages from E9 to E12. (B) Number of SC-SC contacts, (C) Number of HC contacted by a single SC, (D) Number of SC contacted by a single HC, (E) Number of contacts made between HC-HC.

As expected, at E9 Atoh1-gRNA electroporated BP show a greater number of SC-SC contacts, with dramatically reduced SC-HC contacts given the reduced HC numbers in electroporated patches. While around 3-5% of SC are without an HC contact in control and control-gRNA samples, 47% of SC do not have an HC contact in Atoh1-gRNA samples (Fig. 3C). The reduction in SC-SC contacts and the recovery of SC-HC contacts occurs by E12 such that, the number of both SC-SC and SC-HC contacts are similar to those seen in control-gRNA samples (Fig. 3B & 3C). Consistent with this, the number of SC without HC contacts falls to control-gRNA levels by E12.

At E9, substantial HC-HC contacts are observed in Atoh1-gRNA samples. These are rarely observed in control samples (Fig. 3E). These contacts resolve by E12. Surprisingly, the number of HC-SC contacts showed an increase at E12 (Fig. 3D). This may be due to the smaller apical surface area of restored HC.

Proliferation Status of Basilar Papilla After HC Loss

We next asked if HC restoration was associated with changes in proliferation. Embryos electroporated with either control-gRNA or Atoh1-gRNA were grown to E9, E10, E11, and E12. At these stages the BP was explanted and cultured for one day in the presence of EdU (Fig. 4A). After culture, explants were fixed and processed for Sox2 (as a support cell marker) and Myo7a (a hair cell marker) immunostaining, as well as EdU incorporation. Sections of explanted BP showed a clear demarcation between hair cells (HCs) and supporting cells (SCs). HCs were situated closer to the luminal surface, while SC nuclei were grouped closely near the basilar membrane, making them easily distinguishable and countable.

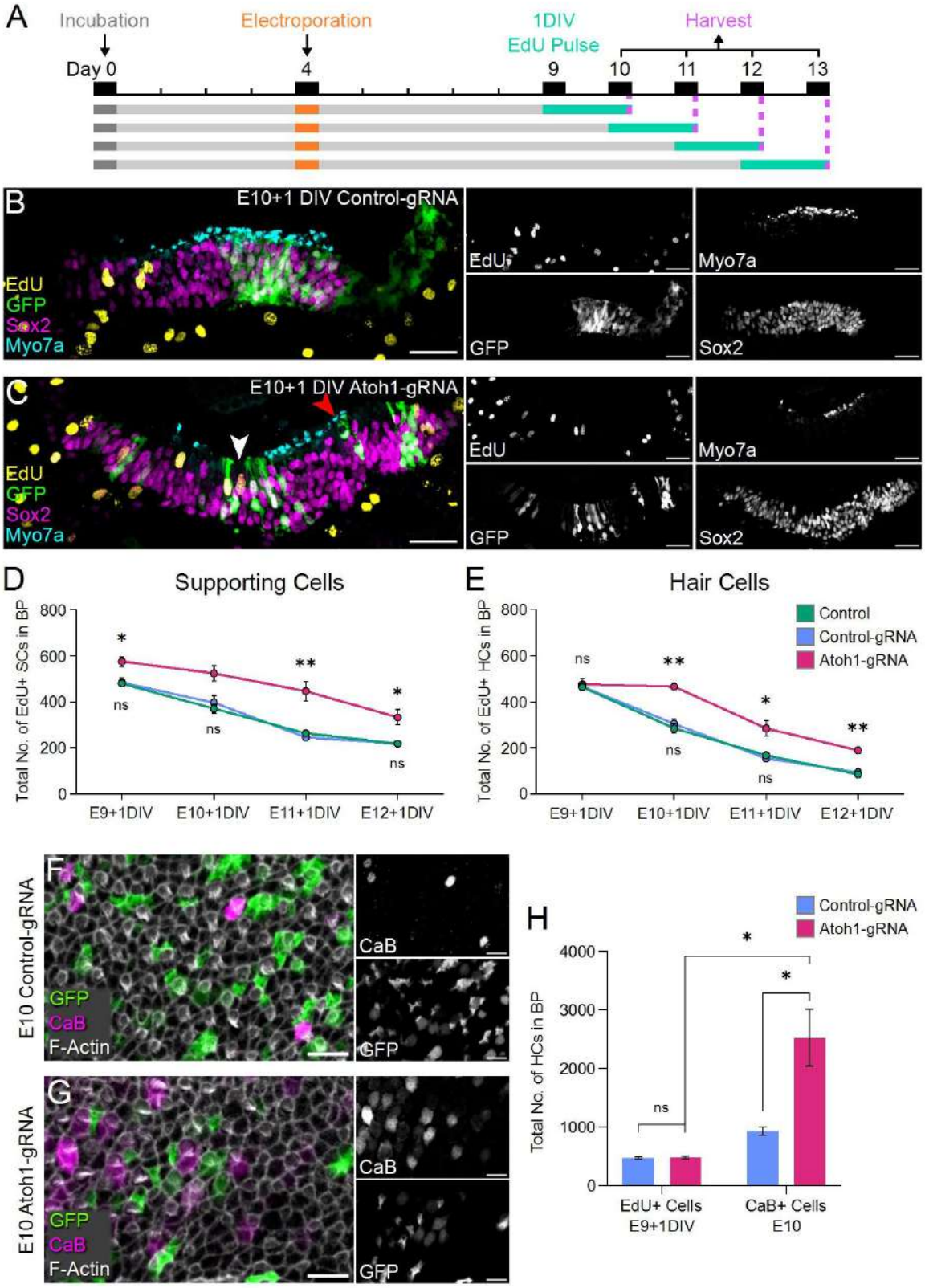

Figure 4: Proliferation dynamics in developing BP. (A) Illustration of the experimental design for EdU pulse treatment. Electroporation is performed on all embryos at E4. At the specified stages of E9, E10, E11, and E12, a one-day EdU pulse was administered through in vitro BP explants, followed by the harvesting of the BP. (B-C)

*Cross-sectional images of E10+1-day in vitro (DIV) BP explants, (Scale bar is 25µm). Myo7a staining HCs in cyan, Sox2 staining SCs in magenta, EdU labeling in yellow, and green indicating GFP expression in Control-gRNA (B) and Atoh1-gRNA BP (C). The white arrow marks the region with missing HCs with an EdU-positive SC beneath it, and the red arrow marks GFP-positive HCs, referred to as "escapers". (D) Graph showing EdU-positive SCs and (E) EdU-positive HCs from embryonic stages E9+1 DIV to E12+1 DIV from control, control-gRNA, and Atoh1-gRNA. (F-G) are whole mount images of E10 BP from electroporated chick embryos (Scale bar is 10µm). Calbindin (CaB)(magenta) marks new HCs phalloidin staining F-Actin (grey), and GFP expression (green) of control-gRNA at E10 (F) and Atoh1-gRNA BPs (G). (H) Graph showing the total number of HCs in both E9+1 DIV BP explant (treated with EdU) and E10 BP with two condition groups: control-gRNA (blue) and Atoh1-gRNA (magenta). *P<0.05 and **P<0.01, ns - non-significant.*

In BP sections, a higher number of EdU-positive cells were observed at E10+1 DIV, coinciding with GFP expression in Atoh1-crispants (Fig. 4C). In contrast, the control-gRNA exhibited sporadic presence of EdU-positive cells (Fig. 4B). At each stage from E9+1 DIV to E12+1 DIV, we detected increased numbers of EdU-positive cells in Atoh1-gRNA electroporated regions, when compared to corresponding regions in control-gRNA or unelectroporated BPs. The numbers of Sox2/EdU double positive cells are enhanced in the Atoh1-gRNA crispants, however the numbers show a gradual decline between E9+1 DIV to E12+1 DIV (Fig. 4D). Myo7a/EdU positive cells show comparable levels between Atoh1-gRNA and control BPs at E9+1 DIV, however at E10+1 DIV there is a significant elevation in these numbers when compared to controls (Fig. 4E). This suggests the generation of new hair cells between E9 and E10 in response to Atoh1-gRNA electroporation. In agreement with this, we could detect Myosin7a and Sox2 double-positive cells in Atoh1-gRNA crispants, suggesting the emergence of new hair cells.

To confirm the presence of newly generated hair cells, we immunostained the BP with Calbindin (Fig. 4F & 4G), which labels newborn hair cells at E10, and compared it to the EdU positive hair cells data from E9+1 DIV Atoh1-gRNA electroporated explants (Chen et al., 2021; Cox et al., 2014). We find significantly more Calbindin-positive (CaB+) new hair cells than EdU-positive hair cells at the same developmental stage (Fig. 4H). This suggests the involvement of additional mechanisms in HC restoration, such as transdifferentiation of supporting cells. In agreement with this, we observed a substantial population of cells within Atoh1-gRNA samples that exhibited co-expression of Myosin7a and Sox2, markers typically associated with newly generated hair cells. These cells did not show EdU incorporation. These findings suggest that hair cell restoration could involve both direct transdifferentiation from supporting cells into hair cells and mitotic division of supporting cells. Transdifferentiation likely initiates earlier at E9+1DIV, while mitotic division becomes more prominent later. This finding aligns with previous research indicating that mitotic division of supporting cells could

play a role in the restoration of basilar papilla tissue (Corwin and Cotanche, 1988; Ryals and Rubel, 1988). Although the primary mode of hair cell regeneration in chick basilar papilla is reported to be direct transdifferentiation of supporting cells (Shang et al., 2010; Stone and Cotanche, 2007).

Molecular Regulators of HC Restoration

To understand the molecular mechanisms that could be involved in HC restoration, we used our explant approach as a proof of principle to screen modulators of signalling pathways that might influence HC restoration. Given the correspondence, we tested small molecules that modulate pathways involved in HC regeneration.

Wnt signalling has been implicated in the development of HC (Jacques et al., 2012; Shi et al., 2014). Activators of the Wnt/ß-catenin pathway increase the proliferation of prosensory cells in the organ of Corti, in the chick BP as well as in zebrafish neuromasts. Wnt activation has also been shown to potentiate regeneration in the zebrafish lateral line, and genes associated with this pathway are robustly induced upon neuromast damage (Head et al., 2013; Jiang et al., 2014). We thus used an inhibitor and activator of canonical Wnt signalling to ask if HC restoration was affected.

Control-gRNA and Atoh1-gRNA were electroporated into the E4 otocyst with a tracer construct. At E10 the BP was dissected. It was then either immediately fixed (E10+0) or treated with XAV939, a canonical Wnt antagonist, or CHIR99021, a Wnt agonist. Explants were cultured for 2 days (Fig. 5A), then fixed and HC and SC numbers assayed.

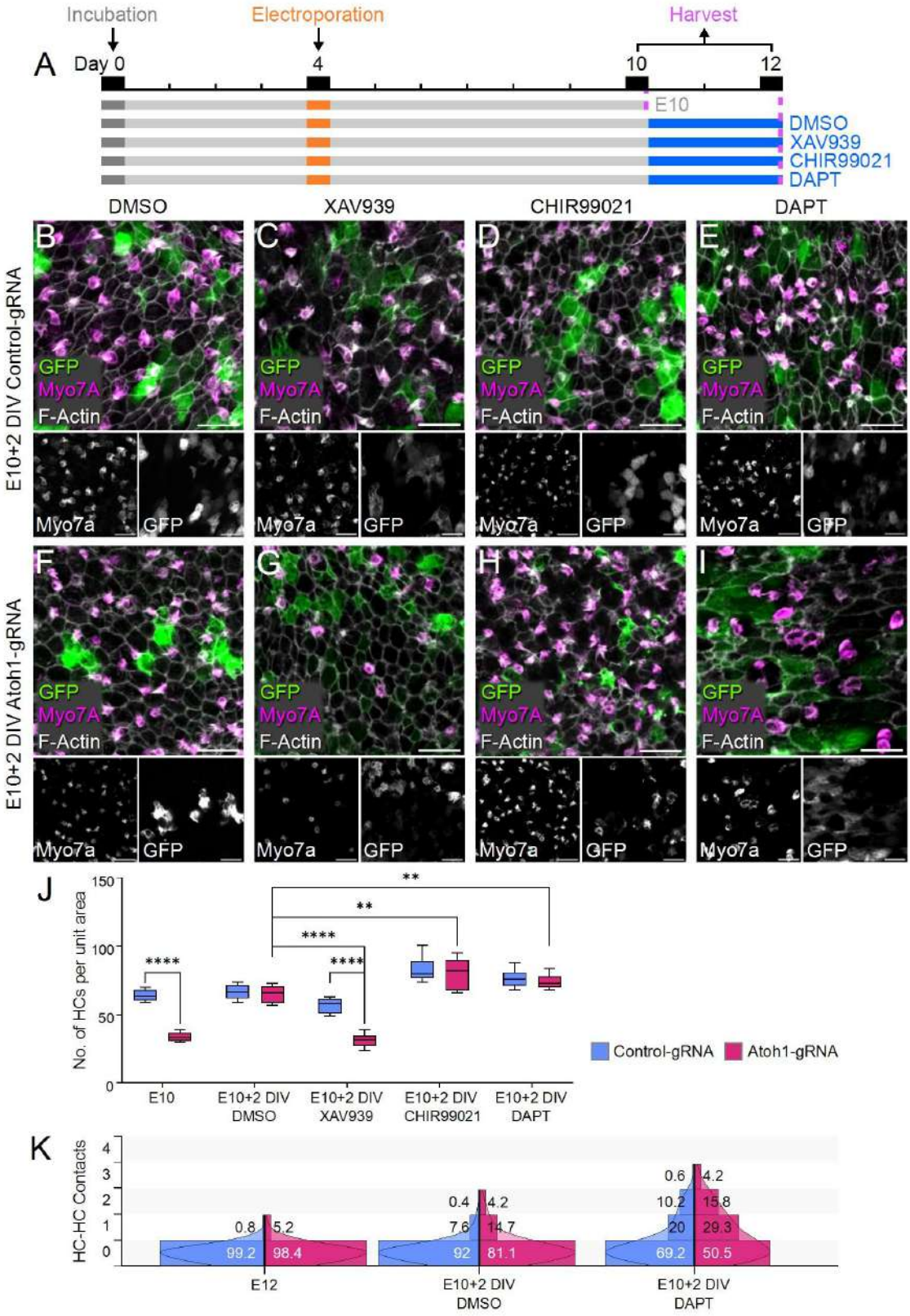
A
Incubation
Electroporation
Harvest
Day 0
4
10
12
E10
DMSO
XAV939
CHIR99021
DAPT
DMSO
XAV939
CHIR99021
DAPT
E10+2 DIV Control-gRNA
E10+2 DIV Atoh1-gRNA
B
C
D
E
F
G
H
I
GFP
Myo7A
F-Actin
Myo7a
GFP
J
No. of HCs per unit area
150
100
50
0
****
****
****
**
**
Control-gRNA
Atoh1-gRNA
E10
E10+2 DIV DMSO
E10+2 DIV XAV939
E10+2 DIV CHIR99021
E10+2 DIV DAPT
K
HC-HC Contacts
4
3
2
1
0
0.8
5.2
99.2
98.4
0.4
4.2
7.6
14.7
92
81.1
0.6
4.2
10.2
15.8
20
29.3
69.2
50.5
E12
E10+2 DIV DMSO
E10+2 DIV DAPT

*Figure 5: Wnt and Notch Pathway Modulation in Atoh1-Crispant Basilar Papilla. (A) Diagram illustrating the experimental setup for the treatment with pharmacological inhibitors and activators. Electroporation is performed on all embryos at E4. At the E10 embryonic stage, a two-day treatment with small molecules is administered through in vitro basilar papilla explants, followed by harvesting the basilar papilla at E10+2 DIV. (B-I) Images of basilar papilla explants from electroporated chick embryos showing F-Actin (gray), Myo7a-labeled hair cells (magenta), and GFP (green). Scale Bar is 10µm. The top panel (B, C, D, E) displays images from basilar papilla explants of control-gRNA electroporated otocysts. The lower panel (F, G, H, I) shows images from the basilar papilla explants of Atoh1-gRNA electroporated otocysts. Explants are treated with DMSO vehicle control (B, F); the Wnt antagonist XAV939 (C, G); the Wnt agonist CHIR99021 (D, H) and an inhibitor of Notch signalling, DAPT (D, H). (J) The graph illustrates the number of hair cells in a unit area in control-gRNA and Atoh1-gRNA basilar papilla explants. E10, serves as zero time point before treatment starts. To assess statistical significance in direct comparisons between the two conditions, Student's t-tests were conducted to calculate P-values, with **P<0.01 and ****P<0.0001 indicating statistical significance. (K) The graphs shows the number of HC-HC contacts in electroporated control-gRNA, and Atoh1-gRNA with E12 control basilar papilla and E10+2 DIV (DMSO & DAPT) treated basilar papilla explant.*

Treatment with XAV-939 blocked the restoration of HC in Atoh1-gRNA electroporated BP explants, with numbers similar to those seen at E10 (Fig. 5G & 5J). In contrast, control-gRNA explants treated with XAV-939 showed normal numbers of HC (Fig. 5C & 5J). In contrast, CHIR99021-treatment did not affect HC restoration in Atoh1-gRNA electroporated E10+2 DIV BP explants (Fig. 5H & 5J). Indeed, when compared to vehicle control (Fig. 5B & 5F), there was mild elevation of HC numbers in both control-gRNA and Atoh1-gRNA electroporated explants after CHIR99021-treatment (Fig. 5J). Taken together, these data suggest that Wnt signalling may play in an aspect of HC restoration.

We next turned to Notch signalling; the role of Notch-Delta signalling in the development and regeneration of HC and SC has been well-established (Chrysostomou et al., 2012; Daudet et al., 2009; Lanford et al., 1999). We thus treated electroporated BP explants with DAPT, an inhibitor of gamma-secretase, important in the activation of Notch. Treatment with DAPT did not affect HC restoration (Fig. 5I), and the numbers of HC in control or Atoh1-gRNA explants were higher than vehicle controls (Fig. 5J). Closer inspection revealed a greater number of HC-HC contacts in the DAPT-treated explants, irrespective of whether they were from control-gRNA or Atoh1-gRNA electroporation (Fig. 5K).

Signalling Activity during HC Restoration

To understand when and where signalling was active during HC restoration, we co-electroporated reporter constructs alongside Atoh1-gRNA CRISPR/Cas9 components. We first looked at Notch signalling. The pT2K-Hes5::nd2mScarlet plasmid consists of the mouse Hes5 promoter driving the expression of a destabilized and nuclear localized mScarlet fluorescent protein in Notch-On supporting cells (Fig. 6A)(Chrysostomou et al., 2012). mScarlet

expression is transient, with its presence limited to cells where Notch is active or has been active within the past 10 hours (Chrysostomou et al., 2012).

We observed a significant reduction in the population of Notch-On cells, expressing high levels of mScarlet, within the basilar papilla of Atoh1-gRNA crispants at E10 (Fig. 6B & 6D). However, a population of cells with lower mScarlet expression was observed at the luminal surface, where hair cells would normally be expected. Staining for phospho-Histone H3 (pH3), a marker of mitotic cells in cross sections of the basilar papilla, revealed a significant

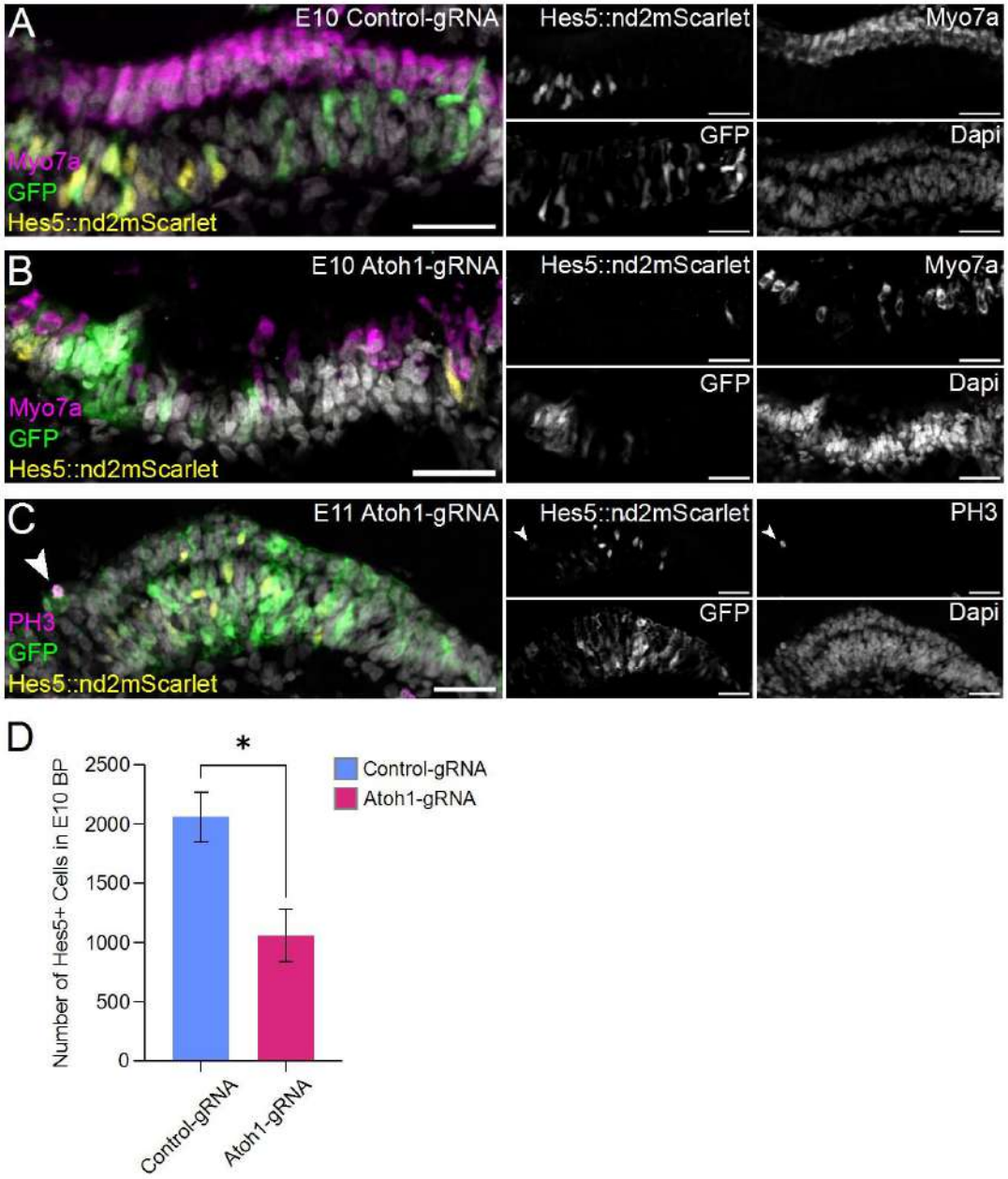

Figure 6: Hes5::nd2mScarlet reporter activity in Atoh1-crispant BP. Cross-sections of BP from electroporated chick embryos. (A, B) E10 BP showing Myo7a (magenta), Dapi-stained nuclei (grey) and Hes5::nd2mScarlett, Notch-on cells (yellow) and GFP (green) in control-gRNA electroporated BP (A) and Atoh1 electroporated BP. (Scale Bar is 25µm). (C) BP of Atoh1-gRNA at E11, which were co-electroporated with pT2K-Hes5::nd2mScarlet showing the mitotic marker Phospho-Histone H3 (PH3) (magenta), nuclei (grey), Notch-on cells (yellow), GFP (green). (Scale Bar is 25µm). (D) The graph shows the total number of Hes5+ cells in the E10 basilar papilla for the two conditions: control-gRNA and Atoh1-gRNA. P-values, with *P<0.05.

co-localization of pH3 positive cells with cells showing diminished mScarlet expression (Fig. 6C). As Hes5 activity is found in supporting cells, the reduced mScarlet expression in these cells may suggest a recent transformation into new hair cells. These findings indicate that the downregulation of Hes5 in supporting cells promotes hair cell differentiation and suggests that supporting cells can be induced to re-enter the cell cycle and give rise to new hair cells.

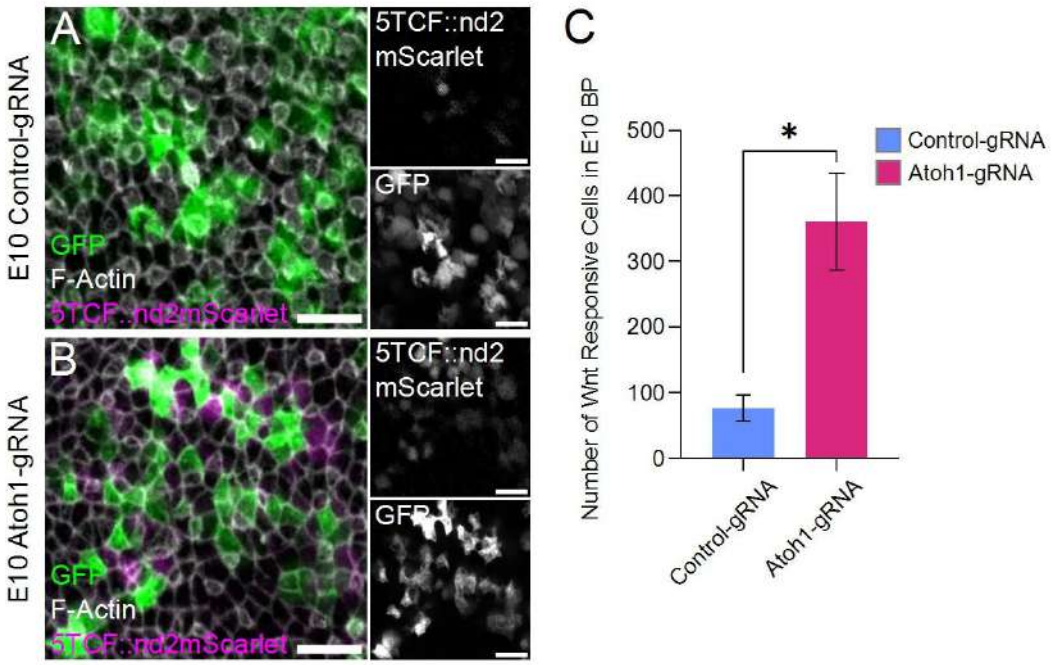

Figure 7: Wnt responsive cells in Atoh1-crispant BP. (A, B) Whole-mount E10 BP at E10 from electroporated chick embryos, showing 5TCF::nd2mScarlet Wnt-on cells (magenta), F-Actin (grey), and GFP (green) from control-gRNA BP (A) an Atoh1-gRNA electroporated BPs (B). (C) The graph showing the total number of Wnt-positive cells in the E10 basilar papilla for control-gRNA (blue) and Atoh1-gRNA (magenta). P-values - *P<0.05.

We next turned to the Wnt pathway, using co-electroporation of a Wnt reporter (pT2K-5TCF::nd2mScarlet). This construct consists of 5 TCF/LEF binding sites driving the expression of a destabilised, nuclear-localized mScarlet protein. Cells in which Wnt signalling

is active, or has been active in the past 10 hours, will show nuclear expression of mScarlet indicating Wnt receiving cells. We observed a significant increase in the number of Wnt-responsive cells within Atoh1-gRNA electroporated BP (Fig. 7B & 7C). These results are consistent with prior research in the field, which highlights the role of canonical Wnt signaling in promoting proliferation in lateral line regeneration (Jiang et al., 2014; Steiner et al., 2014).

Concluding Remarks

Hair cells of the inner ear of birds are replaced after damage. How the BP is able to sense the absence of a HC, what mechanisms are used to activate quiescent progenitors, and what are the steps in HC replacement remain unclear. This has been, in part, due to the inaccessibility of HC regeneration paradigms, requiring post-hatch stages of chicks. In this study, we identify a second wave of hair cell differentiation in the chick basilar papilla, that is revealed by mosaic deletion of Atoh1, and that may provide a model for HC regeneration. We show that even though HC numbers are depleted at E9 after Atoh1 CRISPR-mediate deletion, they are restored by E12. HC Restoration is achieved through non-transfected SC differentiating into HC. Anaylsis of the timing of restoration suggests that it occurs in a distal to proximal fashion mirroring the normal differentiation profile of BP hair cells. Newly generated HCs exhibit a smaller apical area at E12 stage. Some of these newly formed cells lack hair bundles but still express Myo7a. Additionally, we have observed disruptions in planar polarity in Atoh1-crispants, although polarity alignment is restored in the course of BP development (data not shown). The parallels between restoration and regeneration suggest that some aspects of HC regeneration can be modelled through restoration. Moreover, the tractability of the embryonic system to electroporation allows the introduction of constructs into the tissue as HC are restored.

Most hair cells have developed in the chick BP by E9.5 (Goodyear and Richardson, 1997). However, during normal development, around 1000 more hair cells are added over 3 days, such that E12 obtains the final HC number of around 12,000. Between E9 and E12, the BP is also undergoing cellular rearrangements, that are not only responsible for the extension of the BP, but also for the alignment of HC polarity (Goodyear and Richardson, 1997; Prakash et al., 2023). We therefore speculate that during normal development, a second wave of HC differentiation restores the correct number of HC neighbours to SCs that may have lost a neighbour during these rearrangements. At E12 SC have 2 HCs neighbours (Prakash et al.,

2023). In our Atoh1-crispants, there are a substantial number of SC that have no HC neighbour at E9, however by E12 most SC contact 2 HCs.

The mechanisms that sense an inconsistency in the numbers of neighbours is unclear. One obvious candidate would be the interaction between Notch1 (on supporting cells) with Dll1 (on hair cells). In this model, SC fate is maintained through the continued production of NICD after Notch interaction with its ligand (either Dll1, or Jag2) in the HC. In the absence of the ligand, SC differentiate into HC. Previous work suggests Notch signalling itself is not required for the release of quiescence during regeneration, and that DAPT treatment of the adult, undamaged, BP does not result in an increase in HC (Daudet et al., 2009). However it is likely that at embryonic stages, the some of the SC precursors are not quiescent. Consistent with this, we observe a down-regulation of the number of cells showing expression of mScarlet driven from the Hes5-ndmScarlet Notch reporter, in response to Atoh1 downregulation. Control explants treated with DAPT, a gamma-secretase inhibitor that inhibits Notch signaling, show a modest elevation of HC number compared to DMSO control. HC numbers are restored to this value in Atoh1-crispant BP explants. The elevation of HC number is modest, and restoration of HC number after Atoh1-gRNA electroporation is only to this elevated number. This modest elevation suggests that only a subset of SC may have progenitor activity.

In contrast to the suppression of Notch signalling during HC restoration, a canonical Wnt reporter is upregulated in response to mosaic Atoh1 deletion. However, how, and if, these two signalling pathways intersect is unclear. Inhibiting Wnt signalling, using XAV939 prevents the restoration of HC. This suggests that ß-catenin stabilization, as a result of Wnt signalling, is important for the maintenance of the progenitor fate for HC conversion in the BP, and in its absence these progenitor cells enter a quiescent state. In damaged neonatal mouse utricle, stabilized ß-catenin in Lgr5+ cells enhances mitotic activity and HC regeneration (Kuo et al., 2015). Arguing against this, is the effect of the Wnt agonist, CHIR99021. Rather than promoting quiescence, the CHIR compound leads to a modest elevation in HC numbers in both control-gRNA and Atoh1-gRNA electroporated samples compared to the vehicle-treated samples. CHIR99021 is an inhibitor of glycogen synthesis kinase 3 (GSK-3ß) which usually leads to a destablisation of ß-catenin. GSK-3ß can also phosphorylate NICD, protecting it from degradation (Foltz et al., 2002). Thus, it is possible that CHIR99021 could also lead to a degradation of NICD, in effect releasing the Notch-mediated maintenance of SC/progenitor fate. Additional work is required to determine these interactions, however combining mosaic

Atoh1 deletion with co-electroporation of signalling reporters and explant studies can allow imaging experiments and timed inhibitor studies to allow insights into the dynamic regulation of this process.

References

Bermingham, N.A., Hassan, B.A., Price, S.D., Vollrath, M.A., Ben-Arie, N., Eatock, R.A., Bellen, H.J., Lysakowski, A., Zoghbi, H.Y., 1999. Math1: an essential gene for the generation of inner ear hair cells. Science 284, 1837-1841.

Brooker, R., Hozumi, K., Lewis, J., 2006. Notch ligands with contrasting functions: Jagged1 and Delta1 in the mouse inner ear. Development 133, 1277-1286.

Chen, Y., Gu, Y., Li, Y., Li, G.L., Chai, R., Li, W., Li, H., 2021. Generation of mature and functional hair cells by co-expression of Gfi1, Pou4f3, and Atoh1 in the postnatal mouse cochlea. Cell reports 35, 109016.

Chrysostomou, E., Gale, J.E., Daudet, N., 2012. Delta-like 1 and lateral inhibition during hair cell formation in the chicken inner ear: evidence against cis-inhibition. Development 139, 3764-3774.

Coleman, J.W., 1976. Hair cell loss as a function of age in the normal cochlea of the guinea pig. Acta Otolaryngol 82, 33-40.

Corwin, J.T., Cotanche, D.A., 1988. Regeneration of sensory hair cells after acoustic trauma. Science 240, 1772-1774.

Cotanche, D.A., 1987. Regeneration of hair cell stereociliary bundles in the chick cochlea following severe acoustic trauma. Hear Res 30, 181-195.

Cox, B.C., Chai, R., Lenoir, A., Liu, Z., Zhang, L., Nguyen, D.H., Chalasani, K., Steigelman, K.A., Fang, J., Rubel, E.W., Cheng, A.G., Zuo, J., 2014. Spontaneous hair cell regeneration in the neonatal mouse cochlea in vivo. Development 141, 816-829.

Cruz, R.M., Lambert, P.R., Rubel, E.W., 1987. Light microscopic evidence of hair cell regeneration after gentamicin toxicity in chick cochlea. Archives of otolaryngology--head & neck surgery 113, 1058-1062.

Daudet, N., Ariza-McNaughton, L., Lewis, J., 2007. Notch signalling is needed to maintain, but not to initiate, the formation of prosensory patches in the chick inner ear. Development 134, 2369-2378.

Daudet, N., Gibson, R., Shang, J., Bernard, A., Lewis, J., Stone, J., 2009. Notch regulation of progenitor cell behavior in quiescent and regenerating auditory epithelium of mature birds. Dev Biol 326, 86-100.

Driver, E.C., Sillers, L., Coate, T.M., Rose, M.F., Kelley, M.W., 2013. The Atoh1-lineage gives rise to hair cells and supporting cells within the mammalian cochlea. Dev Biol 376, 86-98.

Foltz, D.R., Santiago, M.C., Berechid, B.E., Nye, J.S., 2002. Glycogen synthase kinase-3beta modulates notch signaling and stability. Curr Biol 12, 1006-1011.

Goodyear, R., Richardson, G., 1997. Pattern formation in the basilar papilla: evidence for cell rearrangement. J Neurosci 17, 6289-6301.

Head, J.R., Gacioch, L., Pennisi, M., Meyers, J.R., 2013. Activation of canonical Wnt/beta-catenin signaling stimulates proliferation in neuromasts in the zebrafish posterior lateral line. Dev Dyn 242, 832-846.

Jacques, B.E., Montgomery, W.H.t., Uribe, P.M., Yatteau, A., Asuncion, J.D., Resendiz, G., Matsui, J.I., Dabdoub, A., 2014. The role of Wnt/beta-catenin signaling in proliferation and regeneration of the developing basilar papilla and lateral line. Developmental neurobiology 74, 438-456.

Jacques, B.E., Puligilla, C., Weichert, R.M., Ferrer-Vaquer, A., Hadjantonakis, A.K., Kelley, M.W., Dabdoub, A., 2012. A dual function for canonical Wnt/beta-catenin signaling in the developing mammalian cochlea. Development 139, 4395-4404.

Jiang, L., Romero-Carvajal, A., Haug, J.S., Seidel, C.W., Piotrowski, T., 2014. Gene-expression analysis of hair cell regeneration in the zebrafish lateral line. Proc Natl Acad Sci U S A 111, E1383-1392.

Kiernan, A.E., Cordes, R., Kopan, R., Gossler, A., Gridley, T., 2005a. The Notch ligands DLL1 and JAG2 act synergistically to regulate hair cell development in the mammalian inner ear. Development 132, 4353-4362.

Kiernan, A.E., Pelling, A.L., Leung, K.K., Tang, A.S., Bell, D.M., Tease, C., Lovell-Badge, R., Steel, K.P., Cheah, K.S., 2005b. Sox2 is required for sensory organ development in the mammalian inner ear. Nature 434, 1031-1035.

Kiernan, A.E., Xu, J., Gridley, T., 2006. The Notch Ligand JAG1 Is Required for Sensory Progenitor Development in the Mammalian Inner Ear. PLoS Genet 2, e4.

Kuo, B.R., Baldwin, E.M., Layman, W.S., Taketo, M.M., Zuo, J., 2015. In Vivo Cochlear Hair Cell Generation and Survival by Coactivation of beta-Catenin and Atoh1. J Neurosci 35, 10786-10798.

Lanford, P.J., Lan, Y., Jiang, R., Lindsell, C., Weinmaster, G., Gridley, T., Kelley, M.W., 1999. Notch signalling pathway mediates hair cell development in mammalian cochlea. Nat Genet 21, 289-292.

McGill, T.J., Schuknecht, H.F., 1976. Human cochlear changes in noise induced hearing loss. Laryngoscope 86, 1293-1302.

Monzack, E.L., Cunningham, L.L., 2013. Lead roles for supporting actors: critical functions of inner ear supporting cells. Hear Res 303, 20-29.

Neves, J., Kamaid, A., Alsina, B., Giraldez, F., 2007. Differential expression of Sox2 and Sox3 in neuronal and sensory progenitors of the developing inner ear of the chick. J Comp Neurol 503, 487-500.

Pan, W., Jin, Y., Chen, J., Rottier, R.J., Steel, K.P., Kiernan, A.E., 2013. Ectopic expression of activated notch or SOX2 reveals similar and unique roles in the development of the sensory cell progenitors in the mammalian inner ear. J Neurosci 33, 16146-16157.

Prakash, A., Weninger, J., Singh, N., Raman, S., Kruse, K., Rao, M., Ladher, R.K., 2023. Junctional Force Patterning drives both Positional and Orientational Order in Auditory Epithelia.

Ryals, B.M., Rubel, E.W., 1988. Hair cell regeneration after acoustic trauma in adult Coturnix quail. Science 240, 1774-1776.

Shang, J., Cafaro, J., Nehmer, R., Stone, J., 2010. Supporting cell division is not required for regeneration of auditory hair cells after ototoxic injury in vitro. J Assoc Res Otolaryngol 11, 203-222.

Shi, F., Hu, L., Jacques, B.E., Mulvaney, J.F., Dabdoub, A., Edge, A.S., 2014. beta-Catenin is required for hair-cell differentiation in the cochlea. J Neurosci 34, 6470-6479.

Singh, N., Prakash, A., Chakravarthy, S.R., Kaushik, R., Ladher, R.K., 2022. In Ovo and Ex Ovo Methods to Study Avian Inner Ear Development. Journal of visualized experiments : JoVE.

Steiner, A.B., Kim, T., Cabot, V., Hudspeth, A.J., 2014. Dynamic gene expression by putative hair-cell progenitors during regeneration in the zebrafish lateral line. Proc Natl Acad Sci U S A 111, E1393-1401.

Stone, J.S., Cotanche, D.A., 2007. Hair cell regeneration in the avian auditory epithelium. Int J Dev Biol 51, 633-647.

Stone, J.S., Shang, J.L., Tomarev, S., 2003. Expression of Prox1 defines regions of the avian otocyst that give rise to sensory or neural cells. J Comp Neurol 460, 487-502.

Zak, M., Daudet, N., 2021. A gradient of Wnt activity positions the neurosensory domains of the inner ear. eLife 10.

Zak, M., Klis, S.F., Grolman, W., 2015. The Wnt and Notch signalling pathways in the developing cochlea: Formation of hair cells and induction of regenerative potential. Int J Dev Neurosci 47, 247-258.

List of Publications

1. **Singh, N.**, Prakash, A., Chakravarthy, S.R., Kaushik, R., Ladher, R.K., 2022. In Ovo and Ex Ovo Methods to Study Avian Inner Ear Development. Journal of visualized experiments: JoVE.

2. Prakash, A., Weninger, J., **Singh, N.**, Raman, S., Kruse, K., Rao, M., Ladher, R.K., 2023. Junctional Force Patterning drives both Positional and Orientational Order in Auditory Epithelia. http://dx.doi.org/10.21203/rs.3.rs-2508957/v1.

3. **Singh, N.**, Kaushik, R., Prakash, A., Saini, S., Garg, S., Adhikary, A., Ladher, R.K., 2024. 'Mosaic Atoh1 Deletion in the Chick Auditory Epithelium Reveals a Homeostatic Mechanism to Restore Hair Cell Number. http://dx.doi.org/10.2139/ssrn.4814834.

Chapter 1: Introduction

1.1 Hearing Disorders

Auditory dysfunction, a prevalent neurosensory disorder, significantly impacts global health, affecting 1 in every 500 newborns and over 360 million individuals worldwide. The complexity of this issue is exacerbated by environmental and lifestyle factors, leading to an increasing number of cases beyond congenital hearing loss. This challenge is notably pronounced among the elderly, with over one-third of individuals older than 60 years experiencing significant hearing loss[1]. Moreover, hearing loss spans age demographics, with over 1 billion teenagers and young adults estimated to be at risk[2].

The widespread occurrence of auditory dysfunction primarily arises from sensorineural hearing disorders intricately linked to the loss of sensory hair cells (HCs) within the organ of Corti. In contrast to conductive hearing loss, which obstructs sound waves from reaching the inner ear, sensorineural hearing loss (SNHL) involves challenges in processing sound signals by the ear. SNHL, often irreversible, results from various factors, including the unsafe use of audio devices, prolonged exposure to noisy environments (Noise-induced hearing loss - NIHL), iatrogenic factors like Aminoglycoside ototoxic substances (Drug-induced hearing loss), the natural aging process (Age-related hearing loss - ARHL), and genetic disorders[3,4].

Sensorineural hearing loss (SNHL) significantly impacts an individual's ability to hear faint sounds, understand speech in noisy environments, and discern high-pitched tones. Early identification and intervention are crucial, as sensorineural hearing loss often presents irreversible challenges. Recognizing and addressing hearing loss in its early stages offer numerous benefits, enhancing the overall quality of life for those affected by auditory impairment.

1.2 Anatomy of Inner Ear

A true inner ear, as found in vertebrates, is not present in invertebrates. However, some invertebrate groups have evolved specialized organs that serve similar functions related to hearing and balance. In the evolutionary journey of organisms, particularly in more primitive life forms, the rudimentary hearing apparatus is limited to the presence of vestibular organs, which primarily function as balancing organs. These vestibular structures play a crucial role

in sensing orientation and maintaining balance, representing one of the fundamental sensory adaptations that organisms acquire early in their development. The significance of this adaptation lies in its direct response to the gravitational force, a constant and fundamental aspect of the environment. As organisms navigate their surroundings, the ability to perceive their orientation and balance becomes foundational for survival and effective interaction with their surroundings. This primitive yet essential sensory capacity forms the foundation upon which more complex auditory systems have evolved over time, showcasing the intricate relationship between basic physiological adaptations and the environmental challenges faced by organisms throughout evolutionary history.

1.2.1 Avian Auditory System

The avian ear constitutes a sophisticated sensory system with three main components: an external membrane also known as tympanic membrane, a middle ear, and an inner ear. Unlike mammals, birds lack an external structure resembling the outer ear flap, with the tympanic membrane serving as the outermost covering of the middle ear. This anatomical feature functions to gather sound, setting the stage for the intricate auditory mechanisms of avian species. The middle ear in birds acoustically couples air-borne sound to the fluids of the inner ear through impedance matching. Similar to most vertebrates, the avian inner ear comprises three semicircular canals to determine angular acceleration of the head and three otolith organs for detecting head motion relative to gravity (Figure 1.1 A, B). Notably, birds possess a cochlear duct housing the basilar papilla (BP), a crucial structure for hearing. Sensory hair cells (HCs) on the basilar papilla transduce mechanical energy into signals compatible with the nervous system, responding to sound stimuli with precision.

The avian ear features up to seven distinct sensory epithelia, including three canal cristae (anterior, AC, posterior, PC, and lateral, LC), the utricle macula, saccule macula, lagena, and the basilar papilla. Situated within the tubular cochlear duct, there resides a basilar papilla equivalent to the organ of Corti in other vertebrates; it is a cornerstone in the avian auditory process. Basilar papilla has two anatomical axes: proximal-distal and neural-abneural (Figure 1.1 C). It is harbouring sensory HCs which are surrounded by supporting cells (SCs) in a distinctive “salt and pepper” pattern (Figure 1.1 E, F). In a cross section of the BP (Figure 1.1 D), the nuclei of HCs have a larger, round shape, arranged in a single apical row. The nuclei of SC are located on the basal side of the epithelium, immediately adjacent to the basal lamina, resembling “pearls on the string”, although, unlike HC, SC spans the entirety of the epithelium.

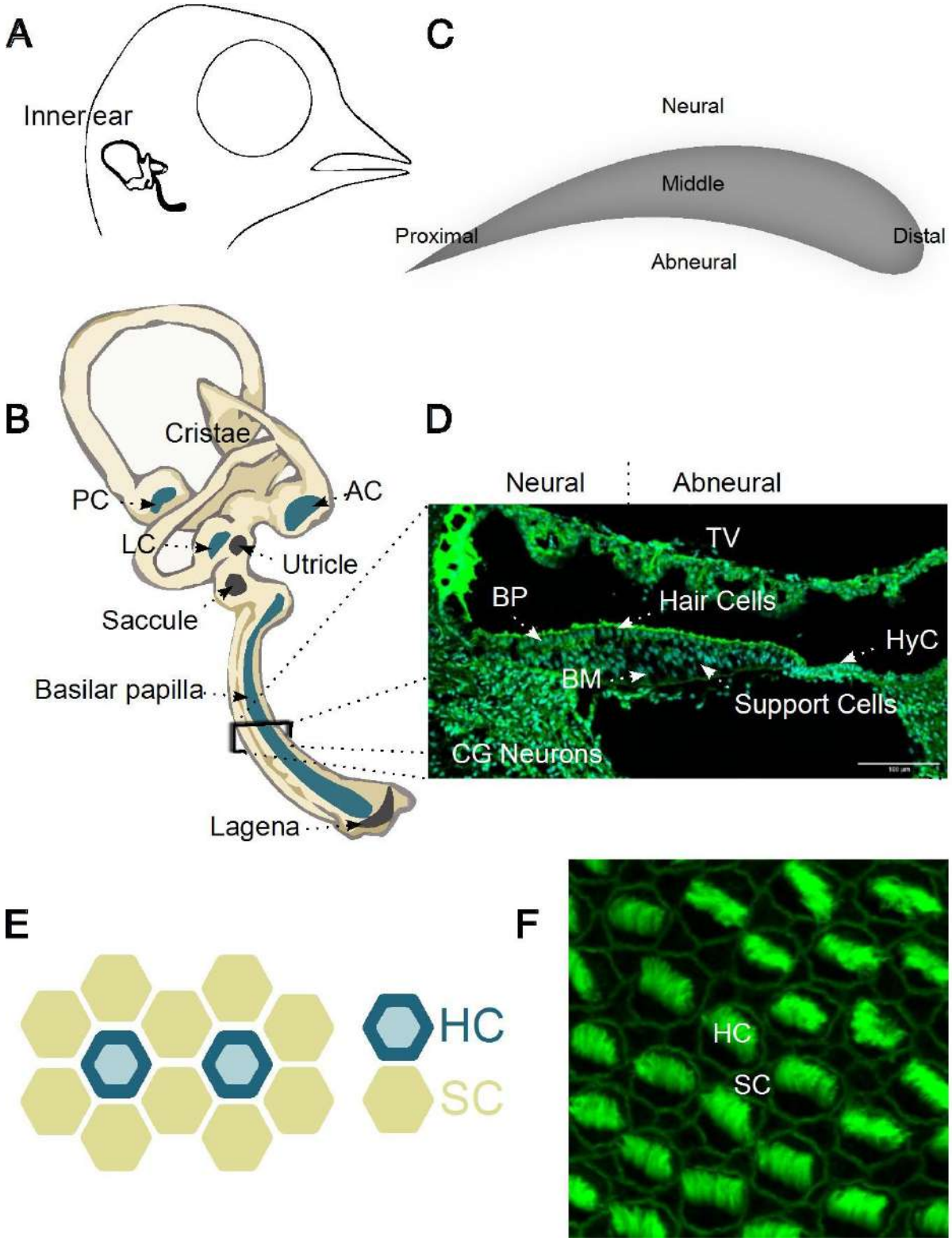

Figure 1.1 Avian Auditory System. (A) Drawing of a chicken head indicating the position of the inner ear. (B) Diagram of the inner ear highlighting each of the sensory organs, the anterior cristae (AC), posterior cristae (PC), lateral cristae (LC) and basilar papilla (BP) are blue. The macula (utricle, saccule, and lagena) are grey. (C) Schematic dividing the BP into three regions: distal, middle, and proximal. (D) Confocal images of horizontal cross sections of cochlear duct are shown with F-actin stained with phalloidin-488 and nuclear staining with Dapi. The vertical dotted mark indicates the dividing line between neural and abneural regions of the BP. Abbreviations: TV, tegmentum vasculosum; BP, basilar papilla; HyC, hyaline cells; BM, basilar membrane. With 100µm scale bar. (E) Diagram showing the apical surface of the BP, where hair cells (HCs) and supporting cells (SCs) are arranged in a regular pattern, with each hair cell being surrounded and isolated by supporting cells. (F) Confocal image corresponding to the diagram with F-actin stained with phalloidin-488.

HCs are highly specialized mechanosensory cells, converting mechanical energy into electrical signals through synapses with the axons of the VIIIth cranial nerve, which encode and transmit the signal to and from the hindbrain nuclei. Hair cells are so-called, due to the hair bundle on its apical surface. This consists of actin-based protrusion known as stereocilia and tubulin-based cilia called kinocilium. In response to a sound stimulus, bending of the hair bundle triggers a cascade of events within the cells. Ultimately, this process culminates in the release of neurotransmitters, stimulating the auditory nerve. The basilar papilla of birds comprises two types of hair cells (HCs), tall hair cells (THCs) and short hair cells (SHCs). THCs are characterized by their tall columnar shape with an elongated hexagonal apical surface, primarily situated on the superior/neural side. In contrast, SHCs are shorter and thicker with a wider surface area, and they predominate on the inferior/abneural side. THCs are mainly located in the distal region of the basilar papilla, whereas SHCs dominate the proximal region and are present on the free basilar membrane. The proportion of SHCs to THCs increases towards the high-frequency proximal end of the BP, which would be consistent with their increased contribution at high frequencies[5]. This intricate arrangement and specialization contribute to the remarkable auditory capabilities of avian species, exemplified by the unique features of the basilar papilla.

1.2.2 Comparative Anatomy of Inner Ear in Vertebrates

While the vestibular part of the inner ear is comparable, a dedicated auditory sensory organ is an evolutionary innovation in vertebrates have undergone significant modifications along the phylogenetic tree[6]. The cochlea is absent in fish and amphibians, with its functions replaced by alternative auditory organs like the saccule and lagena[7,8]. The saccule serves a vestibular function in birds and mammals, while the lagena's functions in birds are still being understood. In placental and marsupial mammals, the lagena is absent. The positioning of the auditory organ within the inner ear has evolved, initially situating itself amidst vestibular organs like the lagena, which existed before the elongation of the auditory sensory tissue to form a tube.

The auditory papilla, a vital anatomical structure found in birds, amphibians, and reptiles, plays a crucial role in transducing sound stimuli into neural signals. The basilar papilla found in birds is shorter and structurally distinct from its mammalian counterpart, potentially accounting for the narrower range of frequencies detected by birds compared to mammals[9,10]. Despite these variations, all organisms share similar hearing organs and similar hair cell types based on the fundamental principle of perceiving sound. The basilar papilla

consists of enclosed structures with sensory epithelia where mechanosensory cells called HCs respond to vibrations. Supporting cells accompany these HCs, akin to glial cells to neurons. While the structures housing these HCs differ in shape and size, they give rise to different frequency hearing and contribute to maintaining hearing sensitivity. Anatomical similarities, as well as distinct differences between the avian basilar papilla and the mammalian organ of Corti, have led to the proposition that these organs and their different hair cell types are analogous[11]. The basilar papilla contains two types of hair cells, tall (THCs) and short (SHCs), resembling the inner and outer hair cells in mammals[9]. Developmental considerations and comparative anatomy, however, support the notion that the basilar papilla and the mammalian organ of Corti arose from a common ancestral structure and represent homologous organs[12].

The auditory system is a specialized organ that demonstrates remarkable diversity across species in both structure and function, highlighting the adaptability of auditory mechanisms in various organisms. Delving into the intricacies of the basilar papilla unveils a captivating narrative of evolutionary adaptations, sensory perception, and the fascinating ways in which various organisms have developed unique auditory mechanisms to navigate and interact with their environments.

1.3 Developmental Program for Inner Ear

1.3.1 From Otic Placode to Bony Labyrinth

The initial development of the inner ear is highly conserved across vertebrates. The sensory and supporting cells, as well as spiral ganglion neurons, originate from the embryonic otic placode, an ectodermal structure adjacent to the hindbrain. While cells for the spiral ligament, otic capsule, and modiolus come from surrounding mesenchymal cells, melanocyte-like cells in the stria vascularis and Schwann cells have a neural crest origin[13–15]. Before the otic placode becomes visible, the ectodermal cells that will form it (Figure 1.2 A), undergoes a genetic program to express pre placodal transcription factors as the Dlx family, Sox9a and Foxi1[16–19]. Following this early induction, the otic placode transforms into the otic cup, eventually closing to form a fluid-filled sac called the otocyst (Figure 1.2 B, C). This transient structure plays a crucial role, containing the necessary information for differentiating into most adult inner ear cell types[20,21].

The dorsal region of the otocyst gives rise to vestibular structures for balance, while the ventral portion forms the auditory part. Within the otocyst, signaling molecules like Notch, Bmp4, Jag1, and Sox2 orchestrate the development of distinct regions called prosensory domains[22–27] (Figure 1.2 D). Notch signaling participates in the earliest induction stages of the prosensory domain. Members of the canonical Notch pathway Notch1, Lunatic fringe (Lfng), Delta-like1 (Dll1), and Hes5 are differentially expressed in the otic placode[17,26,28–30]. The non-prosensory region expresses Hes1 and the Notch ligand Jagged1 (Jag1), but not Lfng and Dll1.

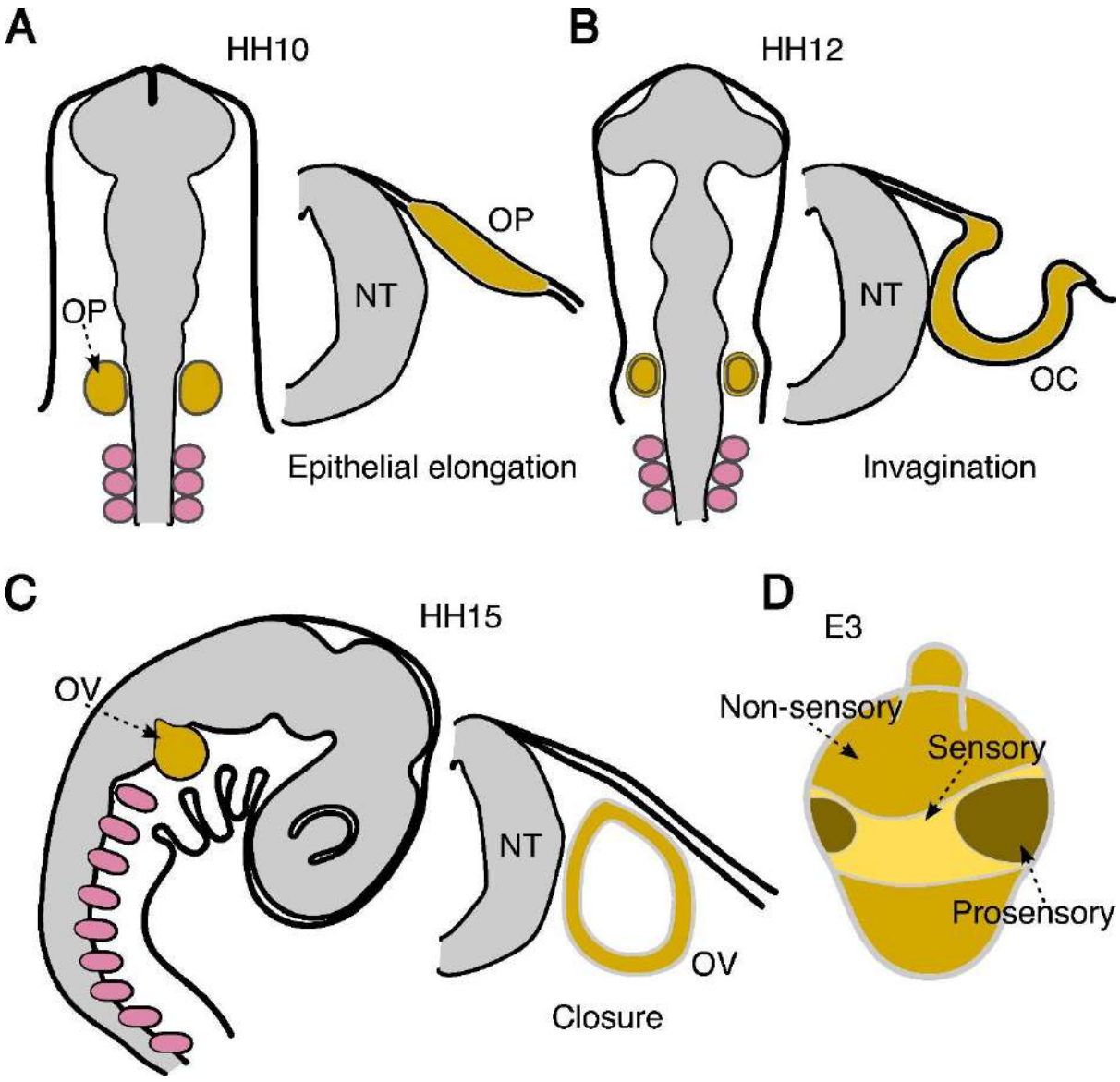

Figure 1.2 Early Development of the Inner ear in Chick. (A) In chick, the otic placode (yellow) became morphologically visible as a thickening of the epithelium by 10 somites (HH10). (B) The otic placode begins to invaginate around the 16 somites (HH12) through a mechanism of apical constriction. (C) The otic cup

eventually pinches off from the adjacent ectoderm, forming the otic vesicle beneath the ectoderm (HH15). (D) Early regionalization and cell fate specification of sensory patches in the otic vesicles.

SOX2, marking both prosensory and proneural domains, underscores the SOX family's role in preserving progenitor self-renewal and pluripotency[31,32]. BMP4 is a member of the TGFβ superfamily of secreted signaling molecules that has been proposed to play a key role in the specification of prosensory patches[26,33,34]. FGF signaling plays a key role during vertebrate inner ear development and participates in the early induction of the otocyst[35,36], in prosensory specification[21,37,38], otic neurogenesis and neuritogenesis[39]. The otic vesicle undergoes morphogenetic movements, generating the complex three-dimensional membranous labyrinth, while surrounding mesenchymal cells form a cartilaginous capsule that eventually becomes the bony labyrinth[13].

1.3.2 Development of Sensory Epithelium

The vast majority of cells that reside within the membranous labyrinth originate from multipotent progenitor cells in the otic epithelia, giving rise to three lineages: proneural cells, comprising auditory and vestibular neurons; prosensory cells, including hair and supporting cells; and nonsensory cells. Neural specification onsets with the expression of proneural genes, being Neurog1 required for the specification of the neuronal fate. HCs and SCs arise following the specification of the prosensory domain[40]. In early development, there appears to be a default program where the first cells specified become hair cells, which then inhibit neighboring cells from adopting the same fate through lateral inhibition. Atoh1, a basic helix–loop–helix (bHLH) transcription factor, is crucial for hair cell production and development[41–43]. Studies on the loss and gain of Atoh1 function have demonstrated its necessity and sufficiency for inducing hair cell formation in both sensory and nonsensory cells[41,44–47]. After hair cells differentiate, the adjacent cells become supporting cells through a mechanism known as lateral inhibition. Hair cell and support cell differentiation are both impacted by the Notch pathway, which was previously involved in prosensory specification. Cells expressing Atoh1 start to produce the Notch ligands Jagged2 (Jag2) and Dll1[25,48,49]. Notch1 is activated as a result, and Notch target genes are then expressed such as Hes and Hey family gene for supporting cell fate[42,50–55].

1.4 Cochlear Cell Types

1.4.1 Sensory Hair Cells

Mechanosensory cells, commonly known as hair cells, trace their origins to chordate ancestors and potentially other invertebrates, making them one of the oldest cell types[56]. Beyond the inner ear, these cells are also found in fish and amphibians' lateral-line organs, offering insights into various stimuli aspects. In the chicken basilar papilla sensory epithelium, the entire set of hair cells is produced during embryonic development, entering a quiescent state post-embryogenesis[57,58].

Hair Cell Architecture and Function

The hair cell, a highly specialized sensory cell, features a unique apical structure known as the hair bundle, composed of stereocilia and a longer projection called the kinocilium. The kinocilium, acting as a specialized primary cilium made of microtubules, is crucial for the hair cell's development and polarization, while the basal body at its base aids in stereocilia orientation. The stereocilia, composed of actin, form a staircase-like arrangement and are linked together by fine thread-like structures known as tip links (Figure 1.3 A). Beneath them, a dense layer of actin filaments forms the cuticular plate beneath them, anchoring the stereocilia[59,60]. These structures are essential for mechanotransduction, where higher stereocilia bend under sound wave influence, mechanically opening mechanoelectrical transducer (MET) channels on lower stereocilia membranes. This process converts the mechanical impulse into an electrical impulse or action potential, facilitated by the entry of K+ and Ca2+ ions through MET channels. While sensory hair cells maintain a similar structure across vertebrates, variations exist in their specifics, suggesting differential responses to stimuli both among taxa and within different end organs of the ear in the same species.

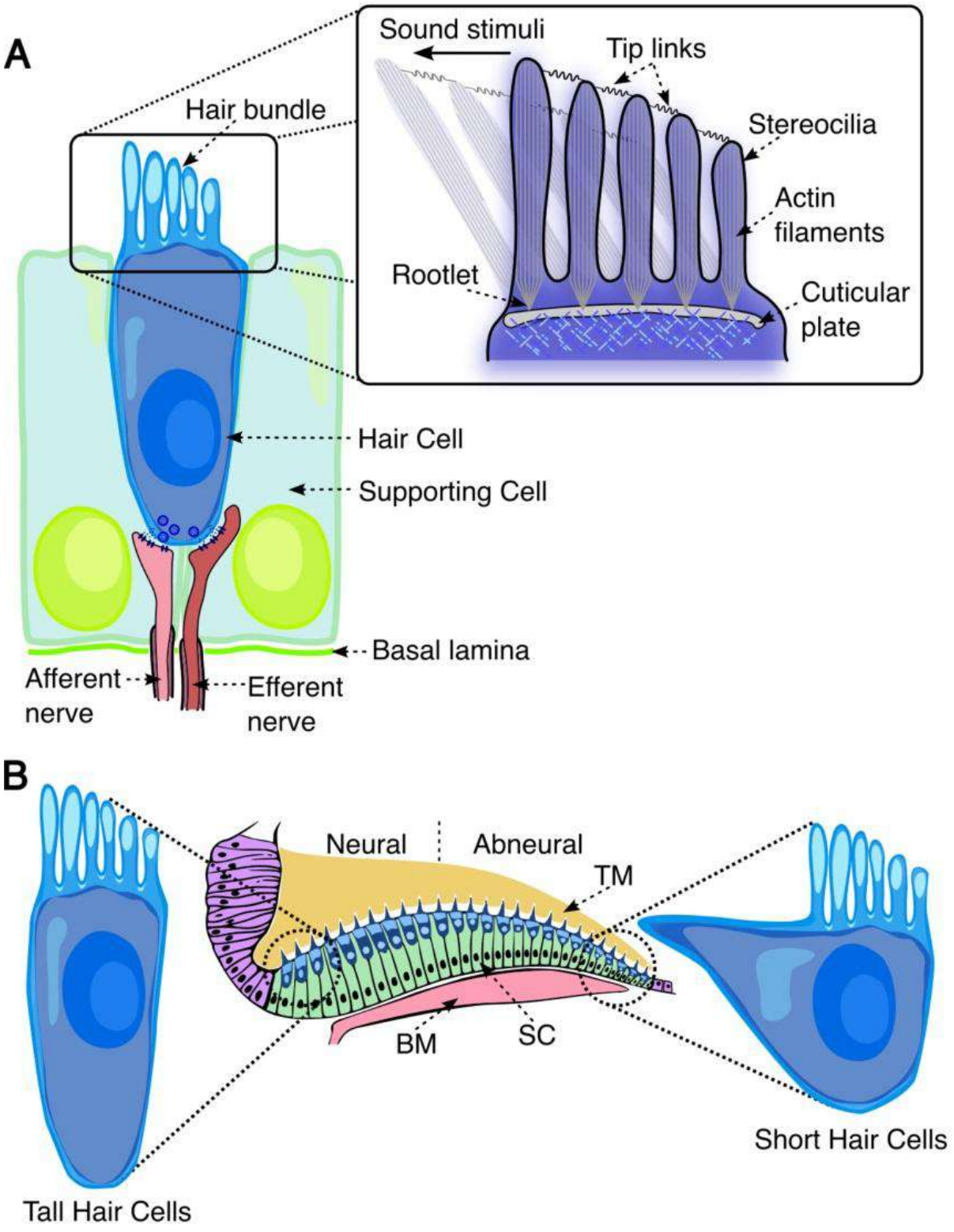

Figure 1.3 Hair Cell Morphology. (A) Hair bundle mechanics, the hair bundles of cochlear hair cells contain 3–4 rows of stereocilia organized like a staircase. Each stereocilium is filled with a dense core of actin filaments that tapers into the cuticular plate at the hair cell apical surface. In response to sound stimuli, the stereocilia deflect elastically around the rootlet. The resulting tension along connected stereocilia opens transducer channels located at the stereocilia tips enabling mechanical sound stimuli to be converted into electrical signals. (B) The chick basilar papilla contains two types of HCs, tall hair cells (THCs), and short hair cells (SHCs).

In birds, cochlear hair cells are classified into two types: tall and short (Figure 1.3 B). Tall hair cells are positioned on the fibro-cartilaginous plate above the auditory ganglion, known as the superior/neural side of the basilar papilla. Whereas, short hair cells are found in the epithelium above the basilar membrane, extending to the inferior fibro-cartilaginous plate, or the inferior/abneural side. These two types of hair cells differ in cytomorphology, the number of stereocilia in their hair bundles, and their innervation patterns. Tall hair cells receive afferent and small bouton efferent fibres, while short hair cells primarily receive efferent innervation characterized by distinct presynaptic cups.

1.4.2 Glia of Inner ear: Support Cells

In all inner ear sensory epithelia, hair cells and supporting cells form a crucial mosaic essential for the proper development of hearing. Some markers selectively expressed in supporting cells, such as Prox1, PLP, GLAST, GFAP, Tak1, Aquaporin4, and S100α, are also found in certain glial cells[61–67]. This underscores the shared functions of supporting cells and glia within their respective organs.

Support Cell Structure and Function

The development, function, and upkeep of inner ear sensory epithelia rely significantly on supporting cells, which reside among hair cells. Unlike hair cells, which only connect to the lumenal surface of the epithelium, supporting cells extend across the entire depth of the epithelium, from the basal lamina to the lumen. These cells are interconnected with each other and with hair cells through tight and adherens junctions, and they directly communicate with neighboring supporting cells via gap junctions. In the mammalian organ of Corti, which exhibits the highest level of supporting cell diversity, there are five distinct types of supporting cells arranged in rows along its length. These include Hensen’s cells, Deiters’ cells, pillar cells, inner phalangeal cells, and border cells, each with unique morphologies. However, all the supporting cells in the avian cochlear system are very similar morphologically, pseudostratified.

Supporting cells play a multifaceted role in the sensory epithelia. They possess sturdy cytoskeletons that uphold the structural integrity of sensory organs during both sound exposure and head movements. Additionally, supporting cells contribute to the maintenance of an environment within the epithelium conducive to the function of hair cells. They aid in various tasks such as recycling K+ ions crucial for sustaining the receptor potential, synthesizing components of essential membranes like the tectorial membrane in the organ of

Corti, and managing the cupula in the cristae ampullaris. In instances of trauma or toxicity, supporting cells can expel damaged hair cells, engulf debris, and potentially facilitate the generation of new hair cells.

1.5 It's All About Atoh1

The discovery of the atonal gene in Drosophila during early 1990s, revealed its role as a crucial proneural transcription factor for the development of mechanoreceptive neurons and photoreceptor cells[68,69]. During Drosophila development, a group of proneural genes known as the Aschaete-Scute complex (ASC), which encode basic-helix-loop-helix (bHLH) transcription factors, was identified as necessary for nervous system development. Atoh1, also known as atonal (ato) in Drosophila, was identified as a novel ASC gene due to its structural similarities with bHLH proteins.

1.5.1 Atoh1 Gene Structure

Atoh1 is an evolutionarily conserved pro-neural basic helix–loop–helix (bHLH) transcription factor. Atoh1, previously referred to as Hath1 in humans, Math1 in mice, and Cath1 in chickens, demonstrates significant sequence conservation between human and mouse genes, with 85.31% homology in the coding region. However, the sequence conservation between mouse and chick is lower at 57.11%. Notably, the basic helix–loop–helix (bHLH) domain of Atoh1 gene is highly conserved (≥80%) among species such as Homo sapiens, Mus musculus, Gallus gallus, Danio rerio and Xenopus laevis (Figure 1.4 B). The bHLH domain comprises a DNA binding basic region and a protein-binding region with two α-helices separated by a variable loop region, enabling heterodimeric interactions with other class I bHLH family members like E47[70]. Additionally, the 3' region of the Atoh1 coding sequence near the stop codon, essential for post-translational modification, is well conserved across these species.

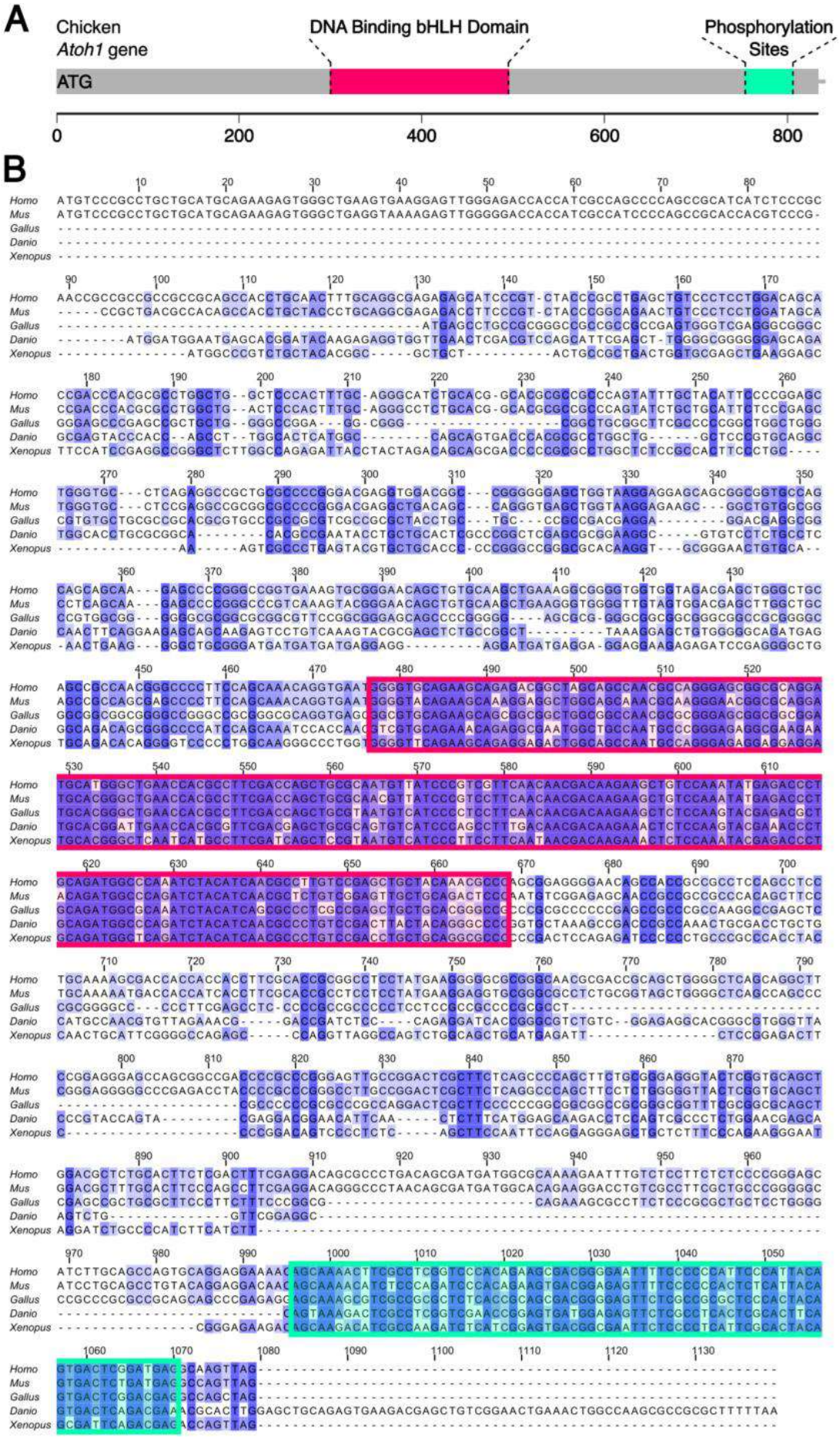
A
Chicken
Atoh1 gene
DNA Binding bHLH Domain
Phosphorylation Sites
ATG
0
200
400
600
800
B
Homo
Mus
Gallus
Danio
Xenopus

Figure 1.4 Conservation of the Atoh1 Gene Across Species. (A) Chicken Atoh1 gene structure. (B) A cross-species comparison of the Atoh1 gene reveals that the bHLH domain (indicated by a pink box) is highly conserved among Homo sapiens, Mus musculus, Gallus gallus, Danio rerio, and Xenopus laevis. Additionally, the 3' coding region, which serves as a regulatory domain for post-translational modification (indicated by a green box), is also conserved across these five species.

In mouse, the Atoh1 open reading frame consists of a 1.053-kb intronless coding region located on chromosome 6, yielding a 351-amino acid protein with a molecular weight of 37 kDa. Two enhancer sites, enhancer A and enhancer B, are located 3.4 kb downstream of the Atoh1 coding region. Enhancer A is characterized by an E-box motif, while enhancer B contains a Hairy preferred sequence along with E-box and N box motifs[71,72]. The interaction between Atoh1 and the E-box site within enhancer B establishes an autoregulatory feedback loop that controls Atoh1 expression[72]. The presence of multiple protein-binding sites within enhancers A and B indicates a complex regulation of Atoh1 expression. Atoh1 enhancers A and B exhibit high evolutionary conservation between mouse and human, with sequence identities of 90.73% and 88.79%, respectively. Comparative analysis of the avian and mammalian Atoh1 gene locus shows that the sequences of the known mammalian 3′ enhancers A and B are also conserved in avian species[73]. Aligning the human, mouse, and zebra finch sequences with the chicken Atoh1 3’ sequence revealed two highly conserved regions in these four species, corresponding to enhancers A and B. The sequence homology for enhancers A and B across these species was found to be 81% and 66%, respectively[73].

Atoh1 is an intrinsically disordered transcription factor, featuring partially unstructured regions that provide flexibility in interacting with various molecular targets. This versatility enables Atoh1 to bind to multiple cellular partners, offering precise control over binding affinity. With a high proline content (35/351 residues), it suggests a role in protein-binding function, while about 33% of the carboxy terminus (aa 325 – 351) comprises serines, indicating the importance of phosphorylation in protein function and regulation. Specifically, serines at sites 328 and 331 are predicted targets for protein kinase C[74]. Notably, the C terminus region harbors several conserved phosphorylation sites, and both the bHLH domain and the proline-rich N terminus are essential for its transcriptional activity.

1.5.2 Atoh1 is Necessary & Sufficient for HCs Differentiation

Atoh1 expression initiates the terminal differentiation of hair cells in the prosensory epithelium of the cochlea, starting at embryonic day 14 (E14) in mouse[41,46] (Figure 1.5 A). Various methods, including in-situ hybridization (ISH), immunohistochemistry, reporter-gene

studies, and qPCR, have been employed to map the spatial and temporal expression of Atoh1 in the mouse inner ear. Atoh1 expression is transient, peaking at the onset of hair cell development and declining as hair cells mature[41]. Inducing ectopic Atoh1 expression in the cochlear sensory epithelium is sufficient to drive a cell towards adopting a hair cell fate[44–46] (Figure 1.5 H-I). Conversely, the cochlea of homozygous Atoh1 mutant mice exhibits a deficiency in differentiated hair cells[41] (Figure 1.5 B-G). Besides the inner ear's developing sensory epithelium, Atoh1 is expressed in the embryonic vertebrate nervous system, particularly in the developing spinal cord and hindbrain.

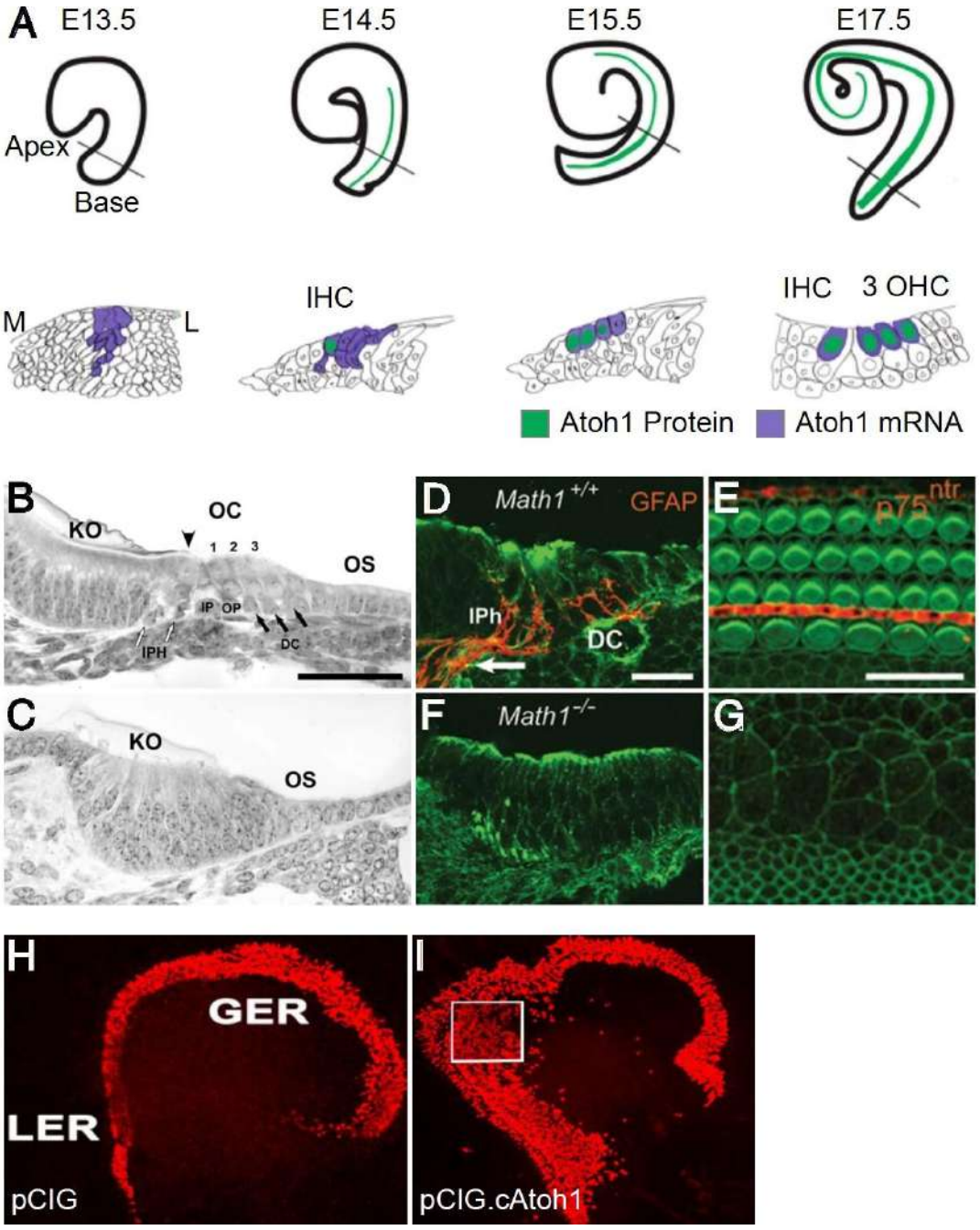

Figure 1.5 Atoh1 is an Essential Transcription Factor in Hair Cell Development. (A) This schematic diagram depicts the progressive expression of Atoh1 (purple: mRNA, blue: protein) in developing mouse cochlea cross-sections (mid-base). At E14.5, Atoh1 mRNA spans the prosensory epithelium, while protein is restricted to a single row of inner hair cells (IHCs) at the base-to-mid region. By E17.5, protein expression expands to include IHCs and three outer hair cells (OHCs), while mRNA is now limited to hair cells (IHCs and OHCs). The solid line indicates the section level. The basal turn of the cochlea in wild-type (B) and Math1-deficient (C) mice is compared in these images. (B) shows a wild-type cochlea with three distinct regions: Kölliker's organ (KO), the organ of Corti (OC), and the outer sulcus (OS). Within the OC, hair cells are visible – inner hair cells (arrowhead) and three rows of outer hair cells (numbered 1-3). Four supporting cell types are also present: inner phalangeal cells (IPH, white arrows), inner pillar cells (IP), outer pillar cells (OP), and Deiter's cells (DC, black arrows). Math1-deficient cochlea (C) lacks the organ of Corti entirely. KO and OS appear normal, but directly adjacent, indicating the absence of supporting cells. Scale bar, 30 μm. (D) and (F) shows cross-sections of the OC at P0 stained with GFAP (glial fibrillary acidic protein). In the wild-type cochlea (D), GFAP expression is visible in DC, IPh, and auditory nerve fibers (arrows). However, the Math1-deficient cochlea (F) shows no GFAP signal. (E, G) Apical view of the OC at P0, stained for p75ntr (p75 neurotrophin receptor). In the wild-type cochlea (E), p75ntr-positive pillar cells separate the IHC and OHC. However, the Math1-deficient cochlea (G) lacks p75ntr expression. Scale bar, 20 μm. (H) and (I) show the effect of overexpressing cAtoh1 in mouse cochlear tissue. Empty plasmid (H) doesn't induce any formation of ectopic hair cells in the greater epithelial ridge (GER) or lesser epithelial ridge (LER). Overexpression of cAtoh1 using pCIG.cAtoh1 (I) leads to robust expression of the hair cell marker Myosin7a (red), indicating the formation of ectopic hair cells. Scale bar, 100 μm.

1.5.3 Atoh1 a Master Regulator for Mechanosensory Cell-Type

Mechanosensory cells, known as "hair" cells, are ancient cell types found in both vertebrates and invertebrates, suggesting a shared evolutionary origin. While vertebrate hair cells are present in the inner ear and lateral-line organs, providing various sensory information, invertebrates also possess similar structures. However, their arrangement and composition may differ. For instance, vertebrate hair cells typically consist of actin-based stereocilia and a single tubulin-based cilium, whereas invertebrate hair cells may have different configurations, such as multiple true cilia or short microcilia. Despite these variations in structure and composition, the core principle remains the same – hair cells in both vertebrates and invertebrates act as specialized vibration sensors. This remarkable convergence highlights the selective pressure that favoured the development of these sensitive mechanoreceptors throughout the animal kingdom. It underscores the elegance of natural selection to identify a design so effective that it has been independently reinvented across countless evolutionary lineages.

Atonal genes evolved with multicellular organisms[75] and represent a rare instance of protein-coding genes exhibiting extensive structural and functional conservation. Orthologues of Drosophila atonal and mouse Atoh1, when interchanged, demonstrate compensatory functions across distant organisms[76]. The remarkable conservation of mechanosensory function is evident, with Drosophila atonal fully rescuing Atoh1 null mutant mouse and mouse Atoh1 (math1) partially rescuing atonal mutant flies. The existence of conservation at

the molecular genetic level, largely based on the observation that the basic helix-loop-helix (bHLH) transcription factor Atonal is needed for both the formation of chordotonal organs in Drosophila and the formation of hair cells in vertebrates (math1), has been the final basis for the argument of homology between invertebrate sensory neurons and vertebrate hair cells. Furthermore, vertebrate Atoh1 genes are expressed in numerous mechanosensitive progenitor cells and are crucial for the development of hair cells are not only in the inner ear, but also in the lateral-line organs of fish and amphibians[77], as well as touch-sensitive Merkel cells in the skin[78,79].

1.6 Hair Cells Regeneration

1.6.1 Regeneration in Sensory Receptor Cells

Our senses, including vision, smell, taste, hearing, and balance, rely on specialized receptor cells housed within epithelial organs. These receptors play a crucial role in capturing environmental stimuli. However, their very location, often exposed to the external environment, makes them susceptible to damage from the very stimuli they detect. For example, olfactory receptor cells have a short lifespan, lasting only a few months on average. Similarly, continuous loud noise can damage auditory hair cells, and prolonged exposure to high light intensity can cause photoreceptor loss in the retina. Furthermore, sensory receptor cells exhibit distinct protein profiles absent in other tissues. Mutations in the genes encoding these proteins, though not inherently lethal due to their limited expression, can trigger specific types of sensory degeneration. Such mutations can have profound impacts in humans, as seen in Usher syndrome. This condition, characterized by mutations affecting both retinal photoreceptors and cochlear hair cells, culminates in profound deafness and blindness.

Unlike most neurons in the vertebrate nervous system, which are generated during development, specific sensory organs have the ability to create new receptor cells throughout life. This process, known as ongoing genesis, is crucial for maintaining sensory function. Olfactory epithelium demonstrates this phenomenon in all vertebrates[80]. Here, a high rate of new olfactory receptor cell production balances their short lifespan of just a few months. This is because olfactory neurons, being the only neuronal cell type in contact with the external environment, are more susceptible to damage[80]. This ensures a stable population of functional receptors for optimal Odor detection. Similar ongoing genesis of mechanosensory hair cells is

observed in the vestibular epithelia of birds[81,82]. Interestingly, these newly generated cells often appear near cells undergoing programmed cell death. Unlike fish where hair cell numbers increase with growth, bird vestibular epithelia maintain a constant population, suggesting a replacement function for ongoing genesis in this case[81,82]. The retina of fish also exhibits ongoing genesis, but specifically for rod photoreceptor cells[83,84]. Unlike olfactory and hair cell regeneration, this process doesn't replace dying cells. Instead, it fuels retinal growth while maintaining a constant rod photoreceptor density relative to the animal's size. This ensures consistent light sensitivity throughout life[85]. These examples highlight the presence of a specialized cell population within sensory epithelia. These cells, similar to stem cells in other tissues, are capable of mitotic division, continuously replenishing sensory receptor cells and maintaining vital sensory functions.

The ability of sensory epithelia to regenerate varies greatly across species and sensory organs. Some, like the olfactory epithelium, exhibit remarkable regenerative potential in all studied animals[80]. In contrast, hair cell regeneration in the auditory and vestibular systems is limited or absent in mammals, but readily occurs in fish, amphibians, and birds[81,82]. Similarly, retinal regeneration is robust in fish and amphibians, with some abilities persisting in birds, while mammals possess minimal regenerative capacity[83]. One intriguing observation is the correlation between ongoing sensory receptor replacement and robust regeneration. Epithelia that continuously generate new receptor cells, like the olfactory epithelium, display exceptional regenerative potential[86]. Damage appears to trigger an increased output from these proliferating cells, allowing for faster restoration. This suggests the preservation of an "embryonic niche" within these tissues, maintaining a microenvironment conducive to regeneration, similar to developmental processes. The increased cell proliferation and fate changes during regeneration likely reflect the same complex developmental signaling pathways governing initial cell patterning. Another interesting finding is the recapitulation of developmental processes during sensory epithelia regeneration. Studies on the inner ear reveal that the same signaling molecules (e.g., Notch) and transcription factors (e.g., Atoh1) used during embryonic development to generate hair and supporting cells are also employed during regeneration. Additionally, a mechanism known as lateral inhibition, crucial for establishing the correct ratio of hair and supporting cells during development, appears to function similarly during regeneration.

In conclusion, sensory epithelia with limited or no regenerative capacity also lack ongoing genesis. Furthermore, these epithelia, like the mammalian inner ear and retina, exhibit minimal cellular proliferation in response to injury. This suggests that the absence of

a proliferative reserve pool and the inability to ramp up cell division after damage contribute to the limited regenerative potential in these organs.

1.6.2 History and Literature from Past: Hair Cell Regeneration

The first observations regarding hair cell regeneration were made in the 1930s when researchers discovered that amphibian lateral line organs regrew following tail amputation, forming regenerative placodes that migrated into the regenerating tail to form neuromasts with new hair cells[87–91]. Unfortunately, many early investigations on nonmammals were neglected or overlooked by prominent auditory researchers only to be rediscovered and embraced 50 years later[87,88]. At a 1978 meeting of the Acoustical Society of America, Robert Capranica presented findings showing that ototoxic aminoglycosides temporarily abolished neurophysiological activity in frogs' inner ears, yet their "hearing" recovered after a few weeks[92]. Subsequent research by Corwin, Cotanche, Rubel, Ryals, and others demonstrated hair cell regeneration in avian ears following acoustic overstimulation and ototoxicity[93,94]. These discoveries challenged the dogma of permanent hair cell loss and irreparability.

1.6.3 Hair Cell Injury and Death

Sensorineural deafness and balance dysfunctions are frequently caused by hair cell loss and the subsequent deterioration of afferent nerve innervation. While these conditions may arise congenitally due to developmental defects or specific genetic conditions, they are more commonly acquired postnatally. Major causes of acquired hearing impairment include aging, noise exposure, and exposure to ototoxic chemicals, notably aminoglycoside antibiotics and cis-platinum have also been implicated in hair cell death and subsequent hearing loss. Ototoxic drugs primarily target and damage hair cells, sparing other structures such as the basilar papilla or tectorial membrane, which are typically affected during acoustic trauma. The mechanosensory function of hair cells depends on the integrity of their hair bundle, with initial damage often occurring to these structures. Tip-links, which connect stereocilia and are crucial for mechanotransduction, can be damaged by various insults, leading to a loss of sensory function[95–97]. While there is rapid morphological and physiological recovery of tip-links after certain types of damage, more extensive damage to the hair bundle may require regeneration for functional recovery[97]. Hair cells can rebuild damaged hair bundles, and in some cases, they can survive without bundles for a period before regeneration occurs[98,99].

Acoustic trauma frequently results in selective hair cell loss on the basilar papilla, with damage beginning at the basal end and extending apically, especially in birds. Similarly,

ototoxic drug treatments exhibit a comparable pattern of hair cell loss, progressing from the base to the apex, with pronounced hearing loss at high frequencies, aligning with anticipated hair cell replacement patterns[100]. In the mammalian cochlea, aging, ototoxic exposure, and noise primarily lead to outer hair cell (OHC) loss, preceding inner hair cell (IHC) loss. IHC absence is typically associated with entire OHC loss, followed by afferent innervation degeneration. Damage to cochlear hair cells, whether caused by noise, ototoxic drugs, or aging, follows a stereotypic pattern in both avians and mammals, progressing from base to apex and, in mammals, from outer hair cells (OHCs) to inner hair cells (IHCs). The susceptibility of outer hair cells (OHCs) to damage stems from their vulnerability to free-radical attack, primarily by singlet oxygen, nitrogen, and hydroxyl radicals. These redox active molecules contain unpaired electrons and can disrupt cellular components, leading to cell death or apoptosis when produced excessively. Excessive noise can also induce free radical generation due to heightened oxidative metabolism[101–103], contributing to cellular and tissue deterioration associated with aging[104]. Neuronal loss, often secondary to hair cell loss, may further exacerbate the damage within the auditory system. The overall pattern of cochlear injury is the sequential depletion of OHCs, IHCs, and afferent nerves.

1.6.4 Proposed Mechanisms for Initiating Hair Cell Regeneration

What triggers hair cells regeneration remains a subject of various hypotheses, yet none have been proven with sufficient data and evidence to refute or ignore the others. However, it is evident that the loss of hair cells serves as a significant stimulus for the regeneration of new ones. In the avian cochleae that remain undamaged, there is minimal or no proliferation of supporting cells observed[58,93,94]. However, laser ablation of auditory sensory epithelium, resulting in loss of hair cells, is adequate to stimulate regenerative proliferation in the surrounding area[105].

The requirement for hair cell loss and the confinement of proliferation to the damaged area imply that hair cells might inhibit proliferation in supporting cells[106]. One hypothesis suggests that hair cells express basolateral membrane proteins that prevent adjacent supporting cells from re-entering the cell cycle[106]. Disruption of in cell-cell contact, such as the loss of hair cell-supporting cell junctions, could trigger the re-initiation of proliferation. One of juxtacrine signaling molecules is Notch that may also contribute in maintaining inhibition of supporting cell proliferation. Although the proliferative response in damaged chick basilar papilla is localized to the vicinity of the lesion, mitotically active supporting cells can be observed up to 180 μm away from the ablation, in seemingly undamaged

regions[105]. This implies that hair cell loss induces proliferation, however it is uncertain if the absence of juxtacrine signaling, such as notch-delta interactions, is a requisite trigger for supporting cell proliferation.

Another hypothesis posits that immune responses may influence sensory hair cell regeneration, as suggested by numerous studies. When axolotls tails are amputated, the recruitment of macrophages at the posterior neuromast lesion prompts the formation of regenerated placodes[107]. Macrophages aid in the migration of mantle supporting cells by breaking down the glycocalyx that ensheathe the outer cells of the neuromast, facilitating regenerative placode formation. In avians, the precise role of macrophages and other immune cells in repair and regeneration of damaged sensory epithelia remains uncertain. However, in damaged basilar papilla, macrophages are recruited to phagocytose cellular debris and produce cytokines[108–110]. Blocking macrophage cytokine production results in reduction of the number of proliferating supporting cells in aminoglycoside treated chick utricles with damaged hair cells, suggesting that macrophage chemical signaling could be crucial[109].

Numerous studies indicate that cell spreading can be a key factor in regulating the growth of hair cells in auditory sensory epithelia. In cultured chick utricular explants, peripheral cells that spread out proliferate, whereas centrally located tightly packed columnar cells do not[111–113]. In damaged basilar papilla with hair cell loss, supporting cells primarily respond by expanding to occupy the space vacated by the missing hair cells[114–118]. This expansion of supporting cells coincides with supporting cells re-entering the cell cycle, returning to normal size with newborn differentiated hair cells and supporting cells[93,117]. These findings support the hypothesis that morphological changes in supporting cells can induce regeneration, however more research is needed to elucidate their precise role in setting on proliferation.

1.6.5 Proliferative Hair Cell Regeneration

In nonmammalian auditory sensory epithelium, the production of hair cells and supporting cells is primarily limited to embryonic development[58,119]. In adult bird's basilar papilla, there is minimal to no cellular proliferation, with zero addition of new hair cells[93,94,120]. However, when hair cell loss is induced, supporting cell proliferation is significantly increased, and an entire pool of newborn hair cells are generated[93,94,121,122]. The asymmetric division of supporting cells facilitates both HC recovery and replenishment of the SC population undergoing mitotic division (Figure 1.6 A).

There is a quantitative, spatial, and temporal correlation between supporting cell proliferation and hair cell demise. Mitotic activity in regenerating sensory epithelia correlates directly with the extent of hair cell loss. Prolonged exposure to noise durations in the chicken basilar papilla results in increased hair cell damage and increased support cell proliferation[123]. Similarly, in the avian vestibular epithelia, the number of supporting cells incorporating BrdU correlates with the number of apoptotic hair cells, indicating a clear link between hair cell mortality and supporting cells undergoing mitosis[124–126].

In the basilar papilla, there are two morphologies of hair cells, tall and short, which are confined to the superior/neural half and inferior/abneural half of the epithelium, respectively. In damaged basilar papilla, most newly regenerated hair cells on the superior/neural side of the epithelium showed EdU-positive nuclei, indicating primarily mitotic origin. However, on the inferior/abneural side, regeneration predominantly occurred through phenotypic conversion, where supporting cells transform directly into hair cells without prior division. Interestingly, there is a higher tendency for direct transdifferentiation in the inferior/abneural half of the epithelium, while mitosis plays a more significant role in the superior/neural half[127,128].

Ototoxic treatment of the chicken basilar papilla results in a hair cell lesion that gradually proceeds from the proximal to the distal region[129]. BrdU labelling of dividing cells at various intervals post-exposure reveals that mitotic activity in supporting cells advances towards the distal region of the basilar papilla that corresponds with the timing of hair cell loss. Initially, dividing cells are observed in the damaged proximal region, with some delay from the onset of hair cell death[130]. It is interesting to note that the duration of delay is similar in all damaging scenarios, regardless of what kind and duration of the adverse treatment[105,110,123]. The delay is likely attributed to the signaling cascades guiding supporting cells/progenitor cells from growth arrest to S phase following hair cell damage[120].

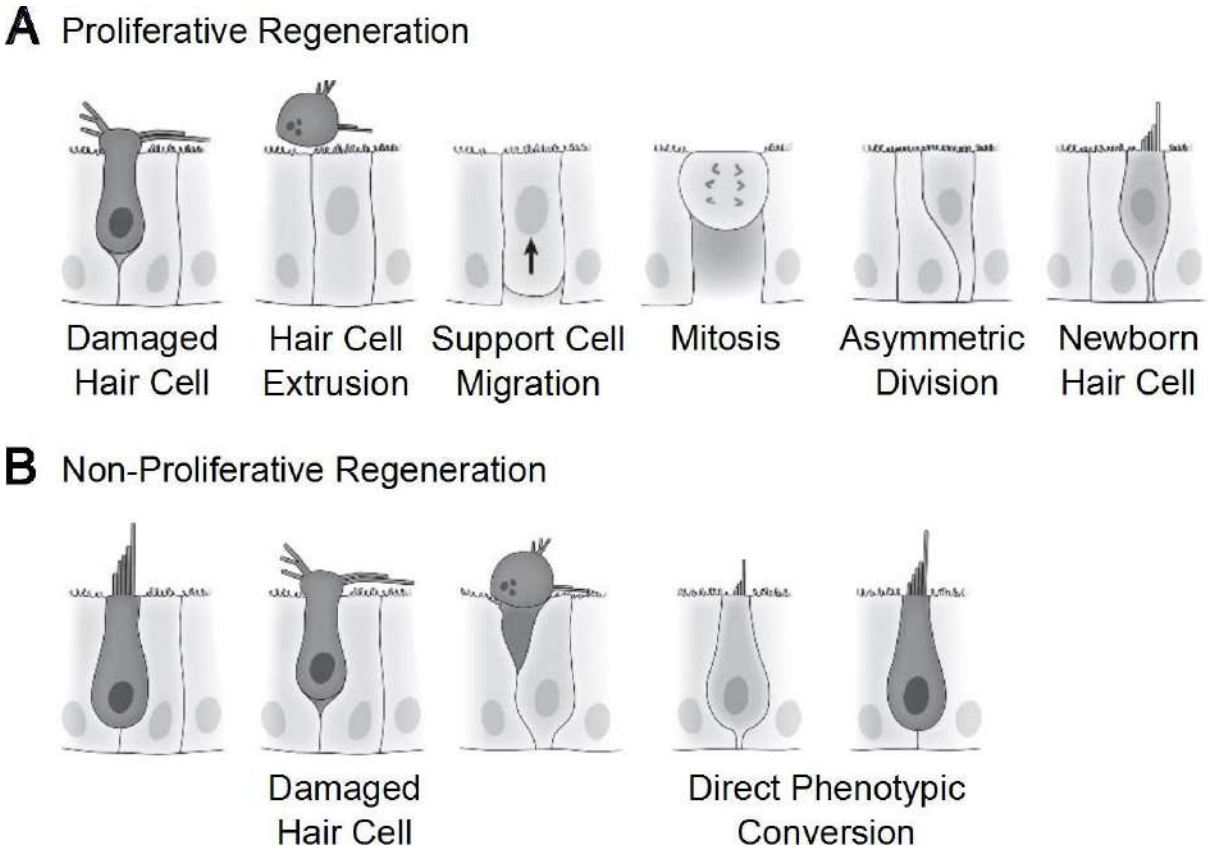

Figure 1.6 Modes of Hair Cell Regeneration. (A) Schematic diagram illustrates the regenerative proliferation driven by SCs. Upon HC loss, the SC nucleus migrates towards the epithelial surface and undergoes mitosis (asymmetric cell division). The resulting daughter cells then differentiate into a new HC and SC. (B) Diagram depicts a proposed mechanism for non-proliferative hair cell regeneration. Following hair cell loss, a neighboring supporting cell, can directly convert into a new hair cell without cell division.

1.6.6 Non-proliferative Regeneration of Hair Cells: Metaplasia

There continues to be evidence that suggests not all of the hair cell recovery following sensory epithelial damage in non-mammals is due to mitotic division of supporting cells. For instance, initial hair cell regeneration in chicks is not marked by BrdU labelling, indicating a different mechanism at play[131]. Moreover, the vestibular epithelial of mammals shows discrepancy between the abundance of newly regenerated hair cells and the limited observed proliferation[132–134]. Additionally, despite the presence of mitotic inhibitors, differentiated hair bundles resurface in the basilar papilla of bullfrogs and chicks, suggesting a potential role for the phenotypic conversion of supporting cells into hair cells without cellular proliferation[99,135,136]. Consequently, two potential mechanisms have been proposed for this hair cells regeneration in the sensory epithelia; mitotic division of supporting cells, followed by differentiation of hair cells and direct transdifferentiation of support cells (phenotypic conversion) (Figure 1.6 B).

In avians, hair cell regeneration begins with direct phenotypic conversion of support cells to hair cells, followed by supporting cell mitotic division[131], primarily in the abneural half of the sensory epithelium[128]. First reports for transdifferentiation were primarily morphological, observed in the bullfrog vestibular epithelia. Following ototoxic drug treatment, supporting cell nuclei migrate from the basilar membrane to the luminal surface adjacent to hair cell nuclei, without substitution of new nuclei in the supporting cell layer[137]. When undergoing transdifferentiation, cells exhibit transitional morphology that bridges between hair cells and supporting cells phenotype, marked by contact with the basal lamina and apical specializations resembling hair bundles[135,138,139].

1.6.7 Quiescent Supporting Cells

In the embryonic chick basilar papilla, the full assembly of hair cells is completed, after which the cells enter a quiescent state[57,58]. Although supporting cells remain dormant until damage triggers cell cycle re-entry, continuous proliferation occurs in the avian vestibular system throughout life. In prenatal basilar papilla, two supporting cell subtypes have been identified with subtle morphological variations; one with thick processes on apex and base of the cell with nucleus positioned at the center and another with thin processes with nucleus positioned towards the lumen[140]. These differences may appear minor, especially while examining SCs in the abneural/inferior edge to SCs situated in between hair cells[141]. However, in the fish vestibular epithelium, these minor variations in nuclear shapes and positions define the status quo of supporting cells, indicating whether they are in S phase or quiescent[141]. Various molecular markers, vary consistently throughout the quiescent supporting cell (SC) population, such as cytokeratins[142], receptor-like protein tyrosine phosphatase (RPTP)[143] and tectorins[144]. Additionally, the homeobox transcription factor Prox1 exhibits variable expression between quiescent supporting cells and mitotically active progenitor cells, with weak expression in a subset of quiescent supporting cells[145]. In ototoxic drug treated basilar papilla, Prox1 expression is heightened in proliferating supporting cells and newborn hair cells, but not in dormant support cells[145]. These observations imply the existence of progenitor populations with varying cell division potentials, influenced by gene expression diversity across the SC population.

In adult basilar papilla, cell proliferation is minimal, with most supporting cells expressing growth arrest G0 markers like statin rather than proliferating G1 markers like PCNA. However, short-term exposure to ototoxic drugs induces complete hair cell damage in the proximal region, altering the expression of these markers. Statin expression declines

throughout the sensory epithelium, whereas PCNA expression rises in supporting cells, even at unaffected distal regions signifying a change in cell cycle phase from G0 to G1[146]. Notably, cell cycle progression to S phase and later stages occurs only in regions of extensive hair cell loss. The widespread presence of signals prompting supporting cells to re-enter the cell cycle G0 to G1 after hair cell loss, coupled with the restricted localization of cues triggering S phase entry only in damaged areas, suggests tightly regulated and diverse signaling pathways controlling support cell proliferation in the sensory epithelium.

Earlier studies in fish lateral line systems have shown that modifying cell death rates alters supporting cell proliferation. Caspase inhibition in neuromast suppresses apoptosis, reducing hair cell death and also decreases support cell proliferation[125]. Similar observations were reported establishing correlation between hair cell death rate and support cells division in chicken vestibular epithelia[126]. This suggests a feedback mechanism wherein hair cells directly influence support cell division. Under normal conditions in the basilar papilla, hair cells act as gatekeepers, suppressing the division of supporting cells. Following hair cell death, the absence of inhibitory signals prompts neighboring supporting cells to proliferate. Thereby, direct signaling between hair cells and supporting cells is likely critical for keeping supporting cells in a mitotically quiescent state[106,121,147].

1.6.8 Newborn Hair Cells

Avian cochlear cells retain their ability to re-enter the cell cycle and generate new hair cells throughout life, despite typically becoming dormant after embryonic development. Following acoustic trauma or exposure to aminoglycosides, newly formed hair cells emerge and migrate towards the luminal surface of the sensory epithelium. The newly regenerated hair cells adopt the structural morphologies of the hair cells they replace[121], indicating the potential transmission of positional identity, especially tonotopy. The newborn hair cells within the damaged region exhibit small apical surface area and small hair bundles reminiscent of immature hair bundles on developing hair cells. These nascent hair cells have rudimentary stereocilia protrusions emerging from their apical surface, morphologically newborn hair cells look spherical while establishing contact with the luminal edge[148,149]. During hair cell differentiation, the cell's shape and connection to the basal lamina alter significantly, but their association with the luminal surface remains intact. In young chicks, new hair cells typically emerge within 3-5 days post-treatment, fully restoring the sensory epithelium within 4 weeks. The highest production of new hair cells typically happens around day 2 or 3 after exposure to noise or drugs[110,123,146,150], followed by a significant decline in mitotic activity by days 5-7,

with almost no proliferation by day 11. Nascent stereocilia emerge on new hair cells approximately 4 to 6 days after injury[121,149], however hair bundle organization remains immature with aberrant orientation. To completely restore stereociliary bundle structure and orientation of newborn hair cells 90 days are required[148,151]. Further, newly regenerated hair cells exhibit afferent and efferent synapses as early as 3-4 days after acoustic trauma, suggesting reinnervation is underway, with synaptic contacts forming at the base of the cell[152].

1.6.9 Mammalian Hair Cell Regeneration

Unlike non-mammalian vertebrates, the development and differentiation of hair cells in mammals are restricted to embryonic stages[153]. Compared to non-mammals, the mammalian organ of Corti fails to produce new auditory hair cells under normal physiology or in response to hair cell damage[154,155]. However, limited proliferation is observed in the vestibular sensory epithelium[132,138]. In contrast to the vestibular system, there is less evidence suggesting mitotic division of supporting cells for hair cell renewal in the mammalian cochlea due to their highly specialized and distinct morphologies[156–160]. The specialization in the organ of Corti may restrict the potential of supporting cells to re-enter the cell cycle, suggesting a higher likelihood of hair cell regeneration in mammalian vestibular epithelia, which share similarities with supporting cells in non-mammalian auditory epithelia. Furthermore, in the organ of Corti, proliferation in supporting cells is actively suppressed with high expression of the cyclin-dependent kinase inhibitor p27Kip1 (Kip1)[161,162]. Knocking out p27Kip1 results in postnatal proliferation and the formation of extra hair cells[161].

During embryonic development of the mammalian cochlea, supporting cells briefly exhibit plasticity to convert into hair cells following neighboring hair cell loss, but this ability diminishes with maturation[163]. Following hair cell loss in the mature organ of Corti, Deiters' cells, surrounding the outer hair cells, undergo morphological changes, forming microvilli bundles that imitate immature hair bundles and often interact with nerve fibres[164–166]. However, these cells do not fully mature into hair cells and eventually are lost from the sensory epithelium[165].

1.7 Molecular Regulation of HCs Differentiation and Regeneration

During embryonic development and regeneration, sensory cells in the inner ear (hair cells and supporting cells) undergo a tightly controlled process where they receive signals from both their surroundings (cell extrinsic) and within the cell itself (cell intrinsic) to transform from unspecialized cells into specific cell types. The observation that similar cell types form in the sensory epithelium during both embryonic development and regeneration suggests that the same molecules might be employed to perform specific functions in both processes.

Numerous studies have highlighted the role of signaling pathways like Notch, FGF, Wnt, and Bmp in embryonic hair cell development[23,38,167,168]. Wnt and Notch signaling are evolutionarily ancient and intricately interconnected pathways, which play vital roles in coordinating the crucial cellular processes involved in the development of sensory hair cells. Wnt and Notch signaling pathways act as master conductors throughout animal development, from the earliest stages of embryogenesis to adulthood. These pathways orchestrate crucial events like cell proliferation, differentiation, and cell fate specification, essentially directing which cells become what. Extensive research has shown that the Wnt and Notch signaling pathways function synergistically in multiple tissues to determine cell fate[167,169–171]. Wnt and Notch signaling pathways act as upstream regulators, controlling the expression of numerous transcription factors that guide inner ear development. Furthermore, after hair cell damage both signaling pathways potentially enable supporting cells to regenerate hair cells.

1.7.1 Wnt Signaling in Hair Cell Development

Wnt signaling is an evolutionary conserved pathway that controls diverse processes like cell fate decisions, cellular proliferation, specification, differentiation and polarity[172]. Notably, Wnt signaling also contributes to maintaining the undifferentiation state of stem cells. Wnt ligand binding to the cell surface triggers diverse intracellular signaling cascades. These include the well-characterized canonical Wnt/β-catenin pathway alongside two distinct non-canonical pathways: the planar cell polarity (PCP) pathway and the Wnt/calcium pathway[173]. Highlighting the canonical pathway, Wnt ligands engage Frizzled receptors and LRP5/6 co-receptors, inducing Dishevelled (Dsh) protein activation within the cell[174]. This activation disrupts the axin2/glycogen synthase kinase 3β (GSK3β)/adenomatous polyposis coli (APC) complex, leading to β-catenin release. The freed β-catenin accumulates in the cytoplasm and translocates to the nucleus[174]. There, it interacts with TCF/LEF transcription factors, regulating the expression of downstream Wnt target genes[175].

Within the cochlea, both the canonical Wnt/β-catenin and non-canonical PCP pathways have been implicated in crucial processes[176,177]. The canonical Wnt/β-catenin signaling pathway plays an essential role in cochlear development, regulating hair cell proliferation, fate specification, and differentiation[176,177]. Experiments employing explant cultures of embryonic cochlea show that hindering Wnt/β-catenin signaling with small molecules inhibitor declines prosensory cell proliferation[176]. On the contrary, Wnt agonist LiCl treatment promotes the formation of the Sox2-positive prosensory domain and increases HC numbers[176]. Furthermore, conditional β-catenin knockout in mouse halts HC differentiation from prosensory cells, while overexpression enhances HC formation[177].

Elucidating the upstream regulators of Atoh1 is critical for understanding its role in hair cell specification, as its activation triggers a autoregulatory self-sustaining transcriptional loop[178]. Atoh1 knockout mice display hair cell deficiency despite retaining promoter activity, highlighting the existence of an independent activation mechanism during embryonic development[154,179]. β-catenin emerges as a potential upstream regulator due to its interaction with Tcf-Lef sites in the Atoh1 enhancer and its earlier expression pattern in the otic placode compared to initial Atoh1 expression[93,180]. These observations suggest a potential role for β-catenin in initiating Atoh1 expression for hair cell formation during inner ear development.

Lgr5, a member of the leucine-rich repeat G-protein-coupled receptor (Lgr) family, is expressed in the developing mammalian cochlea[181,182]. Its ligand, R-spondin, is also present in the sensory epithelium and plays a role in Wnt signaling. During cochlear development, Lgr5 exhibits a specific spatiotemporal expression pattern. Between embryonic day 18.5 and postnatal day 3, it is localized in the third row of Deiters' cells, inner pillar cells, inner phalangeal cells, and the lateral greater epithelial region[181,182]. Notably, activation of the Wnt/β-catenin pathway through Lgr5+ progenitors in the neonatal cochlea promotes cell proliferation and differentiation into hair cells[183]. These findings suggest a crucial role for Lgr5 in Wnt signaling and hair cell development within the cochlea. Furthermore, In the developing cochlea, Lgr5 is initially expressed throughout the prosensory region, becoming restricted to a specific subset of supporting cells (SCs) after birth[181]. These Lgr5+ SCs in newborn mice exhibit remarkable regenerative potential, functioning as hair cell (HC) progenitors. They can regenerate HCs through two distinct mechanisms: direct differentiation and mitotic division[169,183–185]. This implies that Lgr5 expression serves as a marker for a population of SCs with stem cell-like characteristics, capable of replenishing lost hair cells.

While the canonical Wnt/β-catenin pathway is well-established in HC development, the non-canonical Wnt/PCP pathway also plays a significant role. This pathway is known to

mediate the planar polarization of hair cells, ensuring their proper orientation. However, the specific role of Wnt/PCP signaling in hair cell regeneration remains to be elucidated.

1.7.2 Notch Signaling in Inner Ear Development

The Notch signaling pathway, with its external receptor, stands out as a critical extrinsic regulator in inner ear sensory epithelium development[186,187]. The Notch signaling pathway is involved at various stages of ear development, from the emergence of the otic placode to the maturation of mechanosensory sensory structures (hair cells). Notch signaling is an evolutionary conserved pathway crucial for tissue development and homeostasis across diverse species, from fruit flies (Drosophila melanogaster) to humans. Notch signaling is not confined to embryonic development, it orchestrates vital functions in various tissues throughout our lives, from the intricate nervous system to the continuously renewing hematopoietic system[188–190]. Notch activity is necessary for carefully selecting the right starting cells (competent progenitors), guiding them towards their fate (lineage decisions), and ensuring a reserve of stem cells remains in a developing organ system.

Notch signaling begins with the interaction between Notch receptors on one cell and Notch ligands (Delta-like ligands and Jagged ligands) on a neighboring cell, facilitating direct cell-cell communication[191,192]. Notch receptors are transmembrane proteins with extracellular, transmembrane, and intracellular domains. Ligands bind to the extracellular domain of Notch receptors. Upon ligand binding, Notch receptors undergo proteolytic cleavage by enzymes called ADAM metalloproteases and γ-secretase. This cleavage releases the intracellular domain of the Notch receptor (NICD) from the plasma membrane. The NICD translocates into the nucleus of the signal-receiving cell. In the nucleus, NICD interacts with a DNA-binding protein complex called CSL (CBF1/RBPJκ in mammals, Suppressor of Hairless in Drosophila, and Lag-1 in Caenorhabditis elegans). This interaction transforms CSL from a transcriptional repressor into an activator, facilitating the transcription of repressor transcription factors of Myc, P21, HES (Hairy and Enhancer of Split) and HRT (Hairy related Transcription Factor) families[193,194]. The expression of HES suppresses tissue-specific transcriptional activators, affecting cell proliferation and differentiation[193,195].

Notch Pathway Influence on Otic Placode Size

The inner ear originates from a specialized region of thickened surface ectoderm known as the otic placode. Wnt signaling pathways also influence the otic placode's development by regulating the expression of Jag1 (also known as Serrate1 in chicken), a Notch ligand. The

presence of Lef/Tcf binding sites upstream of the Jag1 promoter[196,197], suggests a potential direct transcriptional activation of Jag1 by the canonical Wnt signaling pathway. Here, the Notch pathway is critical for establishing the boundary of the otic placode and segregating it from the surrounding Pax2 positive ectoderm, which develops into other epibranchial placodes and skin epithelia[170]. Conditional deletion of the canonical Wnt signaling effector, β-catenin, within the developing inner ear leads to diminished Jag1 (Notch ligand) expression. Conversely, constitutive activation of β-catenin expands Jag1 expression laterally beyond the neural plate, encompassing the entire Pax2 positive domain[170]. Co-expression of Jag1 ligand and Notch1 receptor within the otic placode suggests a potential positive feedback loop via Notch mediated lateral induction. Functional studies provide evidence that Jag1-Notch1 signaling acts as a potential amplifier of Wnt activity during otic placode induction. N1ICD expression in the Pax2 domain increases the area of otic markers and intensifies Wnt signaling, while Notch1 mutants phenocopy β-catenin conditional mutants, exhibiting a smaller otic placode[170]. These findings suggest a cooperative role for Notch and Wnt signaling to establish otic placode borders.

Notch Mediated Lateral Inhibition for Determining Neurosensory Fate

During invagination of the otic cup, the antero-ventral region, known as the neurosensory domain, initiates neurogenesis. This process, characterized by Neurog1, Dll1, and Lfng expression, concludes with the delamination and migration of neuroblasts from the epithelium. These delaminated neuroblasts form VIIIth cranial ganglion (cochleovestibular ganglion), which later segregates into auditory and vestibular components[28,198–201]. Within the neurosensory domain, Notch signaling determines cell fate decisions, dictating which cells will delaminate and become neural progenitors through a process called Notch mediated lateral inhibition. A low-level and random increase (stochastic upregulation) in the Neurog1 transcription factor within specific cells of the neurosensory domain leads to the expression of the Notch ligand Dll1, marking these cells as putative neuroblasts. Cells expressing Dll1 transmits signals to neighboring cells, through Notch activation in adjacent cells causing a decrease in Neurog1 expression and effectively preventing their neural precursor fate. The Notch mediated lateral inhibition model in inner ear neurosensory fate determination is supported by multiple sets of data. Firstly, Neurog1 deletion in the anterior otocyst ablates Dll1 expression[200]. Secondly, blocking Notch signaling in chick otocysts using the gamma secretase inhibitor DAPT triggers overabundance of neuroblast delamination, extending beyond the anterior domain to include the center of the otic vesicle[202].

Notch Mediated Lateral Induction for Prosensory Domain Development

During early otic development Notch signaling specifies the prosensory domains to define discrete regions of epithelium that would later develop into sensory patch, containing hair cells and supporting cells[198]. This sensory epithelium originates from the prosensory domain, characterized by the expression of the Sox2 and the Notch ligand Jag1. Jag1 is initially expressed in prosensory domains of the otocyst. Following differentiation into the distinct auditory and vestibular sensory organs, Jag1 expression persists specifically in the supporting cells of each organ[28,203]. Functionally, Jag1 acts as a key ligand for Notch receptors expressed throughout the otocyst. This ligand-receptor interaction establishes a positive feedback loop, promoting the prosensory fate in these domains while Notch signaling in the surrounding otic epithelium directs them towards a non-sensory lineage[204]. This Jag1-Notch mediated enhancement of cell fate determination is a well-established mechanism known as lateral induction. Conditional Jag1 deletion in early otic development disrupts vestibular organ formation, characterized by loss of molecular markers and structures, especially semicircular canals[205,206]. Conversely, ectopic Jag1 expression in the chick otocyst expands the prosensory domain via Jag1 and Sox2 upregulation in neighboring cells[186,207].

Notch Mediated Lateral Inhibition for Hair Cell Formation

In birds, the sensory epithelia of the inner ear display a characteristic mosaic pattern of hair cells and supporting cells. Notch-mediated lateral inhibition determines the formation of this mosaic from bipotent progenitor cells. Upon differentiation, nascent hair cells express Delta1-like 1 (Dll1) and Jagged2 (Jag2) ligands, activating Notch1 receptors on neighboring progenitor cells. This triggers Hes1/5 expression in these progenitors, ultimately suppressing the pro-hair cell transcription factor Atoh1[206,208]. Consequently, neighboring cells are prevented from adopting the hair cell fate and instead differentiate into supporting cells, establishing the characteristic salt and pepper mosaic pattern of alternate cell type in the inner ear.

While Notch juxta signaling is crucial for cell fate decisions during inner ear development, its role in postnatal hair cell replacement, both normal physiology and injury induced, remains largely unexplored. In adult chicken, the expression patterns of Notch and its ligands, Delta1 and Jag1 (also known as Serrate1 in chicken), suggest a potential role in hair cell regeneration[149]. In normal physiology, basilar papilla is mitotically quiescent with Notch1 expressed in all supporting cells while Serrate1 is present in both hair cells and support cells. Notably, the Delta1 expression is absent. However, the continuously

regenerating vestibular epithelia exhibit robust expression of Notch1, Delta1, and Serrate1. Interestingly, upon HC injury in the basilar papilla, Delta1 transiently appears at low levels in proliferating progenitors. Post-mitotic sister cells initially exhibit a similar and low level of Delta1 expression; within a 72-hour window, this expression becomes specifically upregulated in hair cell precursors and downregulated in support cell precursors. These findings suggest that Delta1 upregulation in nascent hair cells acts as a lateral inhibitory signal shortly after cell division, preventing neighboring cells from adopting the HC fate during regeneration and therefore maintaining a supporting cell fate.

Notch Signaling in Hair Cells Regeneration

In mature basilar papilla, hair cell injury induced by ototoxic drugs leads to the upregulation of Notch pathway genes in actively proliferating regions. Interestingly, while inhibiting Notch signaling with DAPT promotes hair cell regeneration via supporting cell proliferation and direct transdifferentiation, it had no direct effect on support cells proliferation[209]. This is further supported by the observation that γ-secretase inhibition in undamaged papillae doesn't trigger hair cell production. Conversely, in damaged sensory epithelium, the over expression of NICD in support cells maintain their quiescent state, hindering hair cell regeneration[209]. These findings suggest that Notch signaling is crucial for regulating cell fate choices during regeneration, but may not directly control cell division.

On a mechanistic level, Notch activation suppresses hair cell fate by upregulating Hes1 and Hes5, members of the Hes family genes. Hes5 gene is strongly expressed in progenitor cells and subsequently in supporting cells[42,50,51,210]. Hes5, a downstream effector of Notch signaling, is a potent inhibitor of the pro-hair cell transcription factor Atoh1, thereby preventing progenitor and support cells conversion into hair cell. This is further confirmed by studies in auditory and vestibular sensory epithelium of mouse, where Hes5 deletion leads to hair cell supernumerary[51].

1.7.3 Wnt and Notch Crosstalk in Hair Cell Regeneration

Converging evidence suggests that Wnt and Notch signaling pathways cooperate in regulating cell fate decisions across various tissues[167,169–171]. A key regulatory link between the Wnt and Notch pathways exists through the Notch ligand Jag1, an evolutionarily conserved target of the canonical Wnt signaling pathway. The 5' promoter region of Jag1 contains TCF/LEF binding sites, which recruit β-catenin and promote Jagged1 expression[211].

During otic placode development in mice, Wnt signaling acts upstream of the Notch pathway, effectively regulating the expression of Notch target genes like Jag1, Notch1, and Hes1. In contrast, Wnt inhibition reduces the size of the otic placode. In the zebrafish lateral line system, Notch signaling can hinder SC proliferation and differentiation into hair cells by suppressing Wnt activity in specific regions[212]. These findings collectively point towards a dynamic interaction between Wnt and Notch signaling pathways during development. Previous research in postnatal cochleae, inhibiting Notch signaling promotes proliferation and differentiation of Lgr5+ supporting cells into hair cells[167]. Interestingly, combined Wnt and Notch inhibition decreased HC generation through mitotic division. Hair cell regeneration in the neonatal cochlea after Notch inhibition, wherein hair cells are either generated mitotically with Wnt signaling or directly transdifferentiated from supporting cells into hair cells, without Wnt signaling[167]. However, another study suggests Notch inhibition alone might not be enough, as it failed to stimulate hair cell conversion in β-catenin knockout mice, where Wnt signaling is disrupted[169]. This implies Wnt signaling plays a crucial role in direct transdifferentiation.

Studies on cochlear development reveal that Wnt signaling activation promotes the expression of Atoh1, a critical transcription factor for hair cell (HC) formation[177]. This finding suggests that β-catenin, a downstream molecule in the Wnt pathway, acts upstream to regulate Atoh1 and drive HC development. In contrast, Notch signaling appears to favour the formation of supporting cells (SCs) by suppressing Atoh1 expression[51]. These observations highlight the opposing roles of Wnt and Notch signaling in determining HC fate. However, the precise mechanisms by which Atoh1 interacts with these pathways during the postnatal period remain to be elucidated.

Objectives of the Thesis

This thesis investigates the mechanisms underlying BP tissue homeostasis in recovering hair cell numbers upon mosaic Atoh1 deletion, with the following objectives.

Objective 1: Development of a Non-invasive Method and Model System for Hair Cell Regeneration Studies

The first step in this exploration is to develop a method for studying hair cell regeneration. This non-invasive approach will allow us to observe the process without physically harming the subject. Additionally, appropriate control groups for electroporation and CRISPR will be established, ideal for studying hair cell restoration in detail.

Objective 2: Investigation of Hair Cell Regeneration in the Developing Basilar Papilla

Studying hair cell regeneration in developing basilar papilla of embryonic chicken. The avian auditory organ holds the key to understanding how hair cell regeneration naturally occurs. By studying proliferation dynamics in embryonic BP, we hope to understand of hair cell restoration during early development.

Objective 3: Deciphering the Signaling Mechanisms of Hair Cell Restoration

What signaling mechanisms are involved in maintaining BP homeostasis, this study delves into the intricate cellular communication pathways that orchestrate hair cell restoration, aiming to unlock the potential to stimulate or enhance hair cell regeneration in adult organisms, offering hope for the future of hearing loss treatments.

Chapter 2: Material and Methods

Detailed description of the materials and methods used in this study are published in 'Singh N, Prakash A, Chakravarthy SR, Kaushik R, Ladher RK. In Ovo and Ex Ovo Methods to Study Avian Inner Ear Development. J Vis Exp. 2022 Jun 16;(184). DOI: 10.3791/64172[213].

Table 2.1: List of Reagents Used in the Study.

#	Reagents	Composition	Preparation
Buffers			
1.	Phosphate Buffered Saline (PBS) 10X	80 g Sodium chloride (NaCl) 2.0 g Potassium chloride (KCl) 14.4 g Sodium phosphate dibasic (Na_2HPO_4) 2.4 g Potassium phosphate monobasic (KH_2PO_4)	Adjust the volume to 1 liter with distilled water and pH 7.4. Sterilize by autoclave.
2.	0.719% Saline	7.19 g Sodium chloride (NaCl)	Add 1 liter of distilled water and autoclave.
3.	Ringer Solution	8.5 g Sodium chloride (NaCl) 0.42 g Potassium chloride (KCl) 0.25 g Calcium chloride ($CaCl_2$)	Add 1 liter of distilled water and mix well. Best if prepared fresh.
4.	Pannett-Compton Solution A	121 g Sodium chloride (NaCl) 15.5 g Potassium chloride (KCl) 10.42 g Calcium chloride dihydrate ($CaCl_2.2H_2O$) 12.7 g Magnesium chloride hexahydrate ($MgCl_2.6H_2O$)	Add 1 liter of distilled water to each Solution A and Solution B and mix well. Both solutions A & B are suitable for autoclaving and stored at 4°C. To prepare the solution for use, combine the following components in the specified order: 120 ml of solution A, 2,700 ml of H_2O, and 180 ml of solution B.
5.	Pannett-Compton Solution B	2.365 g Sodium phosphate dibasic dihydrate ($Na_2HPO_4.2H_2O$) 0.188 g Sodium phosphate monobasic dihydrate ($NaH_2PO_4.2H_2O$)	

6.	Hank's Balanced Salt Solution (HBSS)	8.0 g Sodium chloride (NaCl) 0.4 g Potassium chloride (KCl) 0.25 g Calcium chloride ($CaCl_2$) 0.1 g Magnesium sulfate heptahydrate ($MgSO_4.7H_2O$) 0.1 g Magnesium chloride hexahydrate ($MgCl_2.6H_2O$) 0.06 g Sodium phosphate dibasic dihydrate ($Na_2HPO_4.2H_2O$) 0.06 g Potassium dihydrogen phosphate (KH_2PO_4) 1.0 g Glucose ($C_6H_{12}O_6$) 0.35 g Sodium bicarbonate ($NaHCO_3$)	Add 1 liter of distilled water and mix well. Sterilize and store at 4°C.
7.	TAE Buffer 50X	242 g Tris base ($NH_2C(CH_2OH)_3$) 57.1 ml Acetic acid (CH_3COOH) 100 ml 0.5M EDTA (pH 8.0)	Adjust the volume to 1 liter with distilled water and mix well. Storage at room temperature.
8.	Stacking Buffer (0.5M Tris-HCl)	6.057 g Tris base ($NH_2C(CH_2OH)_3$)	Adjust the volume to 100 ml and adjust to pH 6.8.
9.	Resolving Buffer (1.5M Tris-HCl)	18.171 g Tris base ($NH_2C(CH_2OH)_3$)	Adjust the volume to 100 ml and adjust to pH 8.8.
10.	Ammonium Persulfate 10%	1 g Ammonium Persulfate $(NH_4)_2S_2O_8$	Dissolve in 10 ml, create 1 ml aliquots and store them at 4°C.
11.	Lysis Buffer	100 µl Triton X 4.8 mg AEBSF 200 µl 0.5M EDTA 0.1755 g NaCl 2.0 g MS-SAFE Protease and Phosphatase Inhibitor	Dissolve it in 19.7 ml 1X PBS. Filter sterile and store at -20°C.
12.	Resuspension Buffer 10X	59.58 g HEPES (4-(2-hydroxyethyl)-1-piperazineethanesulfonic acid) 37.27 g Potassium chloride (KCl) 43.83 g Sodium chloride (NaCl) 1.09 g Calcium chloride ($CaCl_2$) 50 ml Glycerol	Adjust the volume to 500 ml with distilled water and pH 7.5. Filter sterile and store at 4°C.

13.	Protein Loading Buffer 5X	3 ml 20% SDS 3.75 mL 1M Tris base (pH 6.8) 9 mg Bromophenol blue 1.16 mg DTT (Alternatively add 2.4ml B-mercaptoethanol)	Add water to a final volume of 10.5ml to make 15 ml. Mix the above reagents well. Add 4.5 mL Glycerol and mix well again. Store at 4°C.
14.	SDS Running Buffer 10X	30.28 g Tris base 144 g Glycine 10 g SDS	Adjust the volume to 1 liter with distilled water, pH 8.3. Store at room temperature.
15.	MES Buffer 20X	97.3 g MES (2-(N-morpholino) ethanesulfonic acid) 60.6 g Tris base ($NH_2C(CH_2OH)_3$) 10 g Sodium dodecyl sulfate (SDS) 3 g EDTA	Adjust the volume to 500 ml with distilled water and filter sterile.
16.	MOPS Buffer 10X	41.8 g MOPS (pH 7.0) 20 ml 1M Sodium acetate (CH_3COONa) 20 ml 0.5 EDTA (pH 8.0)	Adjust the volume to 1 liter with distilled water. Filter sterile and store at room temperature.
17.	Transfer Buffer 10X	288 g Glycine 60.4 g Tris base ($NH_2C(CH_2OH)_3$)	Adjust the volume to 2 liters with distilled water. For 1X transfer buffer, 100 ml of 10X transfer buffer, 200 ml methanol and 700 ml of distilled water.
18.	Tris Buffer Saline (TBS) 10X	24 g Tris base ($NH_2C(CH_2OH)_3$) 88 g Sodium chloride (NaCl)	Adjust the volume to 1 liter and pH 7.4. To prepare TBST 100 ml of 10X TBS, 1 ml Tween 20 and 900 ml of distilled water.
19.	5% Non-fat dry milk blocking buffer	5 g Non-fat dry milk (NFDM)	Dissolve in 100 ml TBST (Tris Buffer Saline, Tween 20)
20.	5% Bovine serum albumin blocking buffer	5 g Bovine serum albumin (BSA)	Dissolve in 100 ml TBST (Tris Buffer Saline, Tween 20)
21.	Sodium Citrate Acid Buffer 10X	29.4 g Trisodium citrate dihydrate ($C_6H_9Na_3O_9$) 5 ml Tween 20	Adjust the final volume to 1 liter and pH 6. Store at 4°C.

22.	0.2M Sodium Cacodylate buffer with 0.1% $CaCl_2$	42.8 g Sodium cacodylate trihydrate ($Na(CH_3)_2AsO_3.3H_2O$) 1.0 g Calcium chloride ($CaCl_2$)	Add chemicals to approx. 800 ml of distilled water. Adjust to pH 7.3 with 1N HCl and the final volume to 1 liter with distilled water.
23.	Inoue Transformation Buffer (ITB)	10.88 g Manganese(II) chloride tetrahydrate ($MnCl_2.4H_2O$) 2.20 g Calcium chloride dihydrate ($CaCl_2.2H_2O$) 18.65 g Potassium chloride (KCl) 20 ml 0.5M PIPES (pH 6.7)	Adjust the final volume to 1 liter with autoclave distilled water. Sterilize by filtration and store at 4°C.
24.	3M Na-Acetate	408.3 g Sodium acetate trihydrate ($CH_3COONa.3H_2O$)	Dissolve in distilled water with final volume to 1 liter and adjust pH 5.2 with glacial acetic acid. Store at room temperature.
25.	IPTG (100mM)	238 mg IPTG (Isopropyl β- d-1-thiogalactopyranoside)	Dissolved in 10 ml distilled water. Filter sterile and aliquot at -20°C.

Dyes and Solutions

1.	Orange G DNA Loading Dye	3.9 ml Glycerol 0.5 ml 10% SDS 0.2 ml 0.5M EDTA 10 mg Orange G	Bring mixture to 10 mL with distilled water. Aliquot 1 ml solution in 1.5 mL tube and stored at -20 °C.
2.	Fast Green Dye	0.25 g Fast Green FCF	250 ml 95% ethanol dissolved. Filter sterile and aliquot at -20°C.
3.	Alizarin Red	50 mg Alizarin red 1 L of 1% potassium hydroxide	Final concentration is 0.005% (w/v) alizarin red in 1% potassium hydroxide.
4.	Alcian Blue	1.0 g Alcian Blue 8GX 3.0 ml Glacial Acetic Acid	Add 100 ml distilled water and adjust pH 2.5.

Fixatives

1.	4% Paraformaldehyde	4.0 g Paraformaldehyde	Warm it to a temperature below 60°C in order to dissolve it in

			100 ml of 1X PBS, and adjust pH to 7.4.
2.	2.5% Glutaraldehyde	10 ml Glutaraldehyde, 25% Aqueous Solution	Dissolve it in 100 ml of 0.1M sodium cacodylate buffer pH 7.3 with 3mM $CaCl_2$. Cool before use.
3.	2% Aqueous Osmium Tetroxide (OsO_4)	2.0 g Osmium tetroxide OsO_4 (2x1g ampoules)	Dissolve in 100 ml distilled water. Store at 4°C.

Preparations

1.	DNA agarose gel	1 g Agarose 1X TAE buffer	Dissolve in 100 mL of 1X TAE to make a 1% gel by boiling the mixture.
2.	Protein polyacrylamide gel - 4% Stacking gel	Stacking buffer (Tris-HCl, pH 6.8) 1.26 ml 30% Acrylamide 660 µl 10% SDS 50 µl 10% APS 50 µl TEMED 5 µl Distilled H_2O 3 ml	Clean the casting plates with distilled water followed by 70% ethanol, and allow them to dry. Fix the cast in the mount. Pour 10 ml of resolving gel into the cast, followed by isopropanol to achieve a level surface. Allow the resolving gel to polymerize, then pour the stacking gel. Place a well separator and leave the gel to polymerize.
3.	Protein polyacrylamide gel - 10% Resolving gel	Resolving buffer (Tris-HCl, pH 8.8) 2.5 ml 30% Acrylamide 3.3 ml 10% SDS 100 µl 10% APS 100 µl TEMED 10 µl Distilled H_2O 4 ml	
4.	SOB Media	20 g Tryptone 5 g Yeast extract 0.5 g NaCl	Dissolve in 1 liter of distilled water; adjust the pH to 7.0 with 1 N NaOH; and autoclave.
5.	SOC Media	SOB Media 18 g of Glucose	After the SOB medium has been autoclaved. Add 20 mL sterile 1 M solution of glucose. Dissolving 18 g of glucose in 90 ml of H_2O. Filter by sterile.

6.	LB Agar Plate	5.0 g Yeast extract 10.0 g Peptone from casein 10.0 g Sodium chloride 12.0 g Agar-agar	Dissolve in 1 liter of distilled water, autoclave the mixture for 25 minutes at 120°C. Once cooled to 60°C, incorporate the desired antibiotic, and subsequently pour 10-20 ml into sterile plates. Store the plates at 4°C for a maximum of one week.

Antibiotics

1.	Ampicillin	Stock conc. 100 mg/ml, Working conc. 100 µg/ml.	Dissolve in autoclave distilled water and stored at -20°C.
2.	Carbenicillin	Stock conc. 100 mg/ml, Working conc. 100 µg/ml.	Dissolve in autoclave distilled water and stored at -20°C.
3.	Kanamycin	Stock conc. 50 mg/ml, Working conc. 50 µg/ml.	Dissolve in autoclave distilled water and stored at -20°C.
4.	Chloramphenicol	Stock conc. 25 mg/ml, Working conc. 25 µg/ml.	Dissolve in ethanol and stored at -20°C.

Table 2.2: Primer Information.

#	Primer	Sequence (5'-3')
Atoh1 Cloning		
1.	hAtoh1-His-F	ATATCATATGTCCCGCCTGCTGCATG
2.	hAtoh1-His-R	TAATGGATCCTAACTTGCCTCATCCGAG
3.	mAtoh1-His-F	ATATCATATGTCCCGCCTGCTGCATG
4.	mAtoh1-His-R	TAATGGATCCTAACTGGCCTCATCAGAG
5.	cAtoh1-His-F	ATAGGATCCATGAGCCTGCCGCGGGCCGCC
6.	cAtoh1-His-R	GTCAGAATTCTAGCTGGCCTCGTCCGAGTCACTG
7.	mAtoh1-GST-F	ATAGGATCCATGTCCCGCCTGCTGCAT
8.	mAtoh1-GST-R	ATCATGAATTCTAACTGGCCTCATCAGAGTCACT
9.	cAtoh1-GST-F	AATAGGATCCATGAGCCTGCCGCGGGC
10.	cAtoh1-GST-R	TCAGGAATTCTAGCTGGCCTCGTCCGAGTC
CRISPR/Cas9 chicken Atoh1 gRNA		
1.	Atoh1(+)strand	TTTCGTCTCCATTCGCCGAGCCATGAGCCTGCCGCGTTTAGAGACGAAA
2.	Atoh1(-)strand	TTTCGTCTCTAAACGCGGCAGGCTCATGGCTCGGCGAATGGAGACGAAA
3.	Control(+)strand	TTTCGTCTCCATTCGGCACTGCTACGATCTACACCGTTTAGAGACGAAA
4.	Control(-)strand	TTTCGTCTCCATTCGGGTGTAGATCGTAGCAGTGCGTTTAGAGACGAAA
5.	Atoh1-gRNA-T7-F	ATCTTATTCTGGGGGAGCAG
6.	Atoh1-gRNA-T7-R	CGAGGGCGCTGATGTAGATT

Table 2.3: Antibodies.

#	Antibody	Fixation and Blocking Condition	Incubation Condition	Catalogue No.
Immunoblotting				
1.	cAtoh1	Blocking with 5% Non-fat dried milk in TBST.	1:100 dilution in blocking buffer for overnight at 4°C on a shaker.	custom-built
2.	Anti-His	Blocking with 5% BSA in TBST.	1:200 dilution in blocking buffer for overnight at 4°C on a shaker.	TFS, Cat # MA1-135
3.	GST	Blocking with 5% BSA in TBST.	1:200 dilution in blocking buffer for overnight at 4°C on a shaker.	Abcam, Cat # ab9085
4.	Secondary Rabbit HRP	Blocking with 5% BSA in TBST.	1:1000 dilution in blocking buffer for 1 hr RT.	Sigma, Cat # A0545
5.	Secondary Mouse HRP	Blocking with 5% BSA in TBST.	1:1000 dilution in blocking buffer for 1 hr RT.	TFS, Cat # 31430
Immunohistochemistry				
1.	cAtoh1	4% PFA fixation at 4°C for 12 hrs. Antigen retrieval with citrate buffer. Blocking with 10% Goat serum, 1%BSA in PBST for 1 hour RT.	1:100 dilution for overnight at 4°C on a shaker.	custom-built

2.	Hair Cell Antigen (HCA)	4% PFA fixation at 4°C for 12-16 hrs. Blocking with 10% Goat serum, 1%BSA in PBST for 1 hr RT.	1:4000 dilution for overnight at 4°C on a shaker.	custom-built
3.	Myosin 7a	4% PFA fixation at 4°C for 12 hr. Blocking with 10% Goat serum, 1%BSA in PBST for 1 hr RT.	1:400 dilution for overnight at 4°C on a shaker.	DSHB, Cat# 138-1
4.	Sox2	4% PFA fixation at 4°C for 12 hr. Blocking with 10% Goat serum, 1%BSA in PBST for 1 hr RT.	1:400 dilution for overnight at 4°C on a shaker.	CST, Cat # 2748
5.	Calbindin D28K	4% PFA fixation at 4°C for 12 hrs. Blocking with 10% Goat serum, 1%BSA in PBST for 1 hr RT.	1:100 dilution for overnight at 4°C on a shaker.	TFS, Cat # 711443
6.	Phosphohistone H3 (PHH3)	4% PFA fixation at 4°C for 12 hr. Blocking with 10% Goat serum, 1%BSA in PBST for 1 hr RT.	1:200 dilution for overnight at 4°C on a shaker.	CST, Cat # 9701
7.	Anti-GFP	4% PFA fixation at 4°C for 12 hr. Blocking with 10% Goat serum, 1%BSA in PBST for 1 hr RT.	1:500 dilution for overnight at 4°C on a shaker.	Abcam, Cat # ab290
8.	Arl13b	4% PFA fixation at 4°C for 12 hr. Blocking 10% Goat serum, 1%BSA PBST for 1 hr RT.	1:200 dilution for overnight at 4°C on a shaker.	Abcam, Cat # ab136648

9.	Alexa Fluor-488 anti-rabbit	Blocking with 10% Goat serum, 1%BSA in PBST.	1:2000 dilution in blocking buffer for 1 hr RT.	TFS, Cat # A11008
10.	Alexa Flour-555 anti-rabbit	Blocking with 10% Goat serum, 1%BSA in PBST.	1:1000 dilution in blocking buffer for 1 hr RT.	TFS, Cat # A21428
11.	Alexa Fluor-647 anti-rabbit	Blocking with 10% Goat serum, 1%BSA in PBST.	1:1000 dilution in blocking buffer for 1 hr RT.	TFS, Cat # A21245
12.	Alexa Fluor-647 anti-mouse	Blocking with 10% Goat serum, 1%BSA in PBST.	1:1000 dilution in blocking buffer for 1 hr RT.	TFS, Cat # A21235
13.	Alexa Fluor-488 Phalloidin		1:500 dilution in PBST for 1 hr RT.	TFS, Cat # A12379
14.	Alexa Fluor-647 Phalloidin		1:500 dilution in PBST for 1 hr RT.	TFS, Cat # A22287

Table 2.4: Chemicals, Enzymes and Consumables.

#	Reagents	Catalogue No.
Chemicals		
1.	Paraformaldehyde	Sigma-Aldrich , Cat # 158127
2.	Glutaraldehyde (25 %)	Sigma-Aldrich, Cat # 340855
3.	Penicillin G sodium salt	Sigma-Aldrich, Cat # P3032
4.	N-2 Supplement (100X)	Thermo Fisher Scientific, Cat # 17502048
5.	Fluoroshield™	Sigma-Aldrich , Cat # F6182
6.	Osmium tetroxide (4%)	Sigma-Aldrich , Cat # 75632
7.	Dimethyl sulfoxide (DMSO)	Sigma-Aldrich , Cat # D8418
8.	Fast Green FCF	Sigma-Aldrich , Cat # F7252
9.	Sucrose	Sigma-Aldrich, Cat # 84097
10.	Sodium chloride	HiMedia, Cat # GRM853
11.	TWEEN® 20	Sigma-Aldrich, Cat # P1379
12.	Calcium Chloride ($CaCl_2$)	Thermo Fisher Scientific, Cat # Q12135
13.	DMEM, high glucose, GlutaMAX Supplement, pyruvate	Thermo Fisher Scientific, Cat # 10569010
14.	Click-iT EdU Kit	Thermo Fisher Scientific, Cat # C10338
Pharmaceutical Inhibitor		
1.	DAPT	Sigma-Aldrich , Cat # D5942
2.	CHIR99021	Sigma-Aldrich , Cat # SML1046
3.	XAV939	Sigma-Aldrich , Cat # X3004
Enzymes		
1.	Bovine Serum Albumin	Sigma-Aldrich, Cat # A9647
2.	Goat Serum Sterile filtered	HiMedia, Cat # RM10701
3.	Collagen I, rat tail	Thermo Fisher Scientific, Cat # A1048301
4.	Alt-R S.p. HiFi Cas9 Nuclease V3	Integrated DNA Technologies, Cat # 1081061
5.	Phusion HF DNA Polymerase	NEB, Cat # M0530S
6.	Q5 HF DNA Polymerase	NEB, Cat # M0491S
7.	T4 DNA Ligase	NEB, Cat # M0202S
8.	T7 Endonuclease I	NEB, Cat # M0302S

Consumables

1.	Amicon Ultra Centrifugal Filter, 10 kDa MWCO	Sigma-Aldrich , Cat # UFC901008
2.	HisTrap High Performance	Cytiva, Cat # 29051021
3.	GSTrap HP Columns	Cytiva, Cat # 17528101
4.	Millicell Cell Culture Insert, 30 mm, hydrophilic PTFE, 0.4 µm	Sigma-Aldrich, Cat # PICM03050
5.	Dumont #55 Forceps	FST, Cat # 11255-20
6.	Dumont #5 Forceps	FST, Cat # 11251-10
7.	Noyes Scissors, 14cm (5.5")	World Precision Instruments, Cat # 501237
8.	Standard Glass Capillaries 3 in, OD 1.0 mm, No Filament	World Precision Instruments, Cat # 1B100-3

2.1 Plasmids

2.1.1 Cloning

Bacterial Expression of Epitope-Tagged Recombination Atoh1 Protein

pET15b

To express the recombinant Atoh1 protein with a His tag, restriction digestion method was employed for cloning into the bacterial expression vector pET15b, which features a His tag for Atoh1 purification. Primers were designed for mAtoh1 and cAtoh1 gene amplification, incorporating NdeI in the forward primer and BamHI in the reverse primer. PCR amplification was carried out using Pfu polymerase. Subsequently, the PCR products for genes were purified using the Qiagen kit and then ligated into a pET15b vector that had been digested with NdeI and BamHI. Confirmation of the recombinant plasmids pET15b-mAtoh1 and pET15b-cAtoh1 was achieved through both colony PCR and Sanger sequencing.

pGEX-6P-1

To express the Atoh1 protein with a recombinant GST tag, mAtoh1 and cAtoh1 genes were cloned into the pGEX-6P-1 vector, incorporating the GST tag. The pGEX-6P-1 plasmid serves as a bacterial vector for expressing GST fusion proteins with a PreScission protease site. The primers were designed with BamHI and EcoRI restriction sites for gene insertion through restriction digestion and T4 ligation. Confirmation of the recombinant plasmids, pGEX-6P-1-mAtoh1 and pGEX-6P-1-cAtoh1, was achieved through both colony PCR and Sanger sequencing.

CRISPR/Cas9 Mediated Genome Editing Guide RNA

pcU6.1-sgRNA

For optimal sgRNA expression in chicken, pcU6.1-sgRNA (Addgene # 92395) with modified chick U6.1 promoter that drives the expression of guide RNA. The plasmid consists of tracrRNA and BsmBI-flanked cloning cassette for guide sequence insertion. To clone the guide sequence into the sgRNA scaffold of pCU6.1-sgRNA vector, two complementary oligos with BsmBI restriction site at both ends were synthesized (PAM site is not included in

the sgRNA sequence). Dissolve the sgRNA oligonucleotides into 100μM with autoclaved distilled water. Annealing of the two oligos sense and antisense guides is performed using thermocycler with following parameters; 95°C for 3 min then 37°C for 15 min and then decrease to 4°C slowly. Setup restriction digestion of the annealed oligos and pcU6.1-sgRNA cloning vector with BsmBI enzyme overnight. Setup ligation with gel purifies linear BsmBI-digested pcU6.1-sgRNA vector and digested sgRNA oligos. The mixture is then transformed into the DH5-alpha competent cell and the clones were confirmed by sanger sequencing.

2.1.2 Acquired Plasmids

pCAGGS-T2TP

The pCAGGS-T2TP vector features a CAG promoter, ensuring robust and widespread expression of transposase enzymes. This plasmid facilitates the integration of a transgene into the genome when combined with Tol2 transposase.

pT2K-CAGGS-eGFP

The pT2K-CAGGS-eGFP construct contains the eGFP gene flanked by the left and right ends of Tol2. Co-electroporation with pCAGGS-T2TP facilitates integration of the CAGGS-eGFP construct into the genome, leading to sustained expression of EGFP in the transfected cells throughout their lifespan.

pT2K-Hes5::nd2mScarlet

The pT2K-Hes5::nd2mScarlet construct serves as a Notch reporter, comprising a mouse Hes5 promoter driving the expression of a nuclear destabilized mScarlet protein. Upon co-electroporation with the transposase-containing plasmid pCAGGS-T2TP, this construct integrates into the genome. Expression of mScarlet indicates Notch activity, as the Hes5 promoter drives its expression in Notch-On cells. The destabilized nature of nd2mScarlet enables it to report on recent or active Notch signaling. In the absence of Notch activity for more than 10 hours, mScarlet expression ceases.

pT2K-5TCF::nd2mScarlet

pT2K-5TCF::nd2mScarlet is a transposon construct functions as a reporter for Wnt signaling, containing 5 TCF binding sites upstream of a minimal TK promoter that controls the expression of a nuclear destabilized mScarlet protein in cells responsive to Wnt signaling.

The nd2mScarlet exhibits a destabilized feature, allowing it to report on cells with activated Wnt signaling or those that have recently had Wnt activity. If the cells are not Wnt-responsive or the Wnt activity has ceased more than 10 hours ago, there will be no expression of mScarlet.

2.2 Bacterial Strains

2.2.1 DH5alpha

All the plasmids utilized in the study were cloned and propagated using DH5alpha bacterial strain due to its high transformation efficiency. DH5alpha strain carries the recA1 mutation, which aids in preserving plasmid stability, and the endA1 mutation, which protects the integrity of the plasmid by preventing DNA degradation during propagation within the bacteria.

2.2.2 BL21(DES)pLysS

BL21(DE3)pLysS is a genetically modified strain of E. coli bacteria specifically designed for high-level protein expression using the T7 promoter system. The Wild-type BL21 E. coli strains often have limitations for protein expression, such as the presence of proteases, BL21(DE3)pLysS lacks the genes for Lon and OmpT proteases, minimizing protein degradation. The DE3 component of this strain contains a prophage, λDE3, carrying the gene for T7 RNA polymerase, essential for efficient transcription under the T7 promoter. Additionally, the pLysS component provides two benefits, first the T7 lysozyme expression regulates basal T7 RNA polymerase activity, minimizing unwanted protein production before induction, and second is chloramphenicol resistance which aids in plasmid selection and maintenance. BL21(DE3)pLysS offers high-level protein expression and tight control of expression. The inducible nature of the T7 promoter system enables it to control protein production by adding a specific molecule, isopropyl β-D-1-thiogalactopyranoside (IPTG), at the desired time.

2.2.3 Rosetta-gami B(DE3)

Rosetta-gami B(DE3) is an engineered strain of E. coli tailored for enhanced expression of eukaryotic proteins. It combines features from three bacterial strains: BL21(DE3), providing a protease-deficient background and the T7 RNA polymerase gene; Origami, which reduces

thioredoxin activity to create a more oxidizing environment conducive to disulfide bond formation; and Rosetta, which introduces additional genes encoding rare tRNAs to facilitate efficient translation of eukaryotic protein codons uncommon in E. coli. This unique combination ensures improved expression of eukaryotic proteins in a bacterial system. Additionally, Rosetta-gami B(DE3) utilizes the T7 promoter system, similar to BL21(DE3)pLysS, enabling tight control and high-level expression of the target protein upon IPTG induction.

2.3 Atoh1 Expression & Purification

2.3.1 IPTG Induction for Atoh1 Expression

The BL21(DE3)pLysS bacterial strains were utilized to express His-tagged Atoh1 protein (pET15b-hAtoh1, pET15b-mAtoh1, and pET15b-cAtoh1), while the Rosetta-gami B(DE3) strain was employed for expressing GST-tagged Atoh1 (pGEX-6P-1-mAtoh1 and pGEX-6P-1-cAtoh1). Bacterial cultures containing Atoh1 expression plasmids were cultured in LB media at 37°C until the OD reached between 0.4 and 0.6. Upon reaching this point, IPTG (0.1-1 mM) was added to the media and maintained at 37°C overnight. Afterward, the bacterial culture was centrifuged to collect the bacterial pellet, which was then homogenized using a probe sonicator in the resuspension buffer, identical to the binding buffer. Following sonication, centrifugation was performed to separate the soluble protein fraction (supernatant) from the insoluble fraction (pellet). Both fractions were isolated and subjected to Western blot analysis for Atoh1 protein expression. The IPTG concentration and culture conditions were optimized based on Atoh1 protein expression and production in soluble fraction, with this optimized procedure scaled up to large batch cultivations (liter scale) for Atoh1 protein purification.

2.3.2 Affinity Chromatography

His-tag Purification

The purification of the Atoh1-His tagged protein was carried out using Immobilized Metal Ion Affinity Chromatography (IMAC). To ensure optimal yield and purity, conditions for purifying all recombinant His-tagged enzymes were fine-tuned through nickel affinity chromatography. Our purification setup employed an ÄKTAdesign liquid chromatography

system equipped with a HisTrap™ HP column, prepacked with precharged Ni Sepharose. The binding buffer consisted of 50 mM sodium phosphate, 300 mM NaCl, pH 6.5, and the elution buffer comprised 50 mM sodium phosphate, 300 mM NaCl, 500 mM imidazole, pH 7. Prior to use, the liquid chromatography system tubing was filled with distilled water. Remove the stopper and connect the column to the system tubing “drop-to-drop” to avoid introducing air into the system. Remove the snap-off end at the column outlet. Wash the column with 3–5 column volumes of distilled water. Equilibrate the column with at least 5 column volumes of binding buffer with a flow rate of 1 ml/min for the 1 ml columns. Before applying the lysate to the column, it was filtered through a 45 µm filter to ensure clarity. If the lysate was too viscous, it was diluted with binding buffer to prevent column clogging. Washing with the binding buffer continued until the absorbance at 280 nm reached a stable baseline. Elution was carried out using the elution buffer with a linear gradient of imidazole concentration, typically over 20 column volumes or more, to effectively separate proteins with similar binding strengths. The eluted fractions were subjected to SDS PAGE gel electrophoresis to verify purity and confirm the presence of the protein at the expected size. Fractions containing our protein of interest were pooled and loaded onto centrifugal concentrators to concentrate the purified Atoh1-His tagged protein.

GST-tag Purification

Glutathione S-transferase (GST) tagged Atoh1 proteins were expressed using pGEX-6P-1 expression vectors. These Atoh1-GST tagged proteins can be directly purified from pretreated bacterial lysates. The binding buffer used was PBS, pH 7.5 (140 mM NaCl, 2.7 mM KCl, 10 mM Na2HPO4, 1.8 mM KH2PO4), and the elution buffer consisted of 50 mM Tris-HCl, 10 mM reduced glutathione, pH 8.0. A peristaltic pump was employed alongside GSTrap FF, a prepacked, ready-to-use column. Prior to usage, the pump tubing was cleaned with the binding buffer. The column was connected to the pump tubing "drop to drop" to prevent air introduction, and the snap-off end at the column outlet was removed. Equilibration of the column was carried out with 5 column volumes of binding buffer. Sample application onto the column was accomplished by pumping it at a flow rate of 1 ml/min for a 1 ml column. Subsequent washing was performed with 5 to 10 column volumes of binding buffer or until no material was detected in the effluent. Elution was performed using the elution buffer with a linear gradient of reduced glutathione (10-50 mM). The eluted fractions underwent SDS PAGE gel analysis to identify impurities and confirm the presence of proteins of the correct size. Fractions containing the protein of interest were collected and

then loaded onto centrifugal concentrators to concentrate the purified Atoh1-GST tagged protein.

2.3.3 Size Exclusion Chromatography

Following affinity chromatography purification of both Atoh1-His tagged and Atoh1-GST tagged proteins, further purification was carried out via size-exclusion chromatography using a GE Superdex size exclusion column to enhance protein purity by eliminating impurities. Preparation entails equilibrating the GE Superdex column with the respective elution buffers used previously: 50 mM sodium phosphate, 300 mM NaCl, pH 7 for Atoh1-His tagged protein, and 50 mM Tris-HCl, 10 mM reduced glutathione, pH 8.0 for Atoh1-GST tagged protein, typically requiring approximately 2-3 column volumes. The concentrated purified Atoh1 protein is subsequently loaded onto the equilibrated GE Superdex column, often necessitating the use of a syringe. Elution is conducted using the same elution buffer, with the GE Superdex column separating proteins based on size, resulting in Atoh1 eluting at a specific volume relative to column calibration. Detection and collection involve monitoring the absorbance at 280 nm of the eluent as it exits the column, with Atoh1 exhibiting a peak at its elution volume, facilitating the collection of fractions around this peak for further analysis or storage.

2.4 Custom chicken Atoh1 Antibody Design

Due to the absence of commercially available antibodies for chicken Atoh1 protein, the experiment crucial for this thesis necessitated the development of a versatile antibody suitable for multiple applications, including immunoblotting, immunohistochemistry (IHC), immunoprecipitation (IP), and chromatin immunoprecipitation (ChIP).

2.4.1 Peptide Selection

Specific criteria were established for designing an efficient peptide immunogen, excluding regions containing the bHLH domain to prevent potential cross-reactivity. A peptide with antigenic epitopes at the C-terminal, characterized by surface-exposed, hydrophilic, and flexible regions of cAtoh1 protein, was selected. Two strategies were pursued for epitope selection: first, a peptide based on sequence homology to enable broader protein recognition across species by aligning multiple Atoh1 orthologs (Figure 2.1); second, selecting a unique peptide sequence specific to cAtoh1 to ensure no cross-reactivity with other chicken proteins,

enhancing specificity, reducing background, and improving signal detection. Striking a balance between immunogenicity and specificity, a unique 19-amino acid residue peptide (ERSKASPRSHRSDGEFSPR) was selected in chicken with conserved residues among Atoh1 homologs, ensuring antibody specificity to Atoh1 proteins across different species and avoiding cross-reactivity with other proteins within chicken.

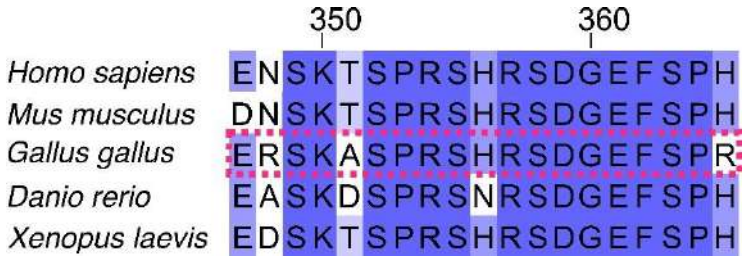

Figure 2.1 Antigen Peptide Selection for Atoh1 Antibody. A 19-amino acid residue peptide, conserved across Atoh1 homologs, was selected in the chick (indicated in pink box).

2.5 Molecular Techniques

2.5.1 Immunoblotting (Western Blot)

Dissected inner ear from chicken/mouse are lysed using micro pestle in PBS containing 0.5% Triton X-100, 150 mM NaCl, 5 mM EDTA, 1 mM AEBSF & 1X MS-SAFE protease and phosphatase inhibitor. Proteins were separated by SDS-PAGE and transferred to polyvinylidene difluoride (PVDF) membranes. The membrane was blocked in 5% BSA in 0.1% TBST and incubated with the primary antibodies at 4 °C overnight and then with peroxidase-conjugated anti-mouse or anti-rabbit IgG (GE Healthcare). Immunoreactive proteins were detected with Amersham ECL Prime Western blotting detection reagent (GE Healthcare).

2.5.2 Immunoprecipitation (IP)

Immunoprecipitation of chicken Atoh1 is performed using custom cAtoh1 peptide antibody. The inner ear from chicken were dissected from E10 stage and are lysed using micro pestle in PBS containing 0.5% Triton X-100, 150 mM NaCl, 5 mM EDTA, 1 mM AEBSF & 1X MS-SAFE protease and phosphatase inhibitor. After incubation at 4 °C for 30 min, lysates were cleared by centrifugation (15,000 x g for 10 min), then further cleared with Dynabeads M-270 Epoxy beads (Thermo Fisher Scientific). The cleared lysates were incubated with custom cath1 rabbit antibody coupled with Dynabeads M-270 Epoxy beads at 4 °C for 2 hrs. The

affinity-purified protein complex was washed three times with lysis buffer and eluted by boiling in SDS-PAGE sample buffer at 95°C for 10 min. The samples are loaded along with molecular weight markers on SDS PAGE gel.

2.5.3 Immunohistochemistry (IHC)

Antigen Retrieval

Slides were initially washed with distilled water for 2 minutes. Antigen retrieval was then carried out by placing the slides in a staining container and subjecting them to steam in a pressure cooker set at high pressure (approximately 120°C). This process was conducted with 200ml of 10mM citrate buffer, 0.05% Tween 20, at a pH of 6, for a duration of 15 minutes. Following antigen retrieval, the slides were allowed to cool within the pressure cooker for 10 minutes before the pressure was released. Subsequently, the slides were moved to hot distilled water for an additional 2 minutes. A thorough flush with running tap water lasting 5 minutes followed. Once these steps were completed, the staining protocol was initiated.

Whole mount Immunostaining

At the desired developmental stage, the inner ear was carefully dissected within ice-cold PBS, without Ca2+ and Mg2+ ions. It was then promptly fixed in 4% paraformaldehyde (dissolved in PBS) at room temperature for a period ranging from 1 to 4 hours on a shaker. Following this, the basilar papilla was meticulously micro dissected in PBS. For the subsequent permeabilization process, the basilar papilla was exposed to a 0.3% PBST (Tween-20) solution for a duration of 20 minutes at room temperature. Following this, a blocking buffer composed of 10% goat serum and 1% BSA within a 0.3% PBST solution was applied and allowed to incubate at room temperature for 2 hours. After this the basilar papilla was subjected to an overnight incubation in primary antibodies, appropriately diluted in the previously mentioned blocking buffer at 4°C, facilitated by a shaker, in a 48-well plate. The subsequent steps involved thorough washing of the samples using PBST, followed by another incubation phase of 1 hour at room temperature, this time with secondary antibodies (at a dilution ratio of 1:500) and Alexa Fluor-conjugated Phalloidin (at a dilution ratio of 1:600). Following this, secondary incubation, the samples underwent further washing. Subsequently, the samples were counterstained using DAPI for a span of 15 minutes, followed by an additional washing step utilizing PBST. Finally, the prepared samples were mounted using fluoroshield. For imaging, the confocal microscopy technique was employed, utilizing the

Olympus FV 3000 inverted microscope located at CIFF NCBS. Images were captured using 40X and 60X oil immersion objective lenses with a numerical aperture of 1.4 and 1.42 respectively, with a step size of 0.5µm.

Cryosection Immunostaining

The inner ear was dissected at the desired developmental stage in ice cold PBS (devoid of Ca2+ & Mg2+). Following this, it was fixed overnight at 4˚C using a 4% PFA solution. Subsequently, the cochlear duct was isolated and subjected to a gradual equilibration process involving successive immersion in 10%, 20%, and 30% sucrose solutions (in PBS). The tissue was then embedded in Leica tissue freezing medium and frozen. Cross-sections of the tissue, measuring 10µm in thickness, were obtained using cryostat starting from the distal side and progressing towards the proximal side of the cochlear duct. These sections were subjected to a drying process at 37˚C for 1 hour, after which they were permeabilized using PBST (0.5% Tween-20) for a duration of 10 minutes. To prevent nonspecific binding of the antibodies, the sections were incubated in a blocking solution composed of 10% goat serum and 1% BSA diluted in PBST for 2 hours. For the immunostaining process, the primary antibody (diluted in the blocking buffer) was allowed to incubate overnight at 4˚C. Following this step, the sections underwent thorough washing with PBST and were subsequently incubated with secondary antibodies (at a dilution of 1:1000) along with alexa fluor-conjugated Phalloidin (dilution 1:1000), both diluted in PBST. After another round of washing, the sections were counterstained with DAPI for 15 minutes and mounted in fluoroshield. The imaging process was conducted using a FV3000 upright confocal microscope situated at CIFF NCBS. The images were captured utilizing 20X water immersion and 40X oil immersion objective lenses, possessing numerical apertures of 1.4 and 1.42, respectively. The imaging procedure employed a step size of 0.5µm.

2.6 Cell Culture

To passage cells, begin by preheating the media at 37°C in a water bath for 5-10 minutes, while also placing the petri dish, 15ml falcon, and serological pipettes in the hood under UV light. Next, wipe the media bottle with alcohol before placing it in the hood. Retrieve the petri dish containing cells from the incubator and carefully remove the media with an aspirator for adherent cells, followed by washing with 5-10 ml of complete media. Add 1-2mL of Trypsin to the cells in the petri dish and incubate them in the incubator for 2-5

minutes to detach the adherent cells. Afterward, add 8-9 ml of complete media to the trypsinized cells, mix well, and centrifuge at 1000 rpm for 1 minute. Discard the supernatant media and resuspend the cells in 5ml of fresh media. Plate the cells either in a 1:5 - 1:10 ratio or at a density of around 2*105 cells / ml after counting, then return them to the incubator.

2.7 CRISPR/Cas9 System for Gene Editing

The CRISPR/Cas9 system stands as a versatile and robust tool for genome editing across a spectrum of organisms, including applications in livestock animals. However, the success of a genome-editing experiment hinges on thoughtful considerations of various factors such as the nature of the target locus, the design of the single guide RNA (sgRNA), and the selection of an appropriate delivery method. In our strategy, a key focus is on selecting sgRNAs that precisely target the Cas9 nuclease to the exons of protein-coding genes. For creating gene knockouts guide RNA should be designed to disrupt the exons region of the gene, preferably closer to the 5' end of the coding region to generate an adequate N-terminal protein truncation. This approach ensures a targeted and specific impact on the genomic sequence. Specifically, in experiments aimed at generating knockouts, our design revolves around disrupting exons that are shared by all transcript variants of a particular gene. This strategic choice enhances the efficiency and effectiveness of the knockout process. Moreover, in certain cases, employing multiple sgRNAs to induce substantial deletions, effectively eliminating entire gene loci. This approach allows for the creation of specific and extensive genomic modifications. Once the Cas9 nuclease induces breaks in the DNA at the targeted sites, the subsequent repair occurs through the error-prone non-homologous end joining mechanism for double-strand breaks (DSBs). This repair process introduces insertions or deletions (indels) at the cleavage site. The indels, particularly in the coding regions of genes, often lead to frame-shift mutations and the generation of premature stop codons. These alterations, in turn, trigger nonsense-mediated mRNA decay, resulting in the elimination of the mutated mRNA.

2.7.1 CRISPOR Guide RNA Designing Tool

Guide RNAs for CRISPR-Cas9 genome editing experiments are designed using the CRISPOR web tool[214]. The specificity and efficiency of cleavage primarily rely on the selection of the CRISPR guide sequence. The browser data is configured for Gallus gallus (chicken), with the protospacer adjacent motif (PAM) sequence set to 5'- NGG -3' for

SpCas9. Potential guide RNAs are chosen from the input sequence and ranked based on various scores that assess potential off-target effects in the genome of interest and predict on-target activity. To design template-specific oligos for guide RNA production, exclude the PAM sequence (5′- NGG -3′) from the output of the guide RNA design tool, as it is unnecessary for targeting but contains the Cas9 cleavage recognition sequence. The remaining 20 nucleotides are then cloned into pcU6.1-sgRNA vector, in frame with scaffold tracrRNA to synthesize full-length sgRNA. The cloned plasmids are pcU6.1-Atoh1-gRNA with chicken Atoh1guide sequence CCGAGCCATGAGCCTGCCGC and pcU6.1-Control-gRNA with control guide sequence GCACTGCTACGATCTACACC, sourced from literature[215] (Figure 2.2).

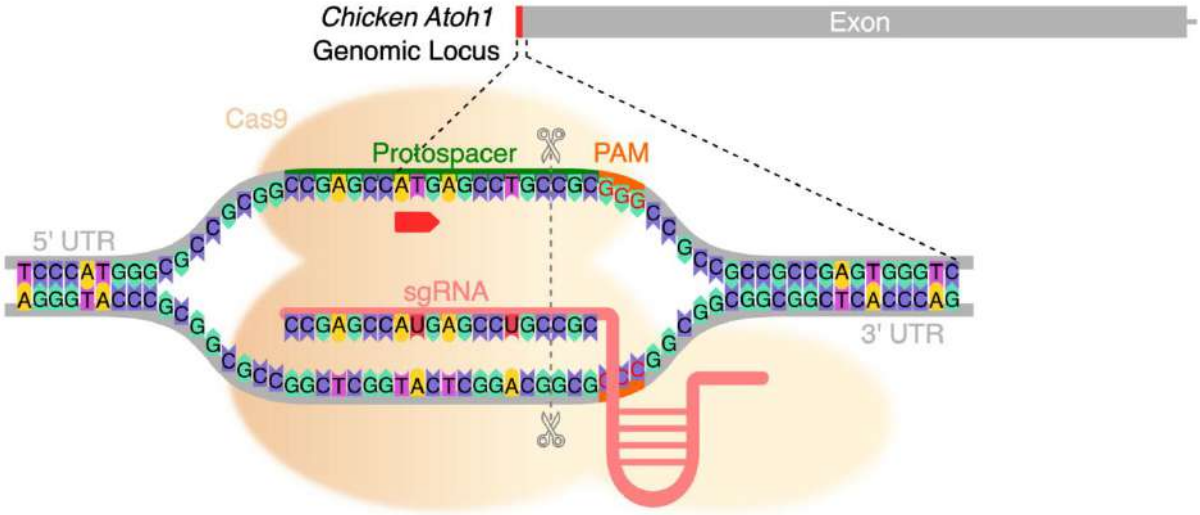

Figure 2.2 Atoh1-gRNA Design. The figure illustrates CRISPR/Cas9-mediated knockout targeting of Atoh1 gene in chick shown by a single gray box, indicating its exonic region. The Cas9 nuclease and sgRNA complex bind to a specific DNA sequence (highlighted in red) flanking the Atoh1 start codon. Target sequence includes a critical motif called the PAM sequence (marked in orange). The protospacer sequence recognized by the sgRNA is labelled in green.

2.7.2 T7 Endonuclease1 Assay

Selecting an effective sgRNA is crucial for enhancing the gene editing efficiency of CRISPR/Cas9 systems, as it plays a pivotal role in ensuring target specificity and cleavage efficiency. A widely used technique for evaluating the effectiveness of sgRNA cleavage is the T7 endonuclease 1 mismatch detection assay, which relies on the identification and cleavage of imperfectly paired double-stranded DNA. The T7 endonuclease assay methodology involves several steps. First, the DNA containing the target site where cleavage occurred was PCR amplified and purified (Figure 2.3 A). Next, the DNA was denatured at

94°C and then annealed to form heteroduplex DNA. Subsequently, T7 nuclease I treatment was performed for 1 hour at 37°C. Finally, the results were analysed using 2% agarose gel electrophoresis (Figure 2.3 B).

To evaluate the effectiveness and assess the cleavage efficiency of Atoh1-gRNA in chicken cells, we transfected pcU6.1-Atoh1-gRNA to DF1 cells, which are chicken embryonic fibroblast cells. After 48-hour transfection period, DNA was extracted for PCR amplification of genomic regions surrounding the Atoh1-gRNA target sites, using the primers Atoh1-gRNA-T7-F: ATCTTATTCTGGGGGAGCAG and Atoh1-gRNA-T7-R: CGAGGGCGCTGATGTAGATT.

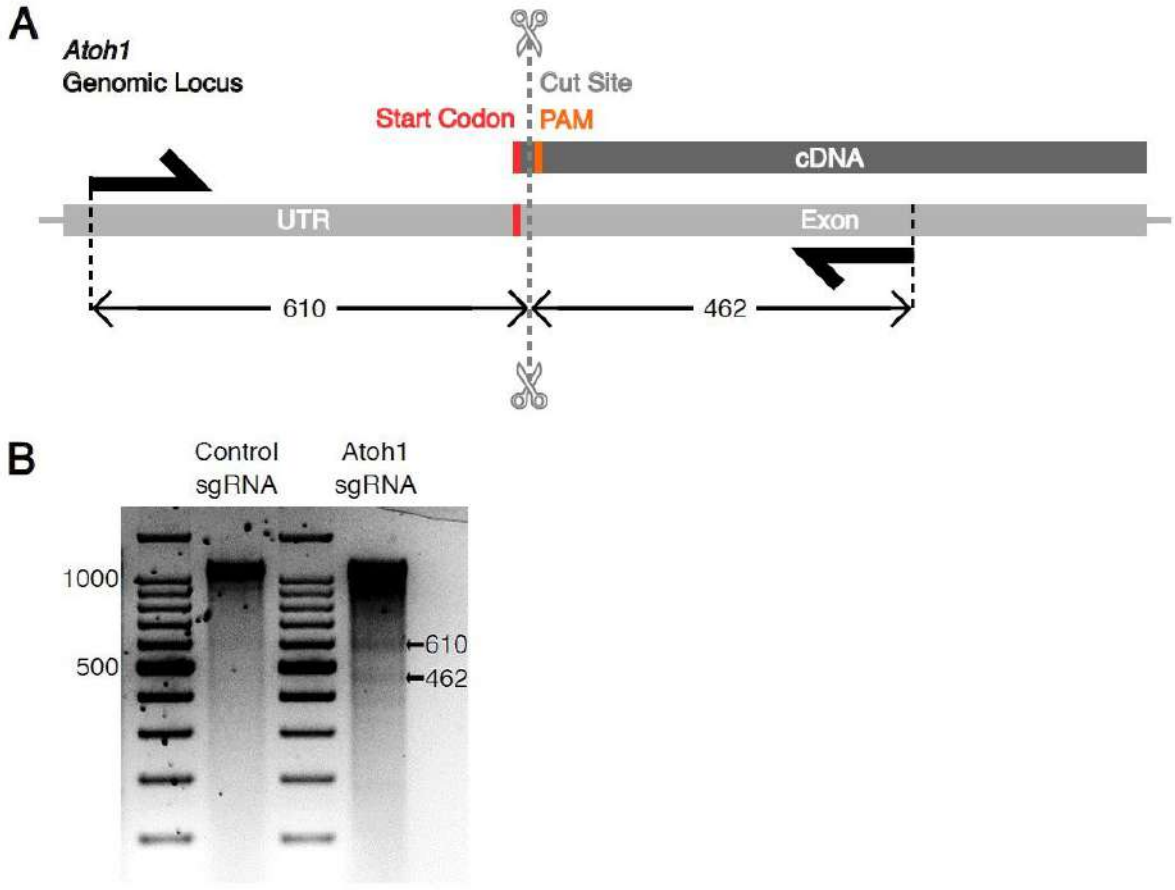

Figure 2.3 T7 Endonuclease 1 Assay for gRNA Cleavage Validation. (A) Chick Atoh1 Locus, drawing highlights the Atoh1 start codon (red) and its nearby PAM sequence (orange), indicating a potential CRISPR/Cas9 cleavage site. Half arrowheads mark the primers used for T7 endonuclease I assay, a forward primer in the untranslated region and a reverse primer within the Atoh1 exon. (B) visualizes the outcome of Cas9 activity using gel electrophoresis. Arrows indicate the sizes of two DNA fragments generated after T7 endonuclease I cleavage, confirming site-specific cleavage by Cas9.

2.8 Chicken Embryo Manipulation

2.8.1 Egg Handling and Windowing

Ensuring embryo viability involves several considerations. It is essential to use fresh eggs, as prolonged storage prior to incubation can lead to increased mortality and abnormal development. To begin, fresh eggs are cleaned and sanitized with 70% ethanol before being placed in an incubator set at 37-38°C with 45% humidity for 3.5-4 days. Before accessing the embryo, the egg is positioned on its side for at least 10 minutes to allow the embryo to reposition to the top of the yolk. Small holes are then carefully made at the blunt end and the top of the egg using forceps. Approximately 2 ml of albumin is extracted through the hole at the blunt end using a 5ml syringe and a 21G needle. The hole is then sealed with scotch tape. Additionally, scotch tape is applied to the top of the shell to prevent eggshell debris from entering during windowing. A window is cut into the eggshell to expose the embryo, and any extraembryonic membranes covering the embryo are removed with sharpened forceps to facilitate direct access.

2.8.2 Otocyst Microinjection

To optimize otocyst microinjection technique, a mixture of two plasmid solutions are needed: one containing pCAGGS-T2TP vector for expression of transposase, and another containing pT2K-CAGGS-eGFP construct expressing eGFP. These plasmid solutions are combined with Fast Green dye and sucrose. Microinjection needles are created by pulling glass capillaries using a pipette puller (Narishige PC-10), with the tip diameter adjusted to approximately 10 µm by breaking off the capillary tip after pulling. At the embryo stage E4, embryos are typically positioned on their left side with the head turned to the right, allowing access to only the right otic vesicle for microinjection. The solution is then injected into the otic vesicle, and the injection volume is monitored by observing the distribution of the green dye, ensuring that the otic vesicle is completely filled.

2.8.3 In Ovo Electroporation

To prepare for electroporation, a few drops of Saline 0.719% are applied on top of the embryo to reduce electric resistance and prevent overheating. Electrodes are positioned parallel along the dorsal-ventral axis of the spinal cord (Figure 2.4). The electroporation process involves transfecting plasmids into embryo cells using a square pulse generator (Nepagene CUY-21), delivering five pulses of 25V each with a duration of 100ms, although

these parameters may need adjustment based on individual electroporation setups. Following electroporation, additional saline 0.719% is added to cool the embryo, and the electrodes are rinsed with distilled water to remove denatured proteins. Finally, the egg is resealed with scotch tape and returned to an incubator set at 37-38°C until the desired stage is reached.

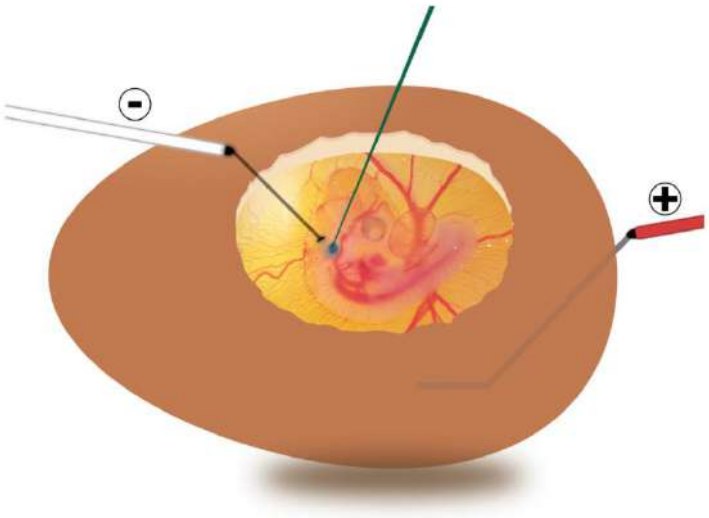

Figure 2.4 In Ovo Electroporation Technique. Schematic depicts the technique of in ovo microinjection and electroporation for targeting the chick otic vesicle at embryonic day 4 (E4).

2.8.4 Basilar Papilla Dissections

Before commencing the dissection process, thorough sterilization of the surgical table, microscope stage, and surrounding area is carried out using 70% ethanol. Additionally, microdissection equipment such as spring-bow scissors, micro-curette, and forceps (including two each of Dumont Inox #5 and #55) are sterilized either through heat or alcohol. Dissection plates including a glass petri dish with a black sylgard base, a 90mm plastic petri dish, and a 60mm petri dish are prepared for use. The dissection media, typically phosphate-buffered saline or Tyrode's solution, is chilled. The egg is gently cracked open into the 90mm petri dish, and the embryo is decapitated with scissors, with the head transferred to the 60mm petri dish containing ice-cold PBS. Next, the embryo is oriented with the beak facing forward, and the eyes are removed using forceps. Following this, the skin over the skull is incised from rostral to caudal, and the brain is scooped out. After adding more ice-cold PBS, two shiny structures representing the otoliths of the lagena at the end of the cochlear duct are located close to the midline. A cut is made between the two lagena to isolate two inner ears, and excess tissue and the vestibule are removed. Subsequently, the cochlea is transferred to a sylgard plate with ice-cold PBS, and using forceps, the cochlear capsule is peeled away to

access the cochlear duct. Finally, the undulated layer (tegmentum) of the cochlear duct is located and removed using forceps to expose the basilar papilla.

2.8.5 Basilar Papilla Explant

The ex-ovo culture of basilar papilla using collagen cultures offers a valuable approach for conducting inhibition studies and live imaging. By culturing basilar papilla explants within a 3D collagen matrix, tissue morphology is well preserved, enabling detailed examination of changes in tissue patterning, polarity, and differentiation. To initiate the culture, a collagen mixture comprising 400µl of 3mg/ml rat tail collagen, 50µl of 10X DMEM, 30µl of 7.5% NaHCO3, and 5µl HEPES is prepared in a tissue culture hood. Subsequently, three drops of the collagen mixture are added into each well of a 4 well plate, and dissected cochlear ducts are transferred to each collagen drop. The plate is then incubated for 10 minutes at 37℃ and 5% CO2 to allow the collagen matrix to cure effectively.

2.9 Pharmacological Treatment with Small Molecules

During Basilar papilla explant culture, specific small molecule inhibitors and activators were added to the culture media. The compounds utilized in this study included DMSO, XAV939 inhibitor, CHIR99021 activator, and DAPT inhibitor. After the designated incubation period, the samples underwent three washes with PBS followed by fixation using a 4% paraformaldehyde solution dissolved in PBS. This preparation aimed to facilitate subsequent immunostaining procedures.

2.10 Proliferation EdU Assay

The necessary components for EdU labeling and detection are included in the Click-iT EdU kits, obtained from the Invitrogen catalogue. EdU, a thymidine analog, is incorporated into DNA during the S phase and serves to assess cell proliferation. At the specified developmental stage, inner ears are carefully dissected using ice-cold PBS and then embedded in a collagen matrix culture. An EdU solution of 10µM in sterile PBS is prepared and added to the explant culture media. The EdU exposure lasts for one day in vitro. Following this exposure period, the samples are fixed using a 4% paraformaldehyde (PFA) solution, after which the cochlear duct explants undergo EdU staining and subsequent immunostaining procedures.

2.11 Image Processing & Analysis

For morphological analysis of the tissue, images obtained from confocal microscopy were segmented using the Tissue Analyzer (TA) plugin within the FIJI software[216]. Manual corrections were applied as necessary to ensure accuracy. Subsequently, cells were categorized as either hair cells (HC) or supporting cells (SC) based on Myosin 7a antibody staining. TA generated comprehensive cell and bond datafiles for each image. Using these datafiles, we calculated the number of neighboring cells for each HC and SC using Excel macro functions. Additionally, the apical surface area of each cell was measured from the TA-derived database. Both manual labeling and automated cell counting techniques within FIJI were employed for cell counting.

2.12 Statistics

To ensure consistent and reliable results, the CRISPR-Cas9 gene manipulation experiments were spread out across different days, minimizing the influence of potential batch effects. Each experimental condition utilized three embryos (n=3). Within each embryo, the left inner ear served as an internal control, while the right inner ear received the injectable control, which involved the electroporation of a control guide. To evaluate the statistical significance of any differences observed between conditions, Student's t-tests were performed. The results are presented using an asterisk notation (*P<0.05, **P<0.01, ***P<0.001, ****P<0.0001) to indicate the level of significance for each comparison.

Chapter 3: Atoh1 Purification and Antibody Validation

Atoh1 is a master regulator of HC differentiation and development, making it a key target for understanding the molecular mechanisms underlying HC formation and regeneration. However, there are currently no commercial antibodies available for performing immunoprecipitation or related applications. Our objective was to perform ChIP-seq to identify Atoh1's downstream targets, which required developing a specific and functional anti-Atoh1 antibody. To achieve this, we generated a recombinant Atoh1 protein to serve as an antigen for antibody production. Chapter 3 outlines the process of purifying the full-length recombinant Atoh1 protein and validating the resulting antibody for its specificity and suitability in various experimental applications.

3.1 Bacterial Expression of Epitope-Tagged Atoh1

3.1.1 Amplifying Atoh1 gene

We amplified the Atoh1 gene from three species: human (hAtoh1), mouse (mAtoh1), and chick (cAtoh1) Atoh1 (Figure 3.1 A, B, C). hAtoh1 and mAtoh1 were PCR amplified from cDNA, while the cAtoh1 gene was amplified using a BAC clone. Refer to the Primer table for primer details. The hAtoh1 gene has a 1062 bp coding sequence (CDS) encoding a 38.1 kDa protein, mAtoh1 has a 1053 bp CDS encoding a 37.8 kDa protein, and cAtoh1's gene, with an 822 bp CDS, encodes a protein of 28.4 kDa in size.

3.1.2 Atoh1-His Tag Protein Expression

The expression of hAtoh1-His tag and mAtoh1-His tag proteins was verified with Western blot using monoclonal Anti-His antibody (Figure 3.1 D). The uninduced IPTG controls exhibited bands at the expected molecular weight, indicating leaky expression from the pET15b plasmid. Additionally, an increase in the soluble fraction expression of both hAtoh1-His and mAtoh1-His was observed with higher IPTG concentrations.

cAtoh1 expression was not detected in the BL21(DE3)pLysS bacterial strain. This could be due to the expression of a eukaryotic protein containing rare codons, prompting us to switch to the Rosetta-gami bacterial strain. However, even after changing the bacterial strain, there was no significant improvement in cAtoh1 expression, although a very faint cAtoh1 expression was detected using Anti-His antibody (Figure 3.1 E). Therefore, we

replaced the His tag with a GST affinity tag, as GST-fused proteins have better cAtoh1 expression and increased solubility.

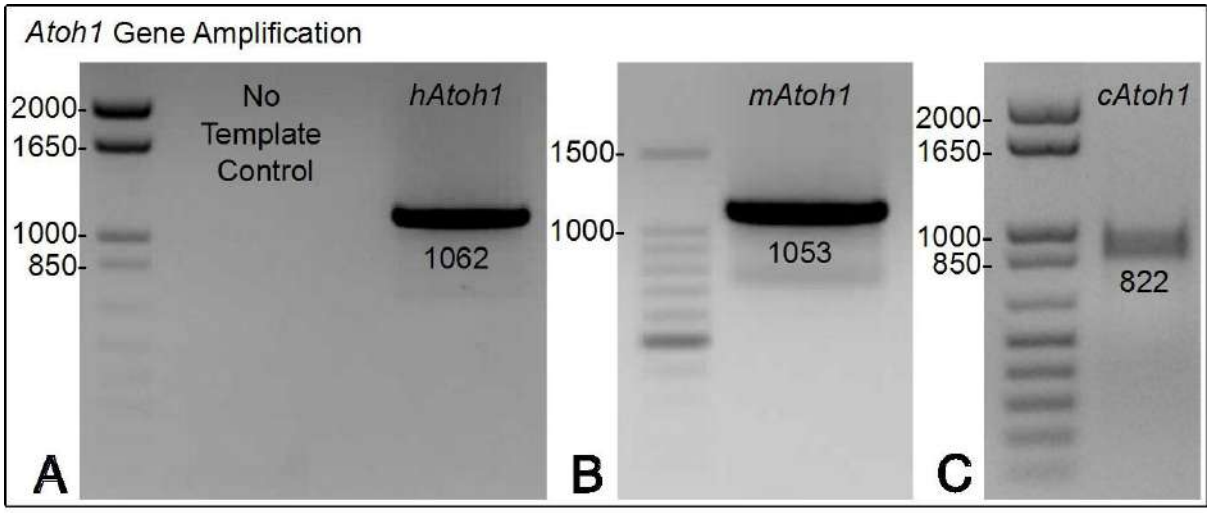

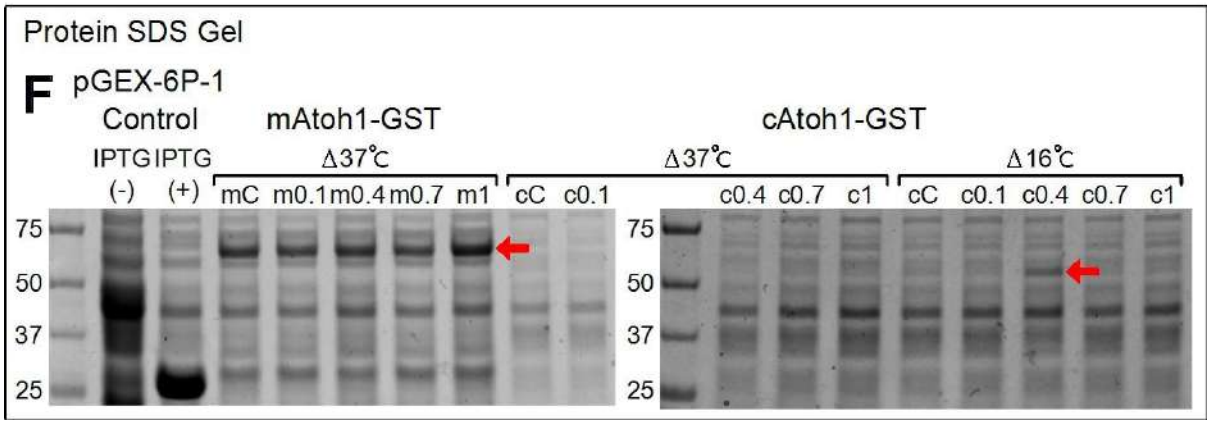

Figure 3.1 Atoh1 Gene Amplification and Protein Expression. Agarose gel electrophoresis of PCR amplification of gene (A) hAtoh1, (B) mAtoh1 and (C) cAtoh1. (D and E) shows protein expression levels. Western blot analysis with an anti-His antibody reveals Atoh1 protein levels in hAtoh1-His, mAtoh1-His, and cAtoh1-His following treatment with varying concentrations of IPTG. The black and red boxes in (D) highlight hAtoh1-His and mAtoh1-His protein bands, respectively. (E) shows the expression of cAtoh1-His protein. (F) SDS-PAGE gels stained with Coomassie blue for mAtoh1-GST and cAtoh1-GST fusion proteins produced under different IPTG conc. and temperature. The red arrow marks the band of interest at the right size.

3.1.3 Atoh1-GST Tag Protein Expression

The pGEX-6P-1-mAtoh1 and pGEX-6P-1-cAtoh1 plasmids are introduced into the E. coli strain Rosetta-gami B(DE3) to boost the expression of the eukaryotic protein and facilitate the formation of target protein disulfide bonds in the bacterial cytoplasm. Glutathione S-transferase (GST) has a molecular weight of 28 kDa. The mAtoh1-GST fusion proteins weigh approximately 65.8 kDa, while the cAtoh1-GST proteins weigh around 56.4 kDa.

To enhance protein expression, we tested various culture conditions with different IPTG concentrations. We analysed mAtoh1 and cAtoh1 expression using SDS-PAGE gel electrophoresis on crude bacterial lysates. The control plasmid without IPTG (P0) showed no GST expression, whereas the IPTG-induced control plasmid (PI) exhibited a GST band of the expected size. mAtoh1-GST protein expression was detected at the desired molecular weight, with mAtoh1 expression notably increasing as IPTG concentration increased. For cAtoh1-GST protein expression, we observed a faint band at the desired molecular weight under one culture condition, however IPTG concentration did not influence its expression (Figure 3.1 F).

3.2 Atoh1 Purification

3.2.1 Ni – NTA affinity purification of mAtoh1 proteins

The mAtoh1 recombinant protein features a His tag at its N-terminus, consisting of six consecutive histidine residues to aid in purification. The His-tagged mAtoh1 protein was purified using Ni-NTA affinity chromatography, following a bind-wash-elute protocol. After column loading, sequential washes were performed with binding buffer (50 mM sodium phosphate, 300 mM NaCl, pH 6.5), followed by elution of mAtoh1 protein using an elution buffer (50 mM sodium phosphate, 300 mM NaCl, 500 mM imidazole, pH 7) with a linear imidazole gradient. Starting at 150 mM imidazole, the concentration increased by 50 mM with each step, reaching 300 mM where an increase in absorbance at both 260 nm and 280 nm was observed (Figure 3.2 B). All eluate fractions were collected and analysed by SDS-PAGE gel electrophoresis to confirm protein size (Figure 3.2 A, B). Fractions containing mAtoh1-His were combined and further purified using a size exclusion column (Figure 3.2 C, D). Protein concentrations were determined using a BCA protein assay with BSA as the standard, resulting in a mAtoh1-His concentration of 550.6 μg/ml.

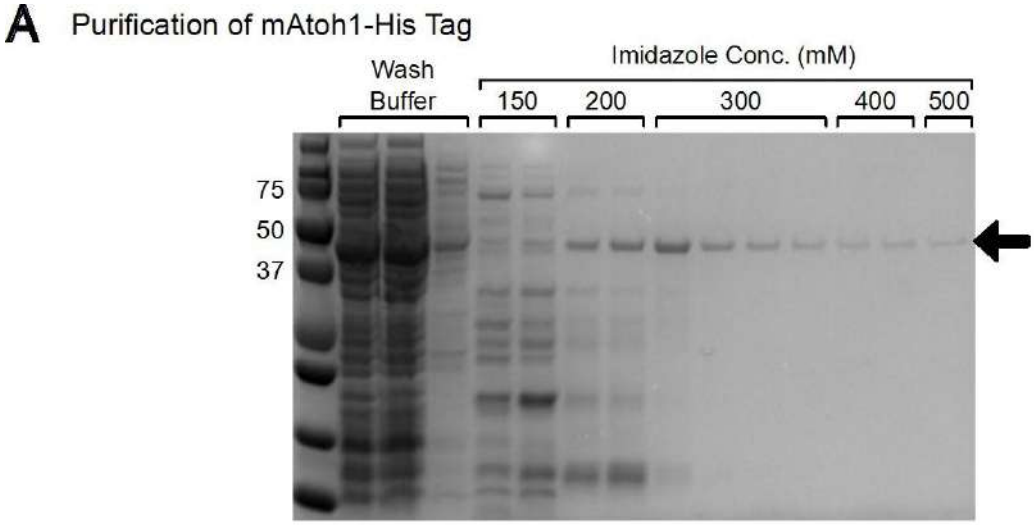
A
Purification of mAtoh1-His Tag
Wash Buffer
Imidazole Conc. (mM)
150
200
300
400
500
75
50
37

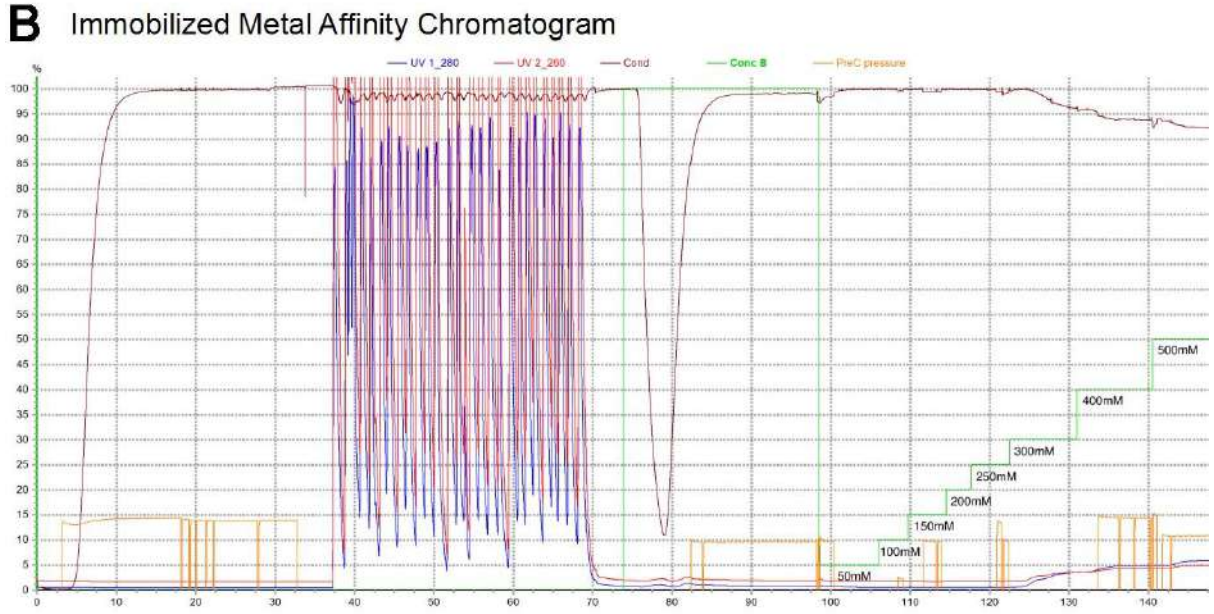
B
Immobilized Metal Affinity Chromatogram
UV 1_280
UV 2_260
Cond
Conc B
PreC pressure
%
50mM
100mM
150mM
200mM
250mM
300mM
400mM
500mM

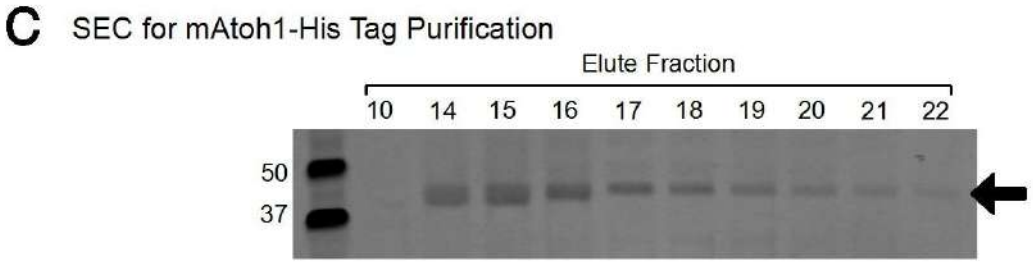
C
SEC for mAtoh1-His Tag Purification
Elute Fraction
10
14
15
16
17
18
19
20
21
22
50
37

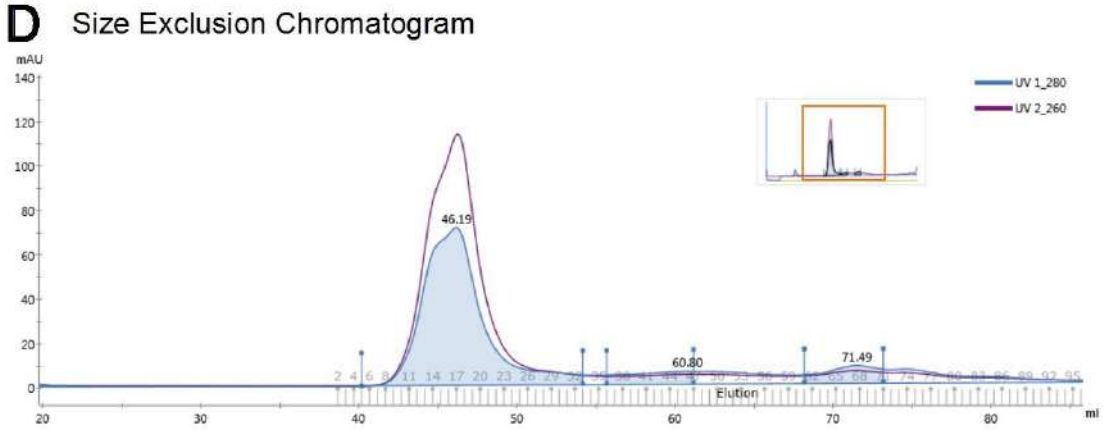
D
Size Exclusion Chromatogram
mAU
UV 1_280
UV 2_260
46.19
60.80
71.49
Elution
ml

Figure 3.2 Recombinant mAtoh1-His Protein Purification. (A) SDS-PAGE gel showing bands of purified mAtoh1-His protein (arrow) in elution fraction at different conc. imidazole. (B) Chromatogram profile for mAtoh1-His purification. (C) SDS-PAGE gel stained with Coomassie dye to visualize elute fractions of mAtoh1-His protein (arrow) purified with size exclusion chromatography. (D) Size exclusion chromatogram for mAtoh1-His protein.

3.2.2 GST affinity purification of mAtoh1 protein

To purify mAtoh1-GST tagged proteins, bacterial pellets are resuspended in a binding buffer (140 mM NaCl, 2.7 mM KCl, 10 mM Na2HPO4, 1.8 mM KH2PO4, pH 7.5) and loaded onto a GSTrap FF column using a peristaltic pump. For elution of mAtoh1-GST protein, an elution buffer (50 mM Tris-HCl, reduced glutathione, pH 8.0) with a linear gradient of reduced glutathione (10-50 mM) is used (Figure 3.3 A). After serial washing with binding buffer, all the eluted fractions are collected and run on SDS PAGE to check for impurities and confirm the protein of the correct size. All fractions containing the protein of interest are collected, and the protein is concentrated using a protein concentrator with a molecular weight cutoff of 10kDa. This concentrated protein is then loaded onto a pre-equilibrated GE Superdex size exclusion column for further purification (Figure 3.3 B, C). The BCA protein estimation assay indicates a mAtoh1-GST protein yield of 1.9 mg. The mAtoh1-GST tagged protein includes a protease site. To remove the GST tag from the fused recombinant mAtoh1 protein, digestion is performed in a dialysis bag using cleavage buffer (50 mM Tris-HCl, 150 mM NaCl, 1 mM EDTA, 1 mM dithiothreitol DTT, pH 7.5) with PreScission protease enzyme overnight at 4°C. Subsequently, reverse phase purification is conducted using the GSTrap FF column, allowing the free GST protein to bind to the column while the cleaved mAtoh1 protein passes through in the flow-through. Unfortunately, a significant amount of mAtoh1 protein is lost after enzymatic cleavage.

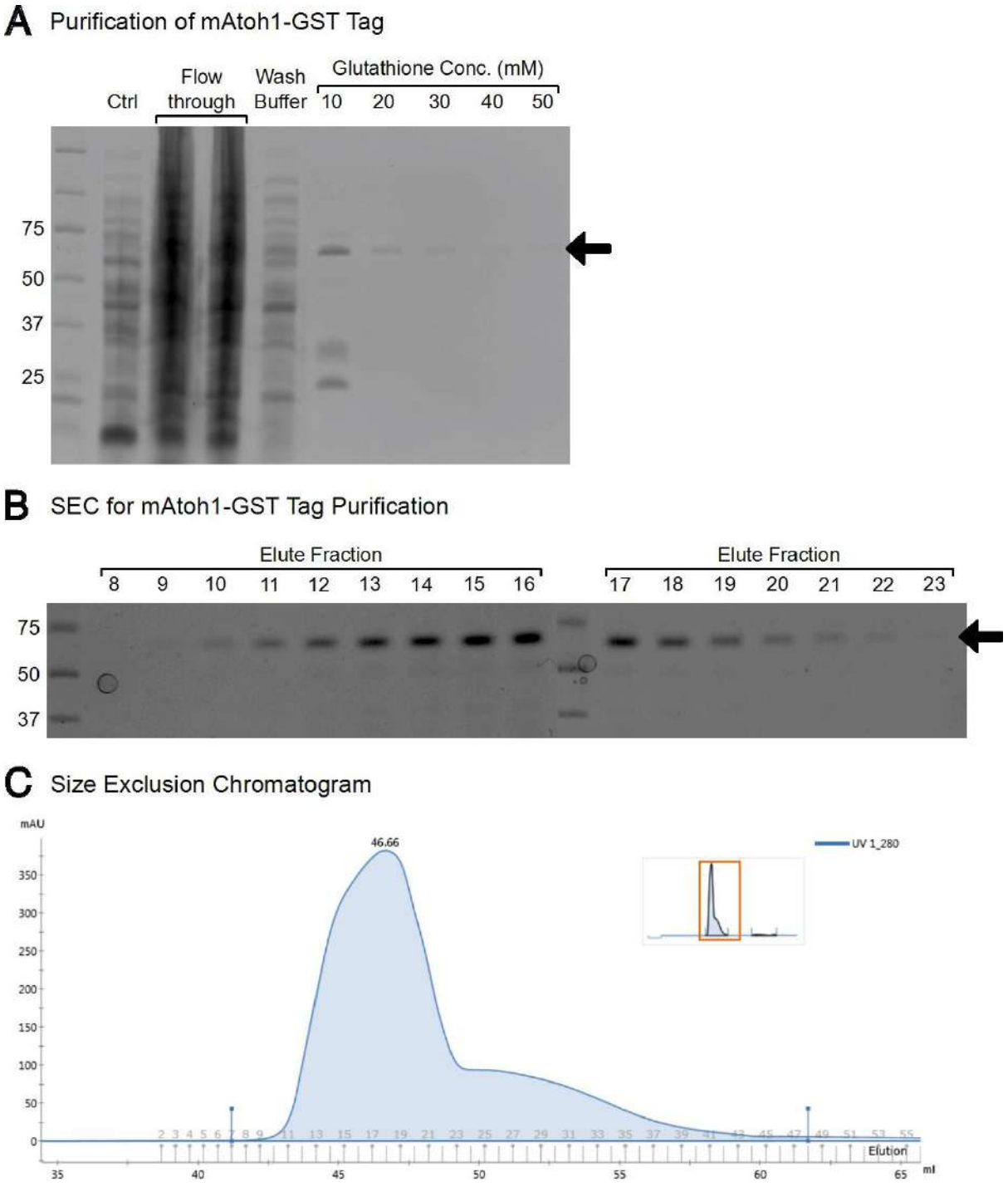

Figure 3.3 Recombinant mAtoh1-GST Protein Purification. (A) Purified mAtoh1-GST protein bands (arrow) from elution fraction at increasing glutathione concentrations shown on an SDS-PAGE gel. (B) Coomassie dye-stained SDS-PAGE gel used to show the elute fractions of mAtoh1-GST protein (arrow) that has been purified using size exclusion chromatography. (C) Size exclusion chromatogram profile for mAtoh1-GST protein purification.

3.3 Characterizing chicken Atoh1 Antibody

Due to the low expression of cAtoh1 protein, achieving a good yield in its purification is challenging. To address this, a peptide-based antigen was designed for generating a cAtoh1 antibody instead of using the full-length protein. A polyclonal cAtoh1 antibody was raised in rabbit, and the resulting immune sera were purified using peptide affinity chromatography and concentrated to 0.57 mg/ml. Validation of the antibody is essential to ensure its sensitivity and specificity, enabling accurate and reliable experimental results.

3.3.1 Immunoblotting Validation

Immunoblotting (Western blot) was conducted to verify an antibody's recognition of a denatured protein/antigen. For this study, cochlear lysate from chick embryonic stage E8 was prepared by dissecting the inner ear and lysing the tissue using a micro pestle in PBS containing 0.5% Triton X-100, 150 mM NaCl, 5 mM EDTA, 1 mM AEBSF, and 1X MS-SAFE protease and phosphatase inhibitor. The custom cAtoh1 polyclonal antibody produced bright bands at the correct size, although there was background noise from nonspecific interactions (Figure 3.4 A).

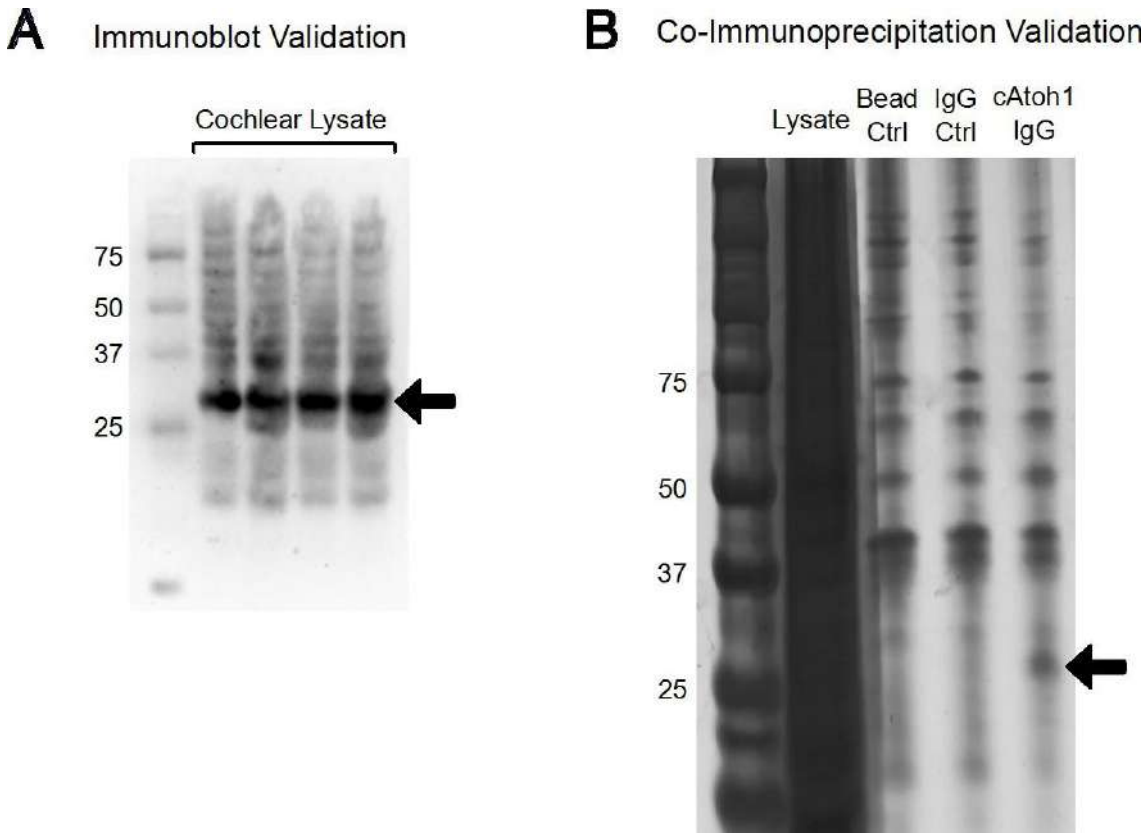

Figure 3.4: Custom cAtoh1 Antibody Immunoblot and Co-Immunoprecipitation Validation. (A) Western blot analysis of Atoh1 protein expression (arrow) from chick cochlear lysate using custom cAtoh1 antibody. (B) Co-

immunoprecipitation (IP) studies with custom cAtoh1 antibody in chick cochlear extracts, pulldown detects Atoh1 protein (arrow) presence.

3.3.2 Immunoprecipitation

To determine if the cAtoh1 custom antibody can perform chromatin immunoprecipitation (ChIP), its efficiency for pull-down assays needs to be verified. This involved performing cAtoh1 antibody immunoprecipitation using cochlear lysate from chick embryonic stage E10. A direct immunoprecipitation method with Protein G Sepharose was employed, where the antibody was first added to the Protein G affinity media to allow binding. The immobilized antibody was then used to purify the cAtoh1 protein from the cochlear lysate. The presence of cAtoh1 protein was detected on a silver-stained gel at the desired size (Figure 3.4 B).

Next, to characterize protein complexes interacting with cAtoh1 protein, immunoprecipitation from the inner ear lysate was followed by mass spectrometry analyses. Unfortunately, the cAtoh1 custom antibody was unable to perform pull-down successfully, as the mass spectrometry results were inconclusive. Therefore, ChIP cannot be performed using the cAtoh1 custom polyclonal antibody, but it works efficiently for detection in western blotting.

3.3.3 Immunohistochemistry Validation

Chick Basilar papilla IHC with cAtoh1 custom antibody

Immunohistochemistry is used to validate an antibody's recognition of the correct native protein/antigen based on cellular localization, confirming specificity by observing cells that either express or do not express the target protein.

Immunostaining was performed on cryosectioned inner ear samples from chick embryos. At embryonic stage E6, the newly differentiating hair cells in the distal region showed green nuclear expression of cAtoh1 and red cytoplasmic expression of Myo7a (Figure 3.5 A). By stage E8, cAtoh1 expression was observed throughout the basilar papilla from the proximal to the distal axis (Figure 3.5 B, C). The custom cAtoh1 polyclonal antibody demonstrated good specificity and minimal background in immunostaining.

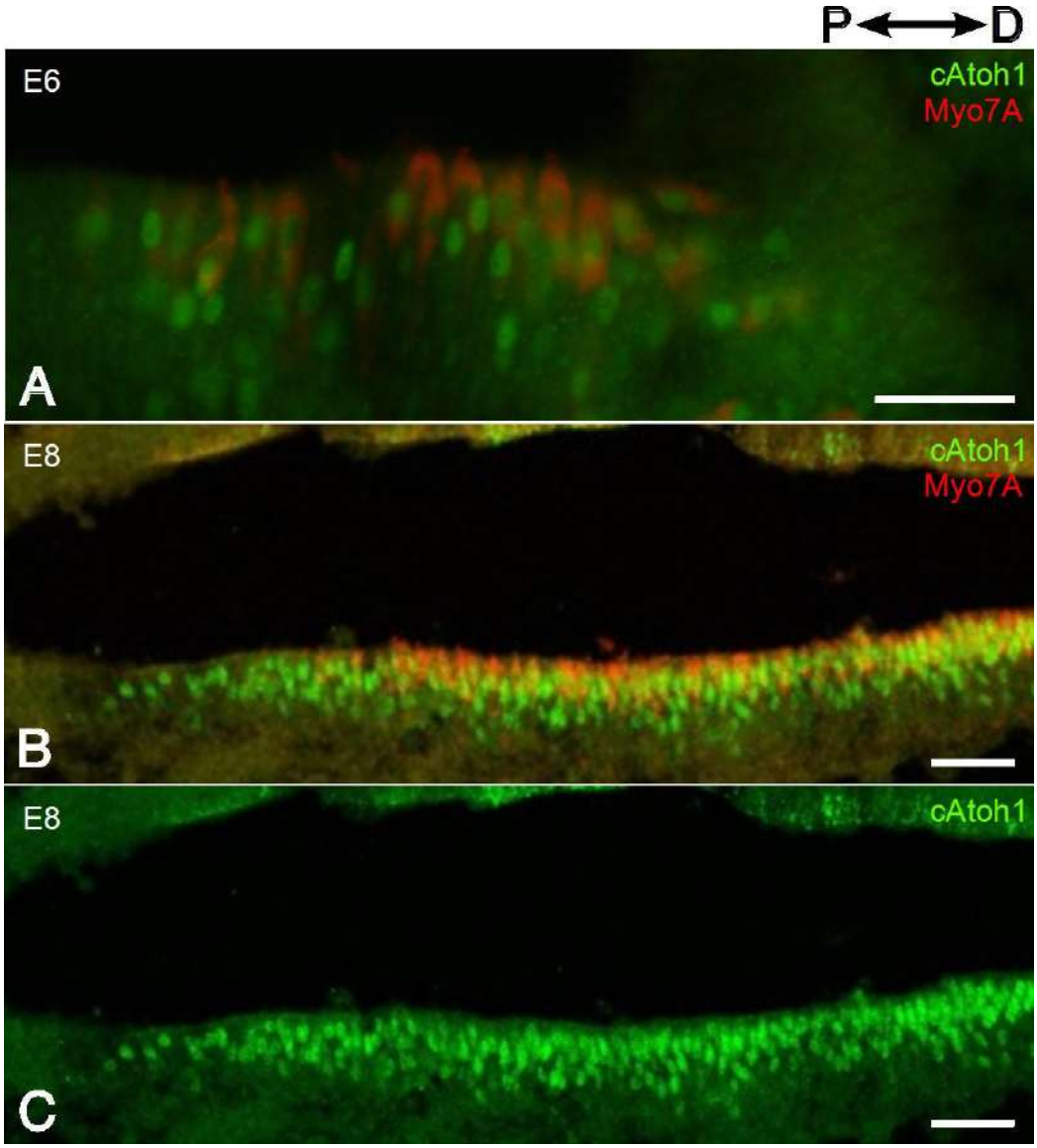

Figure 3.5: Custom cAtoh1 Antibody Immunohistochemistry Validation in Chick BP. Longitudinal section of a chick basilar papilla, oriented from the proximal to the distal end. cAtoh1 (green) marks the nuclei of hair cells, while Myosin7a (red) labels hair cell cytoplasm. (A) Shows early hair cell differentiation at embryonic stage E6, scale bar (50 µm). (B and C) Display HC differentiation from the distal to proximal axis at E8, scale bar (100 µm).

Zebrafish lateral line IHC with cAtoh1 custom antibody

A 19-amino acid peptide with conserved residues among vertebrate Atoh1 homologs was designed. The peptide's sequence homology with Atoh1 proteins from other species suggests that the resulting antibody should be effective across different species. To verify this, immunohistochemistry was performed on the lateral line system of zebrafish at 5 days post-fertilization (dpf). The lateral line system, a sensory organ along the fish's rostro-caudal axis, relies on Atoh1 for hair cell development. Using the custom cAtoh1 antibody, Atoh1 protein

in zebrafish was successfully immunostained. The neuromasts, which contain groups of hair cells, showed green nuclear expression from the cAtoh1 antibody and red cytoplasmic expression from Myo7a, a recognized hair cell marker (Figure 3.6). However, the cAtoh1 custom antibody also showed some nonspecific background.

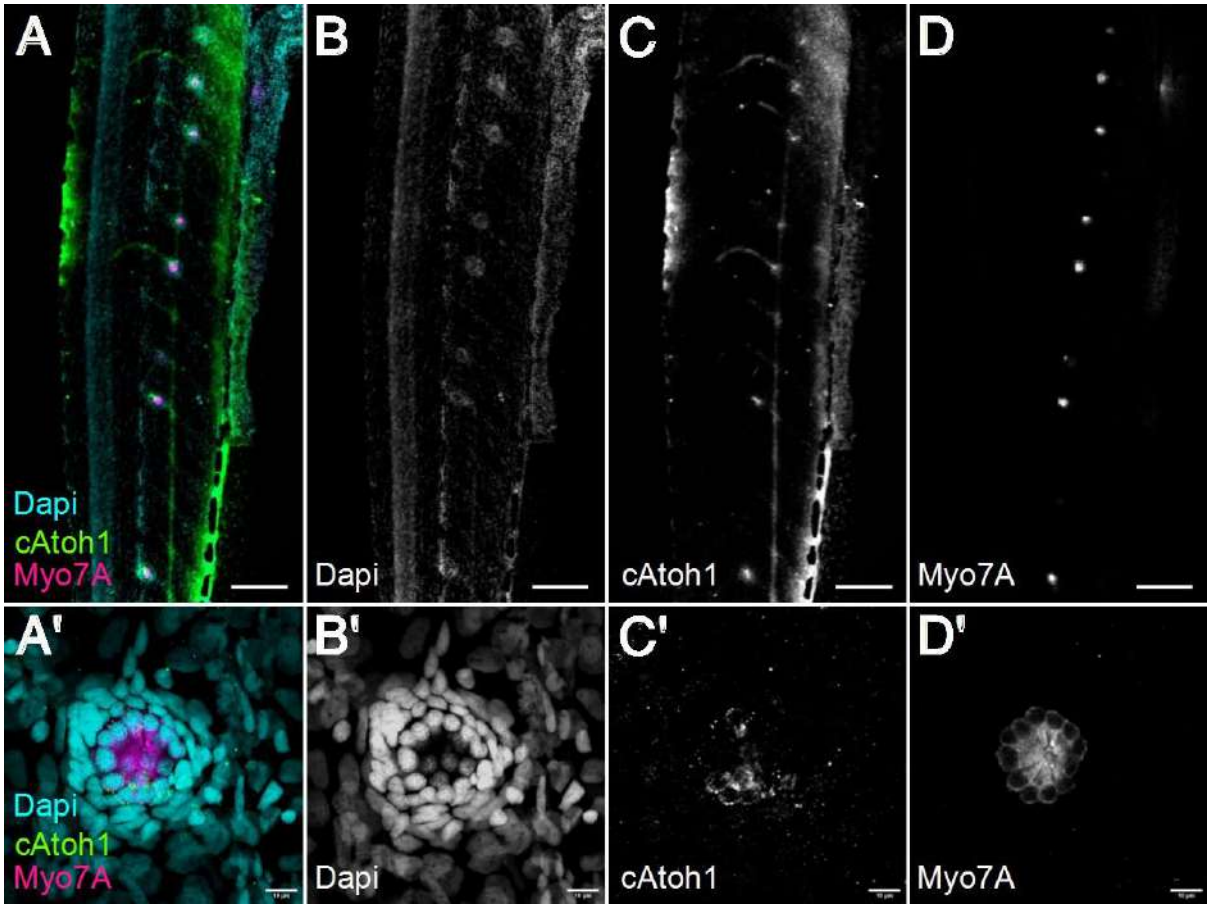

Figure 3.6: cAtoh1 Antibody Immunohistochemistry Validation in Zebrafish Neuromast. (A-D) show lower magnification images of the lateral line system in zebrafish larvae, scale bar 100 µm. (A'-D') display neuromast cells, scale bar 10 µm. (A, A') are merged images stained with DAPI (blue), cAtoh1 (green), and Myosin7a (red).

Chapter 4: CRISPR-Cas9 Atoh1 Gene Editing

This chapter focuses on the use of CRISPR-Cas9 system to genetically ablate the Atoh1 gene in the auditory sensory epithelium to study the resulting phenotypic changes. Atoh1 is a critical transcription factor involved in hair cell differentiation and regeneration, and its disruption provides valuable insights into the molecular mechanisms governing auditory system development and function.

4.1 In Ovo Electroporation of Atoh1-gRNA in Chicken Otocyst

The experimental methodology for in ovo manipulation, involves simultaneous injection and electroporation, carries a potential for low embryo survival and requires both skill and several crucial procedures to achieve optimal transfection. It is crucial to have precise timing for microinjection and electroporation at E4 since otocysts are distinctly visible during this developmental stage, when investigating HC development and differentiation (Figure 4.1 A, B). Due to the typical positioning of embryos at stage E4 (left side down, head turned right), only the right otic vesicle is accessible for injections. This limitation restricts genetic modification to the right basilar papilla in these experiments. The uninjected left otic vesicle, which will develop into the embryo's left inner ear, serves as an internal control and is referred to as the control. To enhance the efficiency of DNA transfection into the sensory domain of the otic vesicle, it's essential to align the electrodes closely with the anterior-ventral region of the otic vesicle near the embryo as demonstrated in (Figure 4.1 A). DNA transfer via electroporation techniques yield genetic alteration in mosaic outcomes.

To prepare for Atoh1 knockout experiments, SpCas9 protein with two plasmid solutions are needed: one containing the Atoh1 guide plasmid pcU6.1-Atoh1-gRNA for the knockout procedure, and another containing a mixture of pT2K-CAGGS-eGFP and pCAGGS-T2TP as a tracer to monitor electroporation efficiency, extent, and mosaicity in the basilar papilla. GFP is integrated into the genome through the Tol2 transposon, which promotes long-term gene expression and assists to determine the cells that have undergone genetic modification. GFP signal in basilar papilla serves as a proxy for cells that experienced change in genetic programming at the progenitor stage, earlier during otic vesicle development (Figure 4.1 C-E).

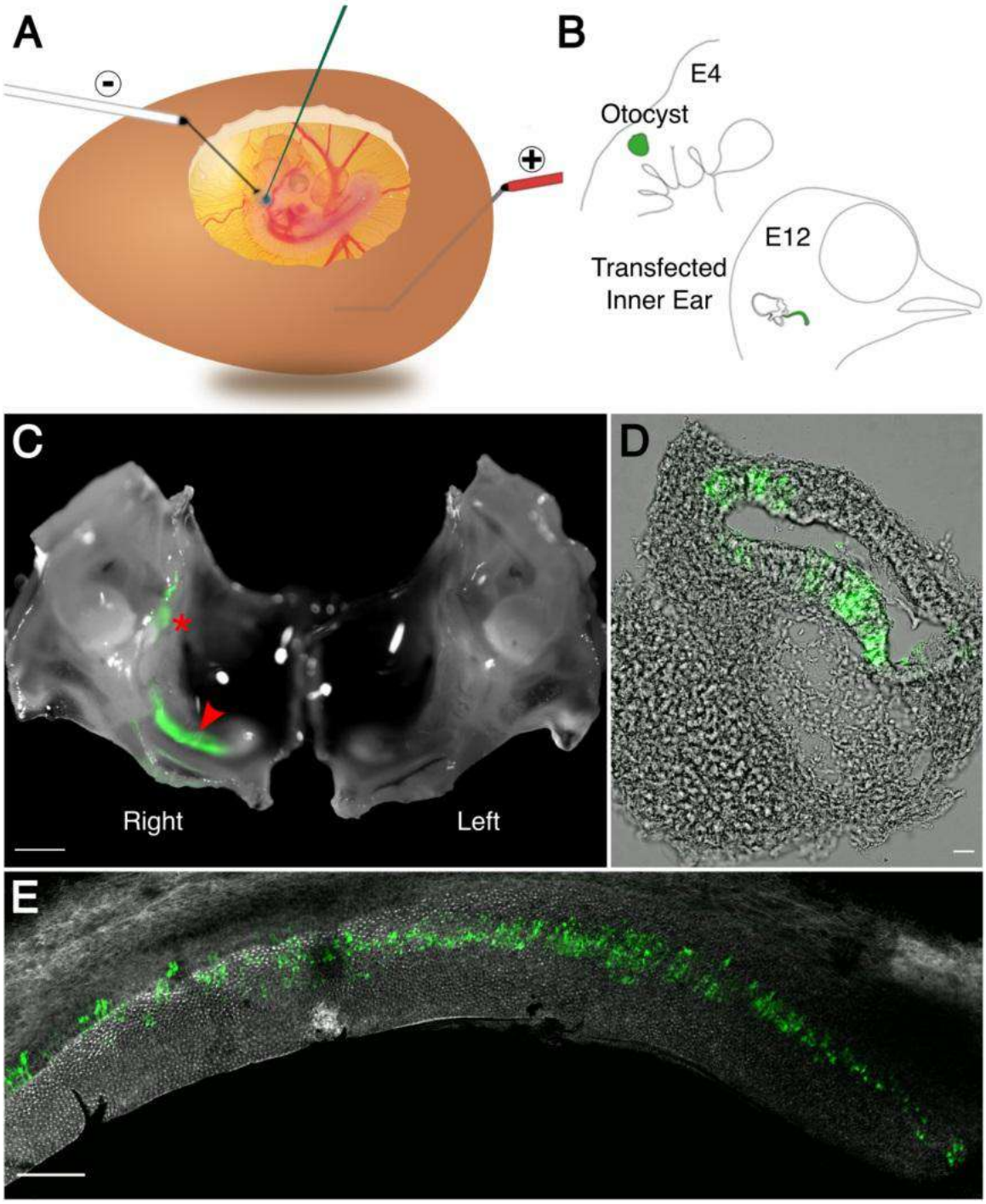

Figure 4.1: In Ovo Microinjection and Electroporation of Chick Otic Vesicle at E4. (A) A schematic illustrating the technique for delivering genetic material and visualization dye (Fast green) to the chick otic vesicle at embryonic day 4 (E4). The injection pipette contains a mixture of guide plasmids, Tol2-eGFP expression plasmids (pCAGGS-T2TP & pT2K-CAGGS-eGFP). Electrodes are positioned parallel to the dorsal-ventral axis of the spinal cord. (B) Diagram of a chick embryo with electroporation targeting the right otic vesicle at E4, grown to E12, illustrating the transfected right inner ear and construct expression. (C) The left inner ear serves as the internal control. The red arrow indicates GFP expression in the cochlear duct of the right inner ear, while the red asterisk highlights GFP expression in the vestibular organs. Scale bar 2 cm. (D) Cross-section of the right cochlear duct shows GFP expression primarily localized to the sensory epithelium. Scale bar 10 µm. (E) Whole mount image of basilar papilla stained with phalloidin, labeling F-actin filaments. GFP expression is observed along the neural side of the BP, extending from the proximal to distal end. Scale bar 100 µm.

4.2 CRISPR-Mediated Atoh1 Knockout Disrupts HC Formation

Embryos were injected with distinct plasmids for targeted experimentation. The first group received pcU6.1-Atoh1-gRNA, labelled as the “Atoh1-gRNA” or “Atoh1-crispant”, specifically designed to target the Atoh1 gene and knock it out. The second group received pcU6.1-Control-gRNA labelled here as “Control-gRNA”, serves as a which is an injectable control since this protospacer contains scrambled sequence is not present in the chicken genome. This control group helps account for any potential effects arising solely from the injection procedure itself, ensuring a more accurate assessment of the Atoh1-gRNA's impact. The uninjected left otic vesicle, which will develop into the embryo's left inner ear, serves as an additional internal control labelled as "control". This internal control allows for a direct comparison between the manipulated and unmanipulated inner ear within the same embryo.

Throughout the development of the basilar papilla during embryonic stages, the arrangement, orientation, shape, and size of hair cells and supporting cells undergo dynamic changes (Figure 4.2 A-D). The apical surface of the basilar papilla was examined in both Atoh1-crispant and control groups from E9 to E12 stages. Observations at embryonic stage E9 reveal a crucial finding. The basilar papilla in the Atoh1-gRNA group exhibits a reduced number of hair cells compared to both the control and control-gRNA groups (Figure 4.2 A, E, I). This finding aligns with observations in mouse models lacking Atoh1, where hair cell development is entirely absent[41]. The presence of these HCs is confirmed through the expression of Myosin7a. Hair cells are eliminated in scattered patches across the sensory epithelium due to genetic mosaicism generated by electroporation. The CRISPR/Cas9 modifications targeting the Atoh1 gene may only affect certain progenitor cells within BP, while others remain unaltered. In the Atoh1-crispants, notable patches of missing hair cells (HC) coincide with areas where GFP expression is observed (Figure 4.2 I-J). This correlation arises due to the presence of Tol2-eGFP, which is co-electroporated alongside the CRISPR components. GFP-positive cells in these regions indicate efficient transfection with the CRISPR construct, signifying genetic alterations targeting the Atoh1 gene.

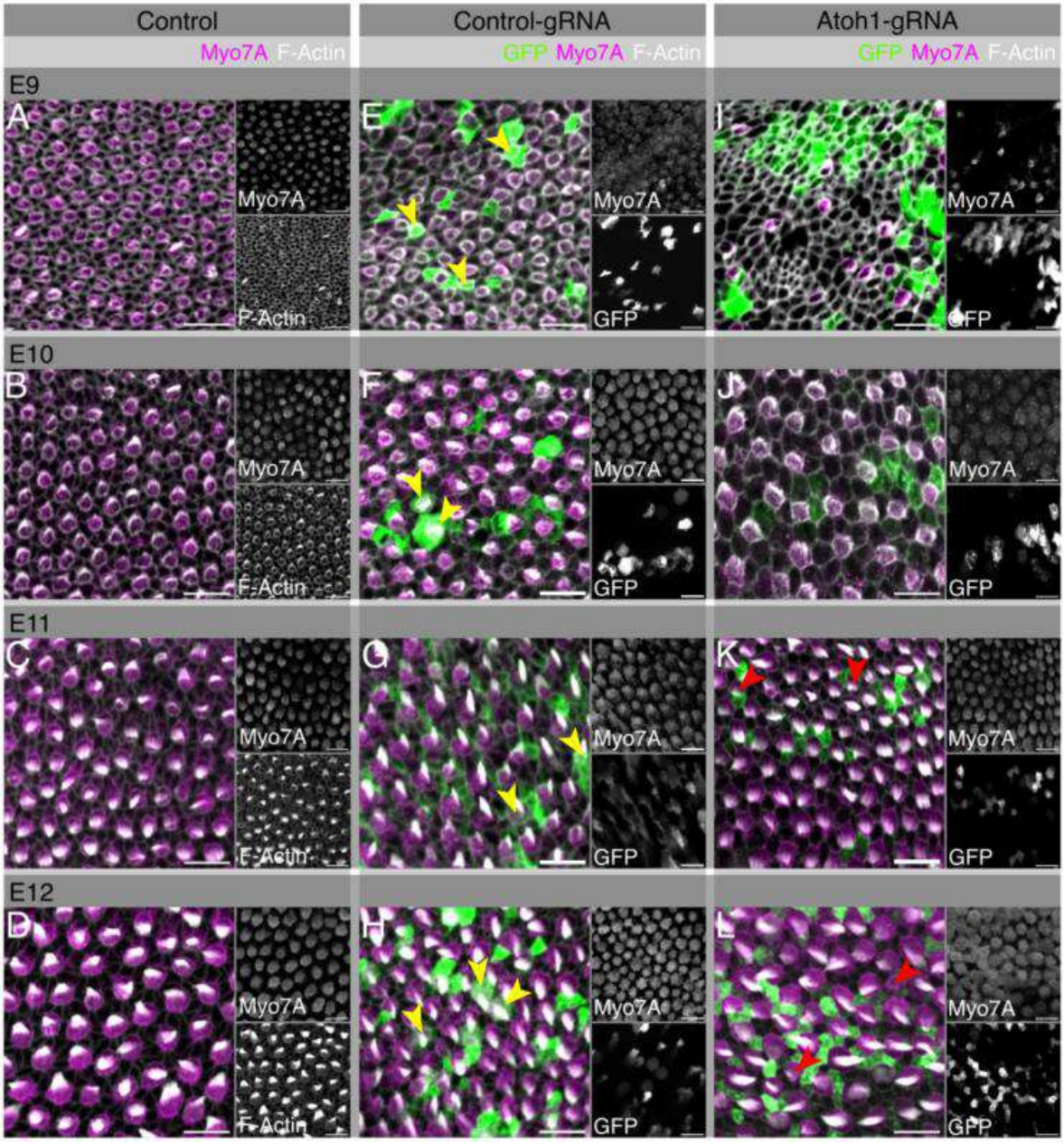

Figure 4.2: CRISPR/Cas9-mediated Mosaic Atoh1 Deletion: From Hair Cell Loss to Recovery (E9-E12). Confocal Images of Chick Basilar Papilla (Scale Bar: 10 µm; FV3000 Microscope). (A-D) Control Basilar Papilla (E9-E12): Merged images show F-actin filaments stained with phalloidin (gray) and hair cells (HCs) labeled with Myo7a (magenta). The left inner ear serves as the internal control in all panels. (E-H) Injectable Control Basilar Papilla (E9-E12): Merged images display F-actin (gray), Myo7a-labeled HCs (magenta), and GFP expression (green). Electroporated with pcU6.1-Control-gRNA, Tol2-eGFP plasmids, and Cas9 protein. Yellow arrows indicate GFP-positive HCs. (I-L) Atoh1 Knockout Basilar Papilla (E9-E12): Merged images show F-actin (gray), Myo7a-labeled HCs (magenta), and GFP expression (green). Electroporated with pcU6.1-Atoh1-gRNA, Tol2-eGFP plasmids, and Cas9 protein. A reduction in HC numbers is evident at E9 in Atoh1 knockout (I) compared to control (A) and injectable control (E) based on Myo7a staining. By E12, HC restoration is observed in the Atoh1 knockout (L) with Myo7a staining. GFP expression is primarily localized in supporting cells (SCs) surrounding the new HCs (indicated by red arrow).

The control-gRNA also exhibits GFP expression patches, with no loss in HCs numbers and more akin to control groups in terms of HC-SC arrangement and overall

organization (Figure 4.2 E-H). The control-gRNA is inert and does not influence the fate of progenitor cells. Therefore, there are more GFP-positive hair cells in the control-gRNA, unlike the Atoh1-gRNA where such instances are rare. Sometimes certain hair cells in the Atoh1-crispants also exhibit GFP positivity, referred to as "escapers". The presence of these escapers, which are GFP positive cells while retaining their hair cell fate, is attributed to the variable performance of the CRISPR construct within each transfected progenitor cell. Such variability in CRISPR efficacy can lead to instances of CRISPR failure, potentially arising from Cas9 cleavage deficiencies, pcU6.1-Atoh1-gRNA degradation, or single-copy deletions of the Atoh1 gene within the transfected cell.

GFP Expression Validates Atoh1 Deletion

The effectiveness of CRISPR/Cas9 targeting in Atoh1-gRNA embryos was evaluated by analyzing GFP expression. The ratio of GFP-positive hair cells to total GFP-positive cells within distinct regions of the basilar papilla was calculated for both Atoh1-gRNA and control-gRNA groups (Figure 4.3). The results revealed a significant difference: Atoh1-gRNA embryos had considerably fewer GFP-positive hair cells compared to the control-gRNA. This finding suggests efficient Cas9 cleavage with Atoh1-gRNA, potentially leading to Atoh1 gene deletion alongside GFP expression.

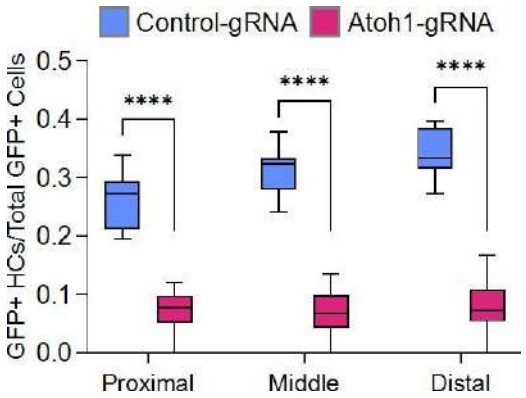

*Figure 4.3: GFP Expression as a Marker for Atoh1 Knockout Efficiency. The graph shows the ratio of GFP-positive hair cells to the total number of GFP-positive cells in different regions of the basilar papilla for Atoh1-gRNA and control-gRNA groups. A significant difference with Student's t-test (****P < 0.0001) is observed between the two groups across all regions. Atoh1-gRNA embryos also exhibit a lower overall number of GFP-positive HCs compared to controls.*

4.3 Hair Cell restoration in Atoh1-Crispants

Observations with extended incubation of Atoh1-gRNA embryo to later embryonic stages revealed a gradual recovery of lost HCs, progressing from E9 to near-complete HCs

restoration by E12. At E12, Atoh1-gRNA basilar papilla exhibits a remarkable restoration of its overall tissue organization. This includes the arrangement of hair cells and supporting cells, which now closely resemble the control and control-gRNA groups. This finding suggests that the basilar papilla has the potential to recover from the initial hair cell loss observed at earlier stages.

The continued presence of GFP expression at E12 provides validation that the GFP-positive cell clusters in Atoh1-crispants underwent genetic program modification, accompanied by the deletion of the Atoh1 gene. Notably, GFP expression is predominantly confined to supporting cells, forming a distinct halo around the hair cells. The majority of the newly generated hair cells do not display GFP positivity. These newly formed hair cells originate from supporting cells, either through asymmetric mitotic division or direct phenotypic conversion into hair cells. This strongly indicates that the population of supporting cells within the GFP expressing patch, which did not undergo CRISPR modification during electroporation and retained the intact Atoh1 gene, gave rise to the hair cells. Notably, the apical surface area of the regenerated hair cells is smaller compared to those in the wild-type basilar papilla, with some lacking hair bundles but still expressing Myosin7a, confirming their identity as hair cells (Figure 4.4).

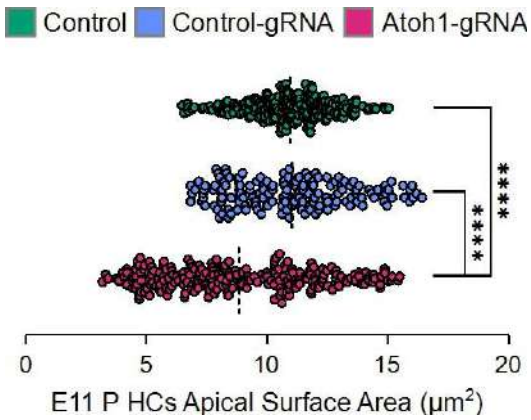

*Figure 4.4: Newborn Hair Cells have Smaller Apical Surface Area. The graph depicts the apical surface area of hair cells in the proximal region of E11 basilar papilla (BP). A Student's t-test was used for direct comparisons between two conditions, resulting in P-values where ****P < 0.0001 indicates statistical significance.*

4.4 Quantifying Hair Cell Recovery Potential

To assess the severity of hair cell loss and potential restoration across different regions of the basilar papilla (BP), we employed a quantitative approach. We calculated the ratio of total hair cells (HCs) to the total number of cells within each designated area - proximal, middle,

and distal (1/3 of the total BP length) (Figure 4.5 A). This ratio provides a metric to compare hair cell density across these regions and between different experimental groups. Hair cell distribution within the BP is not uniform. The ratio of hair cells to total cells varies across the proximal, middle, and distal regions, increasing along the proximal to distal axis of the basilar papilla. These differences in number of hair cell-support cell interactions along the BP influences hair cell packing density and overall tissue organization. To account for this inherent variation, we opted to analyse each region separately throughout the experiment, spanning embryonic stages E9 to E12 (Figure 4.5 B-D). This approach allows for a more accurate assessment of hair cell loss and recovery specifically within each region, taking into account the baseline differences in hair cell density.

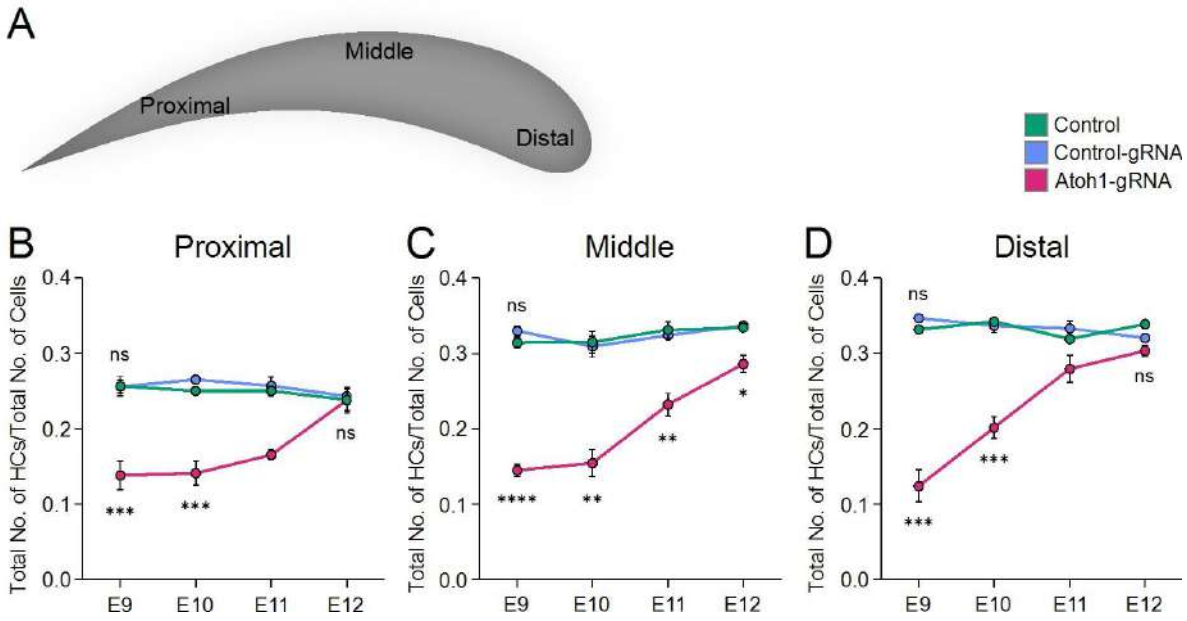

*Figure 4.5: Analyzing Hair Cell Restoration in Developing BP from E9 to E12. (A) Drawing of the BP, divide into proximal, middle and distal regions. (B-D) These graphs display the total number of HCs relative to the total cell count within each region of the BP. They illustrate the HC loss across all regions at embryonic stage E9 and the subsequent restoration of lost HCs in all regions by E12. Statistical significance between two conditions was assessed using Student's t-test, where *P<0.05, **P<0.01, ***P<0.001, and ****P<0.0001 indicate significance, while non-significant differences are denoted as "ns".*

Our findings reveal a substantial decrease in hair cell numbers in Atoh1-gRNA across all three regions of the basilar papilla at E9 embryonic stage. In contrast, the control-gRNA group exhibits a comparable ratio of the total number of HCs to the total cell count when compared to the control. Examination of the graphs suggests that the recovery of lost hair cells initiates early in the distal region at E10, progressing to the middle region by E11, and eventually reaching the proximal region. These findings suggest that the process of hair cell

restoration follows a wave pattern from distal to proximal akin to the differentiation of hair cells during embryonic development, indicating that hair cell regeneration recapitulates the natural process of hair cell development.

4.5 Neighbourhood Analysis

In the basilar papilla, hair cells (HCs) and supporting cells (SCs) are spatially arranged in an intricate pattern of mosaics. During the developmental process of the auditory epithelium, there are variations in the arrangement of HCs and SCs. HCs typically contact SC (HC-SC contact), but rarely contact other HCs (HC-HC contact)[217,218]. SCs can contact both HCs (SC-HC contact) and other SCs (SC-SC contact) (Figure 4.6).

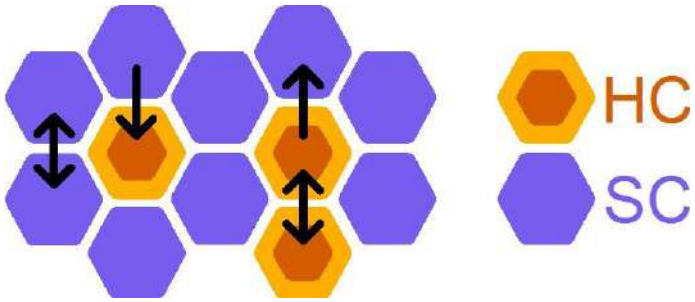

Figure 4.6: Spatial Arrangement of Hair Cells and Support Cells. The diagram illustrates the various connections between HCs and SCs using arrows. These connections include: SC-SC, SC-HC, HC-SC, and HC-HC interactions.

The loss of hair cells in Atoh1-crispants disrupts the organization of HCs and SCs within the tissue. To determine whether HC restoration is accompanied by a restoration in the mosaic pattern of the BP, neighbour number analysis for both HCs and SCs was conducted between E9 and E12.

4.5.1 Support Cell Contacts

At E9, in Atoh1-gRNA electroporated BP show a greater number of SC-SC contacts (Figure 4.7 A), with dramatically reduced SC-HC contacts given the reduced HC numbers in electroporated patches (Figure 4.7 B). While around 3-5% of SC are without an HC contact in control and control-gRNA samples, 47% of SC do not have an HC contact in Atoh1-gRNA samples. The reduction in SC-SC contacts and the recovery of SC-HC contacts occurs by E12 such that, the number of both SC-SC and SC-HC contacts are similar to those seen in control-gRNA samples. Consistent with this, the number of SC without HC contacts falls to control-gRNA levels by E12.

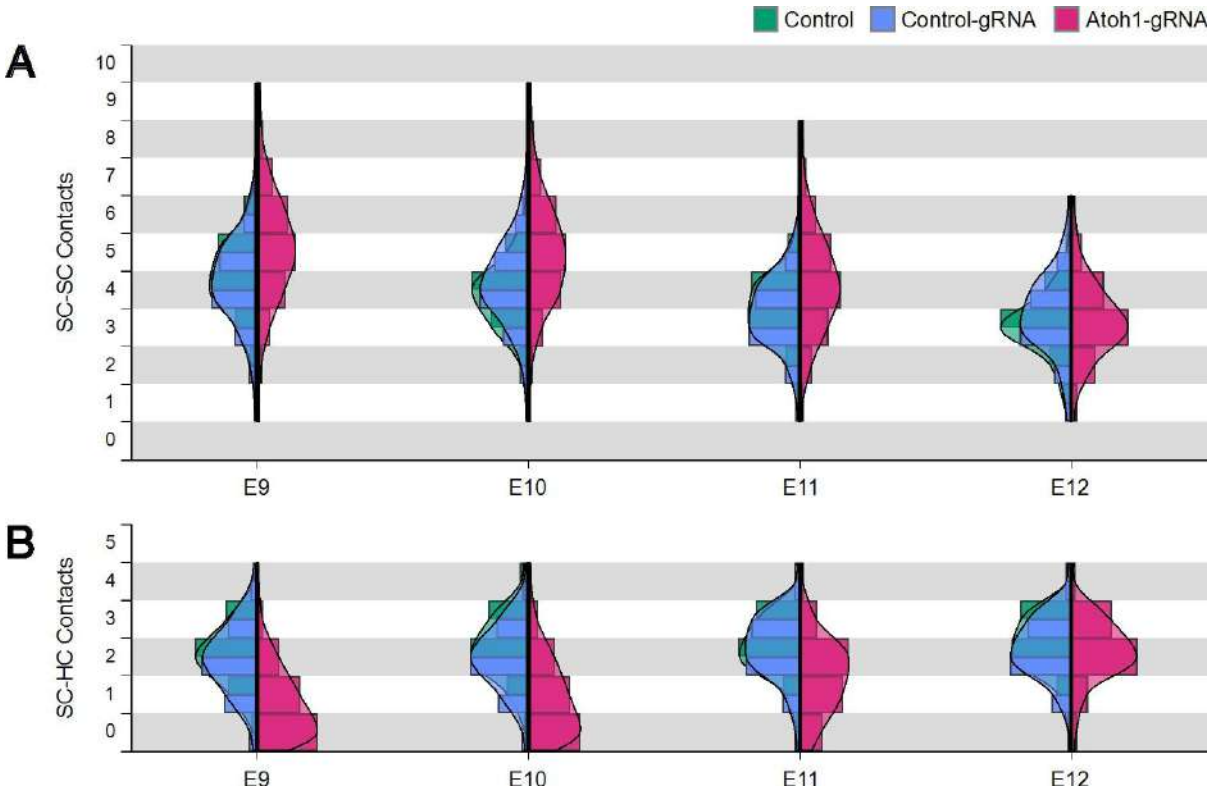

Figure 4.7: Neighborhood Connections of Supporting Cells. (A-B) Graphs analyzing the number of neighboring cells for supporting cell types in control, electroporated control-gRNA, and Atoh1-gRNA at four embryonic stages from E9 to E12. (A) shows interactions between SC-SC, while (B) depicts contacts between SC-HC.

4.5.2 Hair Cell Contacts

The average number of HC-SC contacts, meaning the supporting cells surrounding each hair cell, increases from E9 to E12 embryonic stages, consistent with earlier observations[217]. Additionally, HC-SC contacts in Atoh1-gRNA samples did not show significant changes compared to the control groups (Figure 4.8 A).

Throughout all developmental stages and regions of the basilar papilla, interactions between two hair cells (HCs) were rare, as HCs were predominantly surrounded by supporting cells (SCs). As expected, HC-HC contacts were rarely observed in control and control-gRNA embryos. However, in Atoh1-crispant basilar papilla, HC-HC contacts were more common, with some instances having two or three hair cells clustered together (Figure 4.8 B). This pattern persisted up to E12, with at least one HC-HC contact still frequently observable.

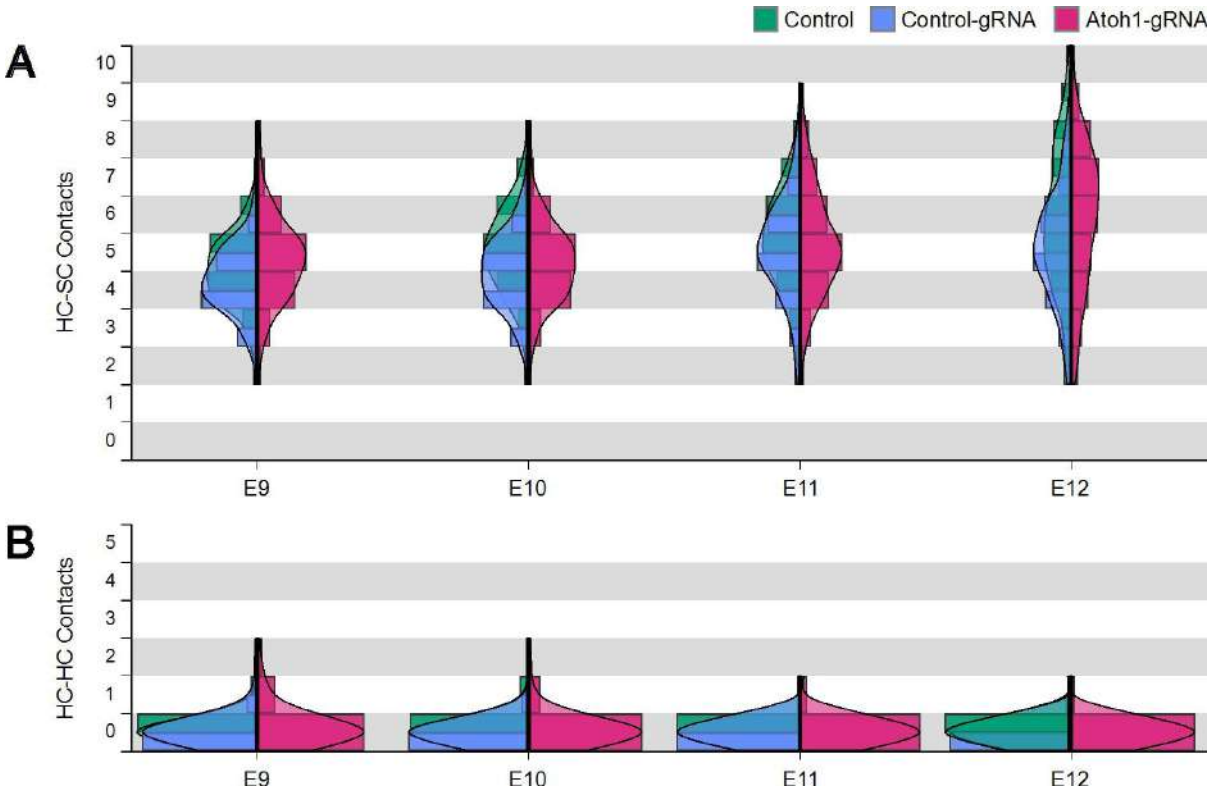

Figure 4.8: Neighborhood Connections of Hair Cells. (A-B) Graphs represent an analysis of the number of neighboring cells for hair cell types in control, electroporated control-gRNA, and Atoh1-gRNA at four embryonic stages from E9 to E12. (A) illustrates interactions between HC-SC, and (B) represents contact between HC-HC.

4.6 Proliferation Potential in Basilar Papilla After HC Loss

Considering the evident hair cell recovery between the E9 and E12 stages, it becomes essential to investigate the proliferative dynamics of the basilar papilla tissue during this critical development window. This period marks a transition in the basilar papilla's development, characterized by an initial phase of exponential HCs differentiation, followed by a shift to a stationary phase where HCs numbers stabilize, resembling the mature basilar papilla. To elucidate whether this transition involves the addition of either hair or supporting cells between E9 and E12, we conducted a proliferation assay utilizing EdU staining on the basilar papilla. The electroporated Atoh1-gRNA, control-gRNA, and unelectroporated control embryos were incubated in ovo until they reached four distinct stages: E9, E10, E11, and E12. Subsequently, a one-day EdU pulse was administered at each stage through in vitro basilar papilla explants to identify and capture EdU-positive cells emerging over next 24 hours (Figure 4.9 A). This approach enables us to track the proliferative activity spanning from E9+1 DIV to E12+1 DIV.

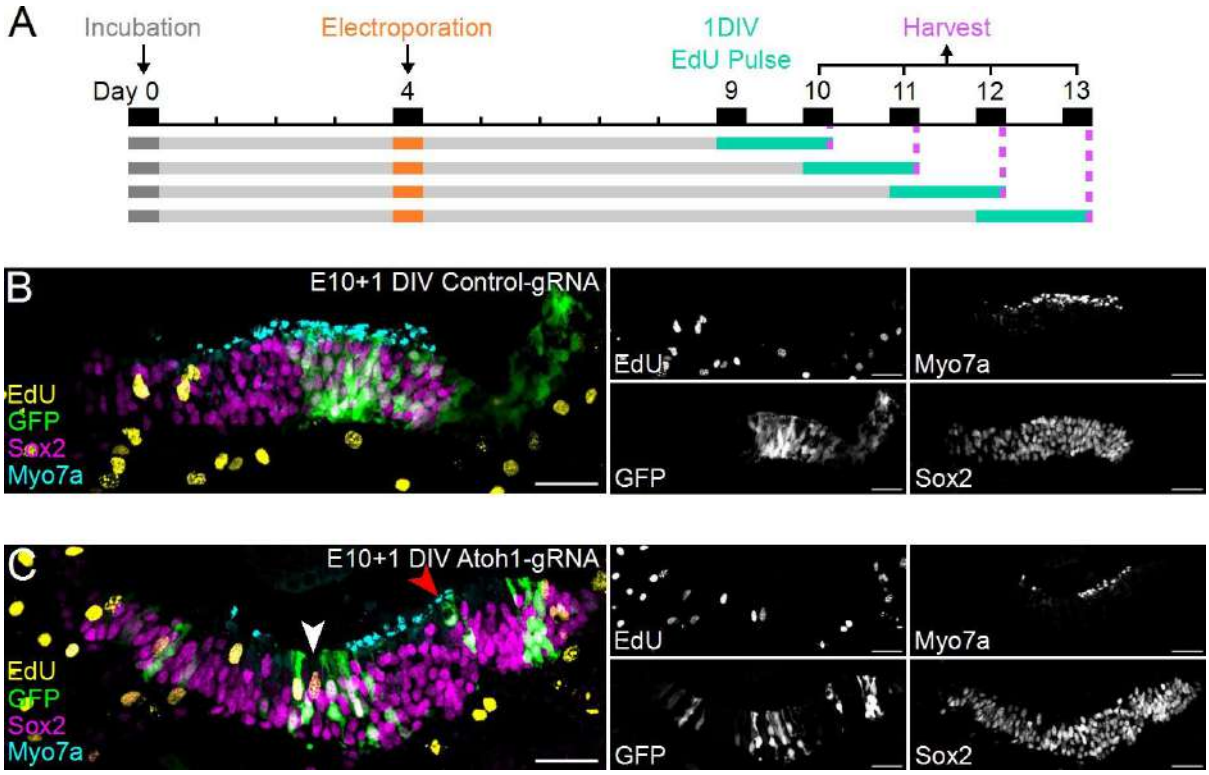

Figure 4.9: Cellular Proliferation in Response to Hair Cell Depletion. (A) Experimental design schematic for EdU Pulse treatment. Electroporation was conducted on all embryos at E4. At E9, E10, E11, and E12 stages, BP explants underwent a one-day EdU pulse in vitro, followed by BP harvesting. (B-C) Cross-sectional images of E10+1-day in vitro (DIV) BP explants, scale bar 25 µm. Hair cells (HCs) stained cyan for Myo7a, supporting cells (SCs) stained magenta for Sox2, actively proliferating cells labeled yellow for EdU, and green indicating GFP expression from Tol2-eGFP plasmids. (B) Control-gRNA BP image and (C) Atoh1-gRNA BP image depicting HC loss. The white arrow indicates a region lacking HCs with an EdU-positive SC underneath, while the red arrow marks GFP-positive HCs known as "escapers".

In the event of hair cell loss, the process of hair cell regeneration relies on supporting cells, which can either undergo asymmetric division or direct transdifferentiation to restore hair cells, or engage in symmetric division to replenish supporting cells that had previously undergone direct transdifferentiation, thereby maintaining tissue homeostasis. To determine the quantity of newly differentiated cells resulting from mitotic division, we counted cells marked as EdU+/Sox2 for supporting cells and EdU/Myosin7a for hair cells within the developing BP from E9+1 DIV to E12+1 DIV. At E10 stage, the sections of the basilar papilla exhibited a clear demarcation between HCs and SCs. HCs were situated closer to the luminal surface, while SC nuclei were grouped closely near the basilar membrane, making them easily distinguishable and countable.

Our analysis revealed key insights into cell proliferation and hair cell restoration in Atoh1-gRNA embryos. In these embryos, regions expressing GFP (indicating Atoh1 gene editing) displayed a clear absence of hair cells. Interestingly, these regions also showed a

higher number of EdU-positive cells at E10+1 DIV, coinciding with GFP expression in Atoh1-crispants (Figure 4.9 C). In contrast, control-gRNA exhibited sporadic presence of EdU-positive cells (Figure 4.9 B). These findings suggest an increased proliferation specifically at the sites where HCs are missing in Atoh1-crispants.

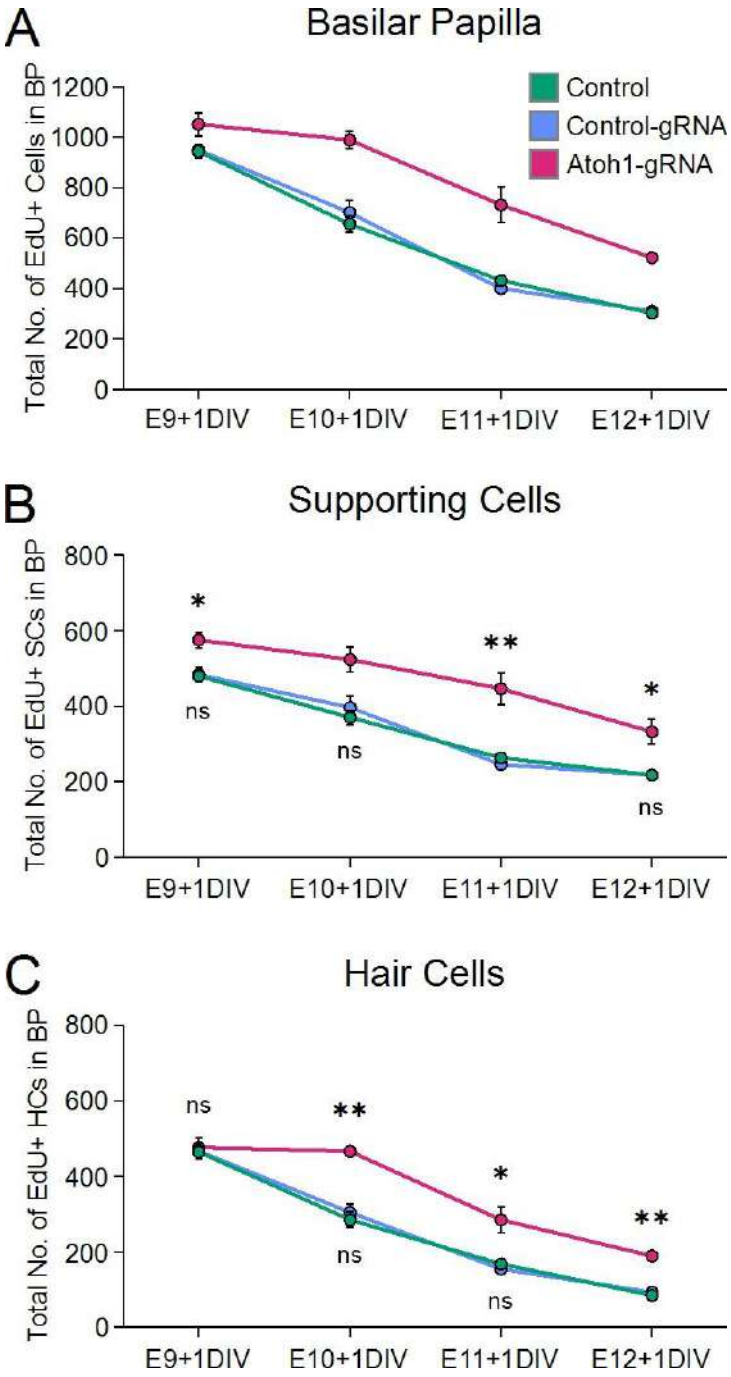

*Figure 4.10: Quantifying Proliferation in Developing BP. Graph represents EdU-positive in (A) basilar papilla, (B) SCs and (C) HCs from embryonic stages E9+1 DIV to E12+1 DIV from control, control-gRNA, and Atoh1-gRNA. Statistical significance in direct comparisons between two conditions was assessed using Student's t-tests. *P<0.05 and **P<0.01 indicate statistical significance, while non-significant differences are denoted as "ns".*

The overall trend of EdU positive cells shows a gradual decline from E9+1 DIV to E12+1 DIV, mirroring the relatively stable HC population after E12 (Figure 4.10 A). Notably, there is no significant difference in the number of EdU positive hair cells and supporting cells between the control and control-gRNA groups at all developmental stages. However, an intriguing observation emerges when comparing Atoh1-gRNA to the control groups. At each stage from E9+1 DIV to E12+1 DIV, Atoh1-gRNA consistently exhibit a higher number of EdU positive supporting cells compared to the control-gRNA and control groups (Figure 4.10 B). We observed that the heightened proliferation of supporting cells begins at E9+1 DIV in Atoh1-gRNA, primarily in the distal region, where a greater number of EdU-positive cells were present. Within 24 hours, by E10+1 DIV, we observed a substantial increase in EdU labelling throughout the entire basilar papilla, surpassing the levels seen in the control groups. However, the complete restoration of hair cells in the entire basilar papilla from distal to proximal region took a longer period, extending until E12.

4.7 HC Restoration from Transdifferentiation

It's interesting to observe that at E9+1 DIV, all three groups Atoh1-gRNA, control-gRNA, and control display an equal number of EdU positive hair cells (Figure 4.10 C). However, at E10+1 DIV, the number of EdU-positive hair cells remains at the same level as E9+1 DIV, which is significantly higher than both the control-gRNA and control groups at E10+1 DIV. This trend continues beyond E10+1 DIV, with Atoh1-crispants consistently exhibiting a significantly higher number of EdU positive hair cells compared to the control groups. Despite this increased proliferation, the number of EdU positive hair cells in Atoh1-crispants remains insufficient to account for the observed hair cells recovery. To confirm the presence of newly generated hair cells, we utilized Calbindin staining[184,219] (Figure 4.11 A-B), which labels newborn hair cells at E10 in Atoh1-crispants, and compared it to the EdU positive hair cells data from E9+1 DIV Atoh1-crispant explants. Surprisingly, there were significantly more Calbindin-positive (CaB+) new hair cells than EdU positive hair cells at the same developmental stage (Figure 4.11 C).

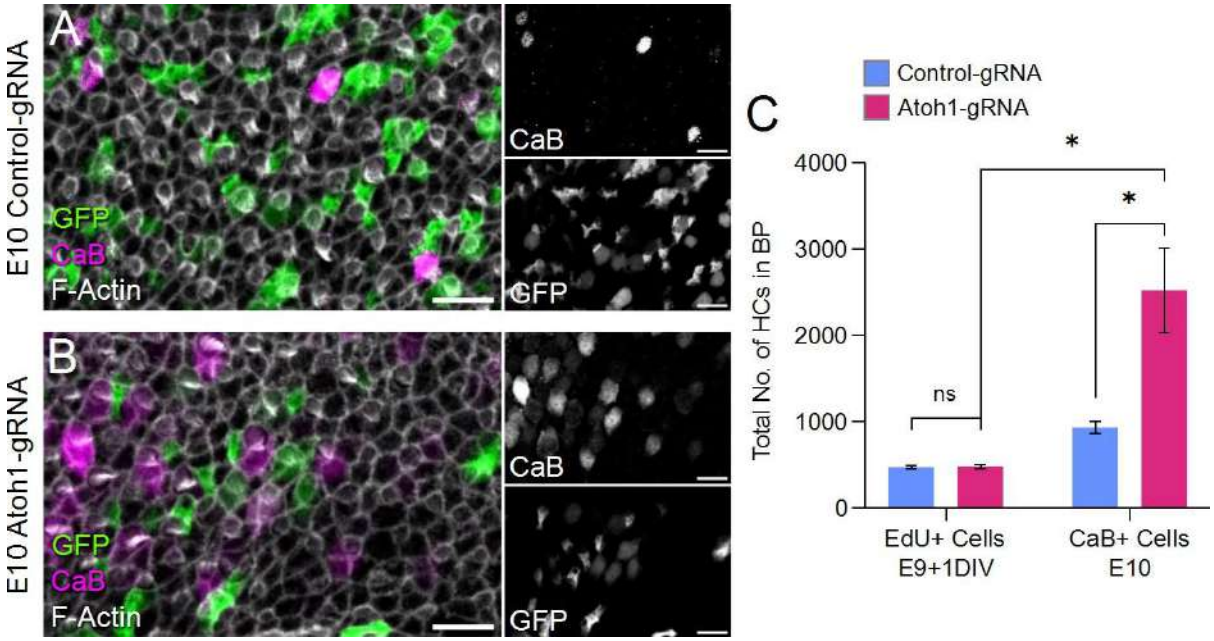

*Figure 4.11: Non-proliferative Hair Cell Restoration. (A-B) Whole mount images of E10 basilar papilla (BP) from electroporated chick embryos, with a 10μm scale bar for reference. The merged images show new hair cells (HCs) positive for Calbindin (CaB) in magenta, F-Actin stained with phalloidin in gray, and GFP expression in green. (A) Represents control-gRNA at E10, while (B) displays images of Atoh1-gRNA. (C) The graph depicts the total number of HCs in E9+1 day in vitro (DIV) BP explants treated with EdU, and E10 BP in two condition groups: control-gRNA and Atoh1-gRNA. Student's t-tests. *P<0.05 indicates significance, while non-significant differences are denoted as "ns".*

This suggests the involvement of additional mechanisms in the hair cell regeneration process, extending beyond mere cell proliferation, such as phenotypic conversion or direct transdifferentiation of supporting cells. In line with the observed HC restoration, a significant population of HCs within Atoh1-crispants exhibited co-expression of Myosin7a and Sox2, markers typically associated with newly generated hair cells. Interestingly, a majority of these recently formed hair cells did not exhibit EdU labelling, indicating that they likely originated from the transdifferentiation of supporting cells. These findings indicate that hair cell restoration involves a dual response from supporting cells, comprising both direct transdifferentiation into hair cells and mitotic division. Our data suggests that transdifferentiation might initiates earlier at E9+1 DIV, while mitotic division becomes more prominent later. These observations are consistent with earlier studies suggesting that the regeneration of basilar papilla tissue may be facilitated by the mitotic division of supporting cells[93,94]. While direct transdifferentiation of supporting cells is thought to be the primary mechanism of hair cell regeneration in chick basilar papilla[220,221].

4.8 Molecular Mechanism of HC Restoration

To investigate the molecular regulators potentially involved in hair cell restoration, an explant approach was utilized as a preliminary test to screen modulators of signaling pathways that might influence HC restoration. Given the correspondence, we tested small molecules that modulate pathways involved in HC regeneration. The electroporated Atoh1-gRNA and control-gRNA embryos were cultured in ovo until E10 and then subjected to basilar papilla dissection for explant culture over a 2-day in vitro period (Figure 4.12 A). It's worth noting that basilar papilla from chick embryos grown in explant culture for 2 days have maintained a morphology akin to that of in vivo basilar papilla. Based on earlier observations, the period between E10 and E12 appears to be the primary timeframe for HC restoration. During this 48-hour window of HC restoration, we administered small molecule treatments to modulate the Wnt signaling and Notch signaling pathway. We employed XAV-939, a Wnt signaling antagonist; CHIR, a Wnt agonist and DAPT, a Notch signaling inhibitor. DMSO served as the vehicle for these treatments and was used as a control.

To quantifying the effects of these pharmacological inhibitors and agonists on the two pathways, we compared the number of HCs, as indicated by Myosin 7a staining, in two groups of embryos: Atoh1-gRNA and control-gRNA. We also compared HC numbers in both these electroporated groups at E10, prior to the 2-day in vitro treatment. The E10 dataset provides an approximate estimate of hair cell numbers during the E10 stage, facilitating a comparison with our explant dataset. Notably, at E10, the hair cell numbers in Atoh1-gRNA BP are approximately half of those in the control-gRNA (p-value). However, when we consider the DMSO vehicle control, Atoh1-gRNA have successfully recovered hair cells during the 2-day in vitro explant culture and are comparable to the control-gRNA after the 48-hour treatment period.

4.8.1 Impact of Wnt Signaling Modulation on HC Restoration

Wnt antagonist XAV939

XAV939 is an effective small molecule inhibitor targeting the Wnt signaling pathway. Its mechanism of action involves selective inhibition of Wnt/beta-catenin-mediated transcription by blocking tankyrase1 and 2[222]. This inhibition results in enhanced protein stability of the axin, consequently facilitating the degradation of β-catenin and thereby inhibiting Wnt pathway downstream actions. It should be noted that XAV-939 treatment failed to restore hair cells in the basilar papilla of E10+2 DIV Atoh1-crispants (Figure 4.12 B, D, G). The number of HCs in XAV939 treated Atoh1-crispants remained unchanged after 2 days of explant culture, akin to the HCs count observed in E10 Atoh1-crispants. Following Wnt pathway inhibition, hair cell restoration in Atoh1-crispants was hindered, resulting in a significantly lower number of hair cells compared to the control-gRNA ($P<0.0001$). However, the DMSO-treated E10+2 DIV Atoh1-crispants demonstrated hair cell recovery (Figure 4.12 B, C, F). This suggests that Wnt inhibition is impeding HC proliferation, thus preventing the generation of new HCs.

Wnt agonist CHIR99021

Derived from aminopyrimidine, CHIR99021 is an effective inhibitor of both GSK3β and GSK3α subunits of glycogen synthase kinase (GSK) 3. As a vital inhibitor of the Wnt signaling pathway, GSK3, a serine/threonine kinase, is effectively antagonized by CHIR99021, resulting in the activation of Wnt signaling. In E10+2 DIV Atoh1-gRNA treated with CHIR99021, we observed hair cell restoration comparable to the control-gRNA under the same treatment, indicating successful recovery (Figure 4.12 B, E, H). Additionally, both Atoh1-gRNA and control-gRNA treated with CHIR99021 showed a modest increase in hair cell numbers compared to those treated with the DMSO vehicle control. These findings suggest that the Wnt agonist CHIR99021 not only stimulates hair cell restoration but also augments hair cell proliferation beyond the levels observed in the DMSO control condition within the same 48-hour timeframe. The resulting number of hair cells surpasses even the natural physiological state of wildtype E12 basilar papilla, indicating a remarkable increase in total hair cell count, leading to a supernumerary effect.

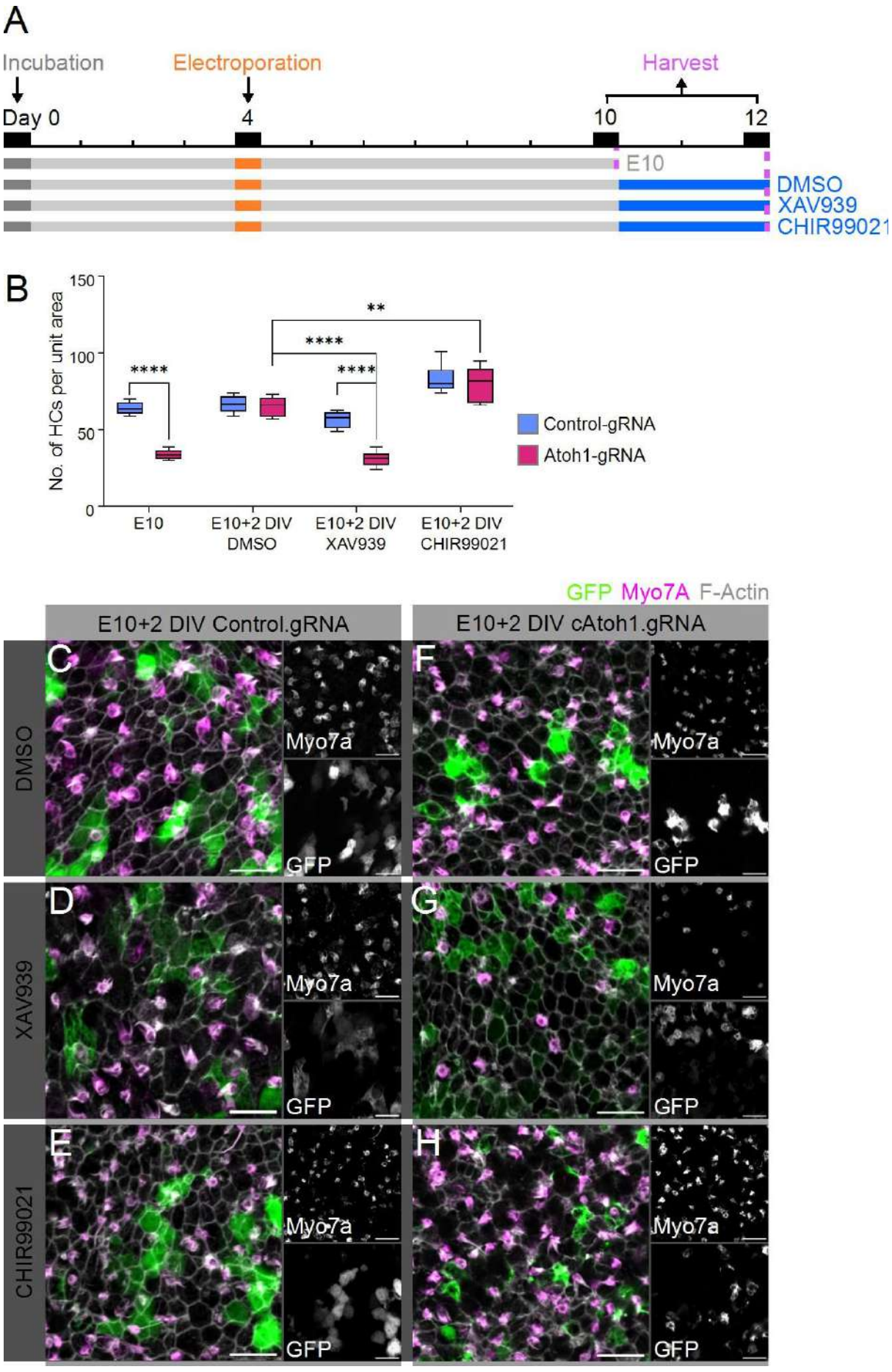
A
Incubation
Electroporation
Harvest
Day 0
4
10
12
E10
DMSO
XAV939
CHIR99021
B
No. of HCs per unit area
150
100
50
0
****
****
****
**
E10
E10+2 DIV DMSO
E10+2 DIV XAV939
E10+2 DIV CHIR99021
Control-gRNA
Atoh1-gRNA
GFP Myo7A F-Actin
E10+2 DIV Control.gRNA
E10+2 DIV cAtoh1.gRNA
DMSO
XAV939
CHIR99021
C
D
E
F
G
H
Myo7a
GFP

*Figure 4.12: Wnt Signaling Effects on Hair Cell Restoration. (A) All chick embryos undergo electroporation at embryonic day 4 (E4). At E10, basilar papilla explants are isolated and treated with DMSO control and Wnt pathway modulators for two days in vitro. Finally, the explants are harvested at E10+2 days in vitro (DIV). (B) The graph illustrates the number of hair cells in a unit area with different pharmacological treatments in control-gRNA and Atoh1-gRNA basilar papilla explants. E10, serves as time point zero before explant starts. Student's t-tests were conducted to calculate P-values, with **P<0.01 and ****P<0.0001 indicating statistical significance. (C-H) Images of basilar papilla explants from electroporated chick embryos, with a 10μm scale bar. All merged images feature phalloidin stained F-Actin in gray, Myo7a-labeled hair cells in magenta, and green indicating GFP expression from Tol2-eGFP plasmids. The left panel (C, D, E) displays images from basilar papilla explants, electroporated with the control guide, Tol2-eGFP plasmids and Cas9 protein. The right panel (F, G, H) shows images from the basilar papilla explants, electroporated with the Atoh1 guide, Tol2-eGFP plasmids and Cas9 protein. (C & F) represents the DMSO vehicle control. (D & G) are images from XAV939 treatment, a Wnt antagonist. (E & H) show images from CHIR99021 treatment, a Wnt agonist.*

4.8.2 Influence of Notch Signaling on HC Restoration

Notch inhibitor DAPT

DAPT is known for its ability to down regulate Notch pathway by gamma secretase inhibition, a protease complex required for canonical notch activation[209,223]. Our study corroborates previous research demonstrating that inhibiting the Notch pathway results in an excess of hair cells in zebrafish, chicks, and mice[209,224–226], highlighting the crucial role of the Notch pathway in hair cell regeneration. In our experiments (Figure 4.13 A), DAPT treatment of E10+2 DIV Atoh1-gRNA led to the recovery of hair cells to a level comparable to that of the control-gRNA under the same explant conditions (Figure 4.13 B, D, F). Similar to CHIR99021, DAPT stimulates hair cell proliferation to a greater extent than the observed hair cell numbers in the DMSO treated E10+2 DIV explants for both Atoh1-gRNA and control-gRNA (Figure 4.13 B, C, E). Furthermore, DAPT significantly influences the organization of HCs and SCs within the basilar papilla by disrupting the Notch pathway, which is crucial for mediating lateral inhibition during their differentiation. This disruption led to a striking increase in the interactions between adjacent HCs, resulting in a higher incidence of HC-HC contact at the E10+2 DIV stage (Figure 4.13 G).

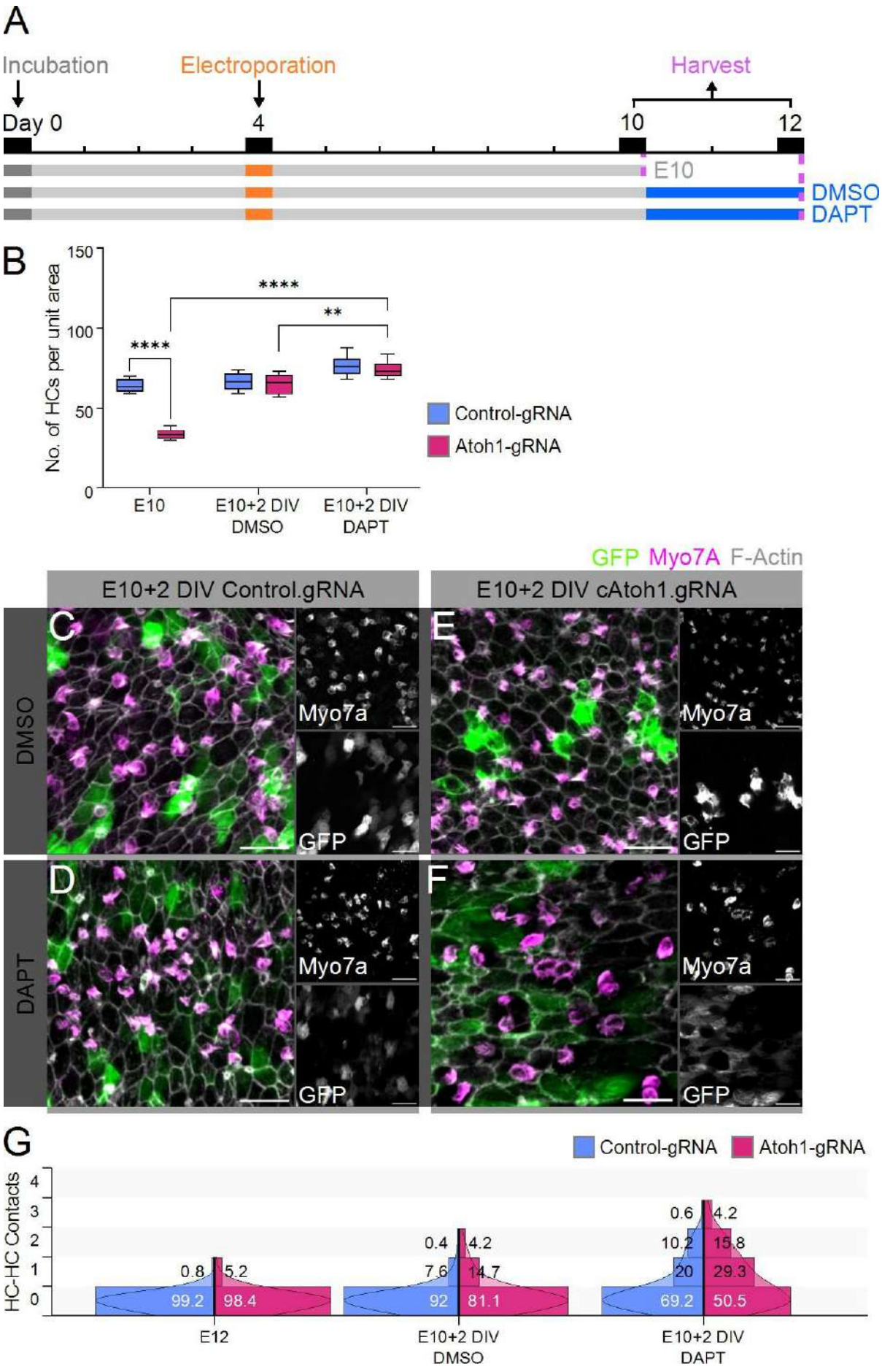
A
Incubation
Electroporation
Harvest
Day 0
4
10
12
E10
DMSO
DAPT
B
No. of HCs per unit area
150
100
50
0
****
**
****
Control-gRNA
Atoh1-gRNA
E10
E10+2 DIV DMSO
E10+2 DIV DAPT
GFP Myo7A F-Actin
E10+2 DIV Control.gRNA
E10+2 DIV cAtoh1.gRNA
DMSO
DAPT
C
D
E
F
Myo7a
GFP
G
Control-gRNA
Atoh1-gRNA
HC-HC Contacts
4
3
2
1
0
0.8
5.2
99.2
98.4
0.4
4.2
7.6
14.7
92
81.1
0.6
4.2
10.2
15.8
20
29.3
69.2
50.5
E12
E10+2 DIV DMSO
E10+2 DIV DAPT

*Figure 4.13: Notch Signaling Effects on Hair Cell Restoration. (A) Diagram of the experimental setup for Notch inhibitor treatment: Electroporation at E4, followed by a two-day small molecule treatment at E10, and harvesting the basilar papilla at E10+2 DIV. (B) The graph illustrates the number of hair cells in a unit area with different pharmacological treatments in control-gRNA and Atoh1-gRNA basilar papilla explants. E10, serves as time point zero before explant starts. Student's t-tests were conducted to calculate P-values, with **P<0.01 and ****P<0.0001 indicating statistical significance. (C-F) Images of basilar papilla explants from electroporated chick embryos, with a 10μm scale bar. All merged images feature phalloidin stained F-Actin in gray, Myo7a-labeled hair cells in magenta, and green indicating GFP expression from Tol2-eGFP plasmids. The left panel (C-D) displays images from basilar papilla explants, electroporated with the control guide, Tol2-eGFP plasmids and Cas9 protein. The right panel (E-F) shows images from the basilar papilla explants, electroporated with the Atoh1 guide, Tol2-eGFP plasmids and Cas9 protein. (G) The graphs illustrate HC-HC contact in electroporated control-gRNA and Atoh1-gRNA, comparing E12 control basilar papilla with E10+2 DIV basilar papilla explants treated with DMSO and DAPT.*

4.9 Signaling Dynamics in HC Restoration

To investigate the spatial and temporal activity of Notch and Wnt signaling during hair cell restoration, we co-electroporated Atoh1-gRNA CRISPR/Cas9 components with reporter constructs for each pathway, one at a time.

4.9.1 Notch Signaling Activity During HC Recovery

In order to understand Notch regulation in Atoh1 knockout basilar papilla, we conducted co-electroporation experiments that combined the pT2K-Hes5::nd2mScarlet plasmid, alongside with CRISPR/Cas9 components featuring either a control-gRNA or Atoh1-gRNA. pT2K-Hes5::nd2mScarlet plasmid is a transposon construct which functions as a reporter for notch activity. The plasmid consists of the mouse Hes5 promoter to drive the expression of a destabilized and nuclear localized mScarlet fluorescent protein in Notch-On cells[227]. The mScarlet expression is transient, with its presence limited to cells where Notch is active or recently active. Beyond a 10-hour timeframe, mScarlet expression diminishes due to its short half-life following Notch inhibition, as documented in prior research[227]. We noted a significant reduction in the population of Notch-On cells within the basilar papilla of Atoh1-gRNA at E10 (Figure 4.14 B, D), in contrast to control-gRNA (Figure 4.14 A), with these cells identified based on the expression of mScarlet.

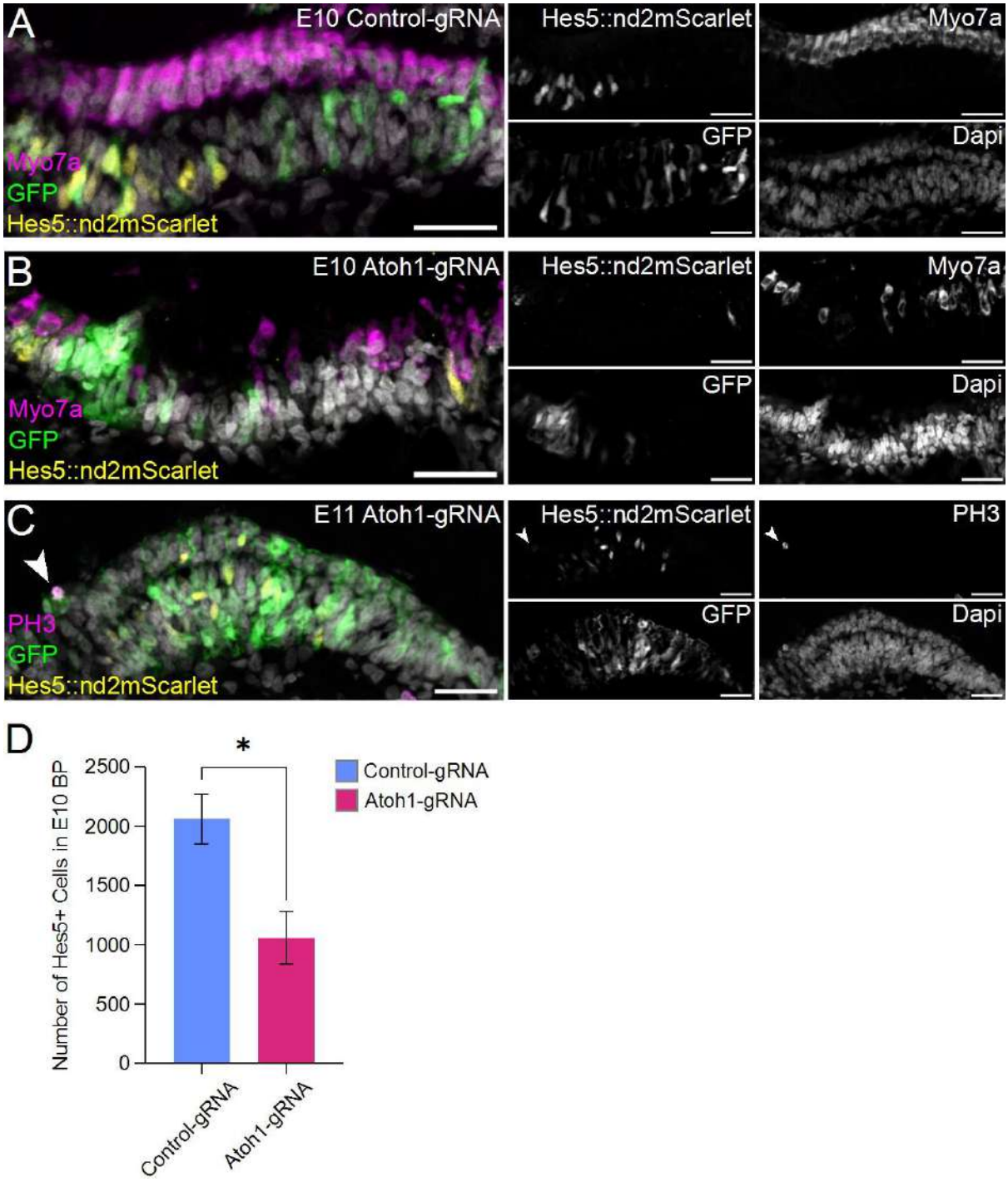

*Figure 4.14: Notch Reporter Hes5::nd2mScarlet Activity during Hair Cell Restoration. The images are cross-sections of the basilar papilla from electroporated chick embryos, with a 25μm scale bar. (A) and (B) are merged images of E10 basilar papilla, highlighting Myo7a-stained hair cells in magenta, DAPI-stained nuclei in gray, Notch-on cells labeled in yellow with the Hes5::nd2mScarlet reporter, and GFP expression in green. (A) depicts control-gRNA samples electroporated with the control guide, Tol2-eGFP plasmids, pT2K-Hes5::nd2mScarlet, and Cas9 protein. (B) shows Atoh1-gRNA samples electroporated with the Atoh1 guide, Tol2-eGFP plasmids, pT2K-Hes5::nd2mScarlet, and Cas9 protein. (C) presents E11 Atoh1-gRNA samples with Phospho-Histone H3 (PH3) antibody-stained dividing cells in magenta, DAPI-stained nuclei in gray, Notch-on cells in yellow, and GFP expression in green. (D) is a graph representing the total number of Hes5+ cells in the E10 basilar papilla for control-gRNA and Atoh1-gRNA conditions, with statistical significance assessed using Student's t-tests, where *P<0.05 indicates significance.*

Hes5 Downregulation and Cell Cycle Re-entry

We observed that Phosphohistone H3 (PH3), utilized for immunohistochemical labeling to identify mitotic cells in cross sections of the basilar papilla, exhibited staining in cells with diminished mScarlet expression located at the luminal surface, where hair cells are should be present (Figure 4.14 C). This intriguing observation is particularly noteworthy because Hes5, which drives mScarlet expression, is exclusively found in supporting cells. The reduced mScarlet expression in these cells suggests their transformation into new hair cells. The plausible explanation for this occurrence is that these cells were Notch-On supporting cells during an earlier developmental stage but subsequently switched off Notch activity to undergo conversion into hair cells. These findings strongly indicate that the downregulation of Hes5 in supporting cells promotes hair cell differentiation and further demonstrates that supporting cells can be induced to re-enter the cell cycle and give rise to new hair cells. Hes5 is a well-known repressor of the Atoh1 transcription factor, playing a critical role in limiting the conversion of supporting cells into hair cells. This repression of Atoh1 by Hes5 is pivotal for maintaining a reservoir of undifferentiated supporting cells in the inner ear, a reserve crucial for hair cell regeneration following damage.

4.9.2 Wnt Signaling Activity During HC Recovery

For examining the Wnt signaling in during HC restoration in Atoh1-crispant basilar papilla, we used a transposon construct pT2K-5TCF::nd2mScarlet. This construct features 5 TCF/LEF binding sites that regulate the expression of a destabilized and nuclear localized mScarlet protein in cells responsive to Wnt signaling during chick inner ear development. The nd2mScarlet exhibits a destabilized feature, allowing it to report on cells with activated Wnt signaling or those that have recently had Wnt activity. If the cells are not Wnt-responsive or the Wnt activity has ceased more than 10 hours ago, there will be no expression of mScarlet. pT2K-5TCF::nd2mScarlet construct is co-electroporated with the pCAGGS-T2TP (transposase) & pT2K-CAGGS-eGFP combined with CRISPR/Cas9 components featuring either control-gRNA or Atoh1-gRNA.

We observed a significant increase in the number of Wnt-responsive cells within the basilar papilla of Atoh1-gRNA compared to those in the control-gRNA at E10 (Figure 4.15 A-C). Wnt-responsive cells were identified by the expression of mScarlet in electroporated embryos. These results are consistent with prior research in the field, which highlights the essential role of canonical Wnt signaling in promoting proliferation in response to hair cell loss[226,228].

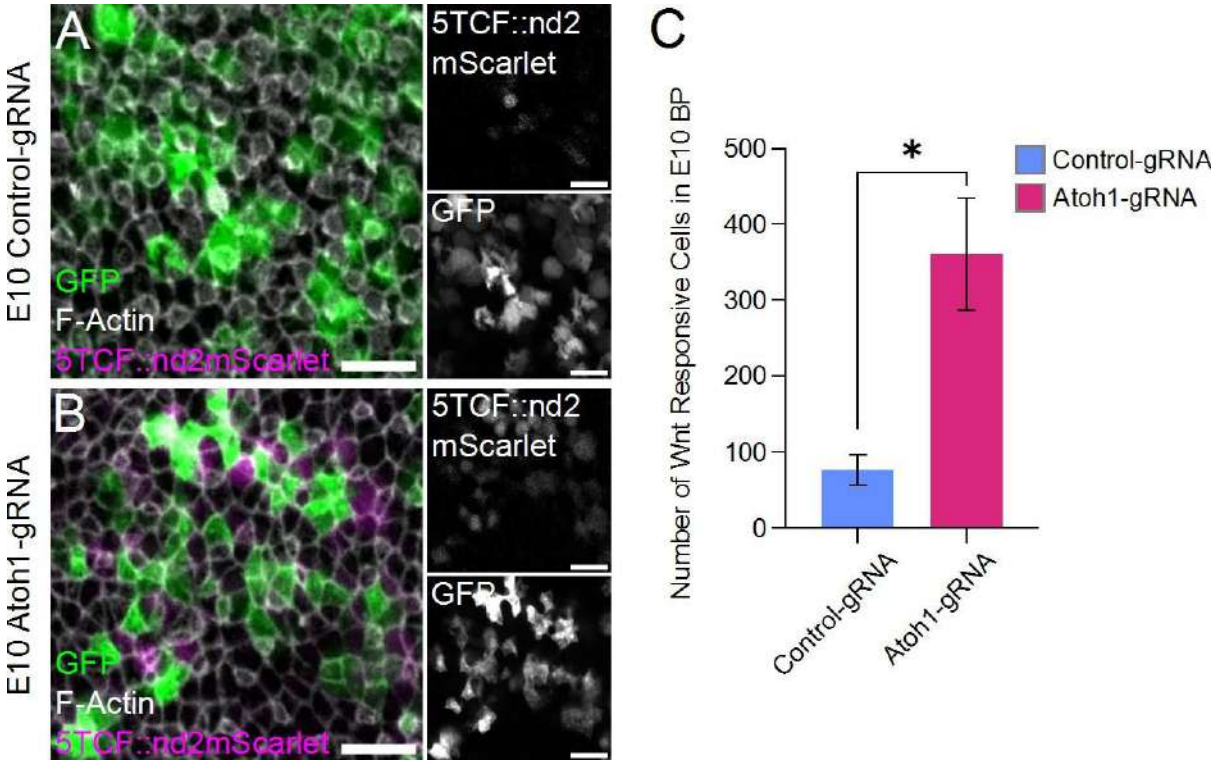

*Figure 4.15: Wnt Reporter 5TCF::nd2mScarlet Activity during Hair Cell Restoration. All the images are of whole-mounted basilar papilla at E10 from electroporated chick embryos, with a 10μm scale bar. (A) and (B) are merged images highlighting Wnt-responsive cells in magenta using the 5TCF::nd2mScarlet reporter, F-Actin stained by phalloidin in gray, and GFP expression from Tol2-eGFP plasmids in green. (A) shows control-gRNA samples electroporated with the control guide, Tol2-eGFP plasmids, pT2K-5TCF::nd2mScarlet, and Cas9 protein. (B) displays Atoh1-gRNA samples electroporated with the Atoh1 guide (pcU6.1-Atoh1-gRNA), Tol2-eGFP plasmids (pCAGGS-T2TP & pT2K-CAGGS-eGFP), pT2K-5TCF::nd2mScarlet, and Cas9 protein. (C) presents a graph illustrating the total number of Wnt-positive cells in the E10 basilar papilla for both control-gRNA and Atoh1-gRNA conditions. Statistical significance for comparisons between the two conditions was evaluated using Student's t-tests, with *P<0.05 indicating significance.*

Chapter 5: Discussion

This thesis investigates the regenerative potential of the chick auditory epithelium following the targeted deletion of Atoh1, a critical gene for hair cell differentiation. Utilizing CRISPR-Cas9 in ovo electroporation, we observed a remarkable capacity of the chick basilar papilla to restore hair cell numbers despite significant disruption of Atoh1. The targeted deletion of Atoh1 enables precise genetic manipulation, minimizing off-target effects and providing robust evidence for Atoh1's essential role in hair cell differentiation. Furthermore, this study underscores the significance of Wnt and Notch signaling pathways in the hair cell restoration process.

This finding is particularly intriguing when compared to the mammalian auditory system, where supporting cells (SCs) in the organ of Corti exhibit a more specialized and limited regenerative capacity. In contrast, the chick basilar papilla contains a more homogenous and regenerative SC population[229]. While adult mammalian cochlear SCs generally lack regenerative potential, some studies suggest a possibility for limited regeneration in the neonatal cochlea and the adult vestibular system[230]. Birds can replace damaged hair cells in the inner ear. However, the mechanisms by which the basilar papilla senses the absence of a hair cell, activates quiescent progenitors, and proceeds with hair cell replacement remain unclear. This challenge is partly due to the inaccessibility of hair cell regeneration paradigms, which often require post-hatch stages of chicks. This study highlights the potential of the embryonic chick model to contribute valuable insights into the mechanisms underlying hair cell regeneration.

5.1 Experimental Framework & Genetic Mosaicism

In this study, we demonstrate a non-invasive approach to investigating hair cell differentiation and regeneration in the basilar papilla. Instead of using pharmacological drugs, acoustic trauma, or physical damage to eliminate hair cells, we employed a genetic ablation strategy targeting the Atoh1 gene using CRISPR-Cas9. This method allows for a controlled and precise manipulation of hair cell populations.

Our experimental methodology is robust and includes two control groups: one with no injection, serving as an internal control, and another with a control-gRNA injection to account for potential electroporation-induced effects. Generating transgenic chickens presents a significant challenge due to the intricate structure of chicken zygotes and the unique

organization of chick embryos, making it difficult to produce germline genetically modified chickens. Moreover, Atoh1's essential role in various embryonic functions, particularly in neurogenesis, makes its deletion from germ cells embryonically lethal. Therefore, localized otic vesicle in ovo electroporation emerges as the optimal approach for knocking out the Atoh1 gene. In ovo electroporation enables the efficient delivery of the CRISPR-Cas9 system to the developing chick inner ear, facilitating targeted gene editing within the basilar papilla. We introduced CRISPR-Cas9 components along with Atoh1-gRNA, confining the genetic manipulation to the inner ear and avoiding interference with the rest of the embryo. This approach induces an inner ear-specific phenotype and generates genetic mosaicism within the basilar papilla, resulting in a mix of cells with distinct genotypes.

This mosaicism creates a spatial variation in gene transfer within the tissue, providing an opportunity to assess the cell autonomy of a specific genetic modification or phenotype. By having a mixed population of cells—some with functional Atoh1 and others lacking it—we can make direct comparisons and gain insights into cell-autonomous versus non-autonomous effects. To track mosaic expression, we utilized Tol2-eGFP plasmids (pCAGGS-T2TP & pT2K-CAGGS-eGFP), which integrate into the genome, marking GFP-positive cells as indicators of CRISPR-Cas9 editing and genetic alteration. However, in some instances, cells may be GFP-marked without undergoing successful CRISPR-Cas9 editing, resulting in no genetic modification. This failure could occur if a subset of cells received the Tol2-GFP plasmid but not the pcU6.1-Atoh1-gRNA construct, despite co-electroporation of both constructs. Other potential reasons include inefficient Cas9 cleavage, degradation of pcU6.1-Atoh1-gRNA, or single-copy deletions of the Atoh1 gene within the electroporated cell. These instances are referred to as "escapers". Despite these caveats, this methodological approach provides a tool for understanding the mechanisms of hair cell differentiation and regeneration and offers insights into the potential for cell-specific genetic interventions.

5.2 Homeostatic Control of Hair Cell Differentiation

The homeostatic mechanism for regulating hair cell (HC) numbers in the chick basilar papilla, as identified in this study, has not been previously explored. Following Atoh1 deletion at embryonic day 9 (E9), the epithelium manages to recover HC numbers completely by E12. This recovery is spatially organized, mirroring the natural progression of HC differentiation. The process of HC restoration can be described as either "Delayed Development" or "Ongoing Genesis". Delayed development refers to the disruption of the

normal timing of hair cell differentiation, resulting in a shifted timeframe for HC formation. Alternatively, ongoing genesis reflects the recovery of HC numbers to near-normal levels by E12 through homeostatic renewal.

The differentiation of HCs after mosaic deletion throughout the basilar papilla involves signals acting on progenitor cells in the sensory epithelium. In areas where HCs were deleted, surrounding supporting cells that did not receive the Atoh1-gRNA convert into HCs. This ongoing genesis is part of a homeostatic mechanism ensuring the proper number of HCs required for the physiological process of hearing. The tissue homeostatic mechanism maintains equilibrium in HC numbers for auditory sensory response, potentially involving the resurrection of HCs for tissue maintenance.

The observed embryonic stages from E9 to E12 are critical for several reasons. First, these stages capture the transition from exponential growth to a stationary growth phase of HC differentiation within the basilar papilla. E9 represents the exponential phase with increased HC differentiation, while by E12, HC numbers stabilize, reaching a plateau similar to mature basilar papilla levels[217]. Second, significant changes in the arrangement of hair and supporting cells occur between E9 and E12, marking a crucial developmental period. At E9, most cells in the basilar papilla exit the cell cycle, and by E12, the apical surfaces of supporting cells compress, resembling the pattern seen in the mature papilla. In wild-type basilar papilla, hair cell differentiation reaches a stationary phase by E12. However, in Atoh1-crispants, this process is delayed, leading to continued exponential HC differentiation and an increased number of HCs even at E12. This secondary HC formation provides valuable insights into the restoration process, cellular proliferation, cell fate determination, and the establishment of polarity. The disruption caused by the absence of HCs in tissue organization closely resembles scenarios with reduced HC numbers compared to the wildtype.

5.3 HC Restoration as HC Regeneration Model

This study proposes that hair cell restoration, observed after Atoh1 depletion in the chick basilar papilla, can serve as a valuable model for understanding hair cell regeneration. Despite being distinct processes with different initiating factors, restoration and regeneration share significant similarities. Both rely on Wnt and Notch signaling pathways to regulate cell fate decisions and promote hair cell formation. Additionally, both processes can utilize proliferative and non-proliferative pathways, or even transdifferentiation, to generate new

hair cells. These shared mechanisms support the use of restoration as a model to study the broader phenomenon of hair cell regeneration. Further strengthening this connection is the observed "restoration wave" in our study. Unlike previous hair cell regeneration models where newly generated cells filled damaged areas, our Atoh1-depleted regions exhibited restoration progressing from the distal to proximal side, mimicking the natural development pattern of hair cells. This suggests potentially shared regulatory mechanisms between embryonic development and regenerative self-repair.

Interestingly, the basilar papilla in our study maintained its overall size despite targeted hair cell loss through Atoh1 deletion. This suggests that the "absent" hair cells might exist in a progenitor state, unable to differentiate due to the genetic alterations. However, neighboring supporting cells demonstrate a remarkable ability to transdifferentiate into hair cells, compensating for the loss. The observed proliferative dynamics further support this notion. In the regenerating chick cochlea and utricle, there is a peak in proliferation at 48 hours after ototoxic injury[231]. We observe similar dynamics in Atoh1-crispants, with direct transdifferentiation initiating as early as within 24 hours. The recovery of hair cells by E12 demonstrates the remarkable ability of the basilar papilla's homeostasis to rapidly compensate for missing hair cells. These findings underscore the importance of studying E9 to E12 embryonic stages for a comprehensive understanding of hair cell development and related research.

5.4 Supporting Cells are Hair Cell Progenitors

The restoration of hair cell numbers in regions where Atoh1-gRNA specifically restricted hair cell fate highlights the remarkable plasticity and dynamic nature of supporting cells within the sensory epithelium[232]. Their characteristic pseudostratified morphology, allowing for movement within the epithelium, could facilitate migration and restoration of hair cell-depleted patches through mitotic division or transdifferentiation. This pseudostratified morphology might also contribute to preserving "stemness," the ability to self-renew and differentiate into other cell types. These characteristic positions supporting cells as potential progenitors in hair cell regeneration. However, the specific subtypes of supporting cells involved in regeneration remain unclear in avian models. It is suggested that only specific types of supporting cells that possess the competence to undergo the transformation are required for hair cell regeneration, although concrete evidence supporting this notion is currently absent.

In our investigation of Atoh1-crispants, we began to question the identity of the cells that had taken the place of the missing hair cells. These cells could potentially represent sensory precursors, progenitors, or are just supporting cells. Our hypothesis is that all supporting cells have the potential to become hair cell progenitors. Based on their morphology and the expression of the Hes5 repressor, it is likely that these cells are indeed supporting cells. The decline in Hes5 expression, as demonstrated in this study, reflects the shift from the quiescent state of supporting cells to re-entering the cell cycle. However, findings in the study from inhibitory explant using DAPT, a Notch signaling inhibitor, present a contrasting view. Control-gRNA explants treated with DAPT displayed a modest increase in HC number, similar to the level of hair cell restoration observed in Atoh1-crispant BP explants treated with the same DAPT treatment. This modest increase suggests that only a subset of supporting cells might possess progenitor potential, and HC depletion might be stimulating these specific progenitor-competent supporting cells to differentiate into hair cells.

Furthermore, we observed that the initiation of supporting cell transdifferentiation precedes that of supporting cell asymmetric mitotic division. Interestingly, the restorative process primarily occurs via transdifferentiation, which significantly outpaces the contribution of asymmetric mitotic division in terms of hair cell replenishment. When hair cells die, they are extruded, creating voids in the sensory epithelium. These voids are filled by supporting asymmetric cell division, generating new hair cell and replenishing the supporting cell undergoing division. However, in our experimental Atoh1-crispant basilar papilla phenotype, hair cell death is absent. The preference for transdifferentiation can be ascribed to the abundant reservoir of supporting cells in the tissue. Opting for mitotic division as the dominant mode for hair cell generation could risk disturbing the intricate organization and arrangement of the sensory epithelium.

5.5 Signaling Mechanism of HCs Restoration

Our neighbour number analysis of the Atoh1-crispants BP has provided valuable insights into the disrupted arrangement and organization of hair cells and supporting cells. It appears that this disruption is sensed by supporting cells, which recognize the absence of neighbouring hair cells, triggering a molecular switch within the supporting cells to initiate the process of hair cell regeneration. We propose a two-phase model for hair regeneration involving: an initial "trigger" phase followed by a subsequent "switch" phase, each with distinct cellular

signalling. Our hypothesis suggests that the initial trigger for supporting cell conversion into hair cells is facilitated through juxtacrine signaling. Once the trigger is activated, Wnt/β-catenin signaling takes over, driving hair cell regeneration. Our research highlights a coordinated interplay between the Notch and Wnt signaling pathways in orchestrating the complex process of hair cell regeneration, with Notch serving as the initiator and Wnt as the subsequent driver of this remarkable regenerative phenomenon. For hair cell regeneration, active canonical Wnt signaling promotes sensory hair cell production, especially in non-mammalian vertebrates like avians, while its inhibition hinders hair cell proliferation and regeneration. Both the Notch and Wnt signaling pathways wield their influence over Atoh1, albeit with opposing effects: Notch acts as an antagonist, while Wnt functions as an agonist.

In the Atoh1-crispant phenotype, supporting cells lacking neighboring hair cells experience disrupted Notch signaling due to the absence of Notch-Delta interactions. This leads to a reduction in NICD that normally suppresses Atoh1 expression via Hes5 regulation. Our findings corroborate this by demonstrating reduced pT2K-Hes5::nd2mScarlet reporter activity during hair cell restoration. It does imply that SC fate needs to be maintained by continuous Delta interaction and in the absence of NICD, Atoh1 expresses due to the subsequent loss of Hes5 inhibition, initiate a compensatory hair cell fate determination pathway. In contrast to the suppression of Notch signalling during HC restoration, a canonical Wnt reporter pT2K-5TCF::nd2mScarlet is upregulated in response to mosaic Atoh1 deletion. Downstream Wnt molecule β-catenin regulates Atoh1 expression due to its interaction with Tcf-Lef sites in the Atoh1 enhancer[93,180]. Our observations align with previous studies, where Notch inhibition induces the overexpression of β-catenin and activation of Wnt target genes in the supporting cells of postnatal mice cochlea[167]. These findings suggest a potential role for β-catenin in initiating Atoh1 expression, facilitating hair cell formation during HC restoration.

Understanding the impact of impairing both the "trigger" (Notch) and the "switch" (Wnt) on supporting cell-to-hair cell conversion during HC restoration, we conducted a two-day in vitro pharmacological treatment in control-gRNA and Atoh1-gRNA basilar papilla. Inhibition of Wnt signaling using XAV939 prevents HC restoration, suggesting that Wnt signaling is essential for maintaining a progenitor pool capable of generating new hair cells. This implies that β-catenin stabilization is crucial for HC conversion in the BP, and in its absence these progenitor cells/supporting cells enter a cell cycle exit (G_0 phase). The Wnt agonist CHIR99021, an inhibitor of GSK-3β, promotes a modest increase in hair cell numbers. Given that GSK-3β also regulates Notch signaling by phosphorylating NICD, the

observed effects of CHIR99021 could be attributed to alterations in both Wnt and Notch pathways[233]. It is possible that GSK-3β-mediated NICD degradation effectively releases the Notch mediated maintenance of SC/progenitor fate. The precise nature of the crosstalk between Wnt and Notch signaling pathways remains elusive, with the mechanisms underlying their potential interactions yet to be elucidated.

5.6 Implication of the Studies

Our knowledge of auditory biology has greatly progressed with the identification of particular genes related to inner ear function[234,235]. The lack of function in these genes leads to the degeneration of several cell types, especially HC[236–239]. Many cases of hereditary deafness are caused by mutations in genes encoding for cytoskeletal, structural, or channel proteins. This study demonstrates the feasibility and effectiveness of CRISPR/Cas9 gene editing in the chick embryo basilar papilla. Further, the ability to test small molecule pharmacological inhibitors and activators on genetically altered Crispant BPs can facilitate understanding signaling pathways involved in hair cell regeneration.

In this study, by precisely altering specific genes within the basilar papilla, we genetically ablated Atoh1, the master regulator gene for hair cells, resulting in a reduced number of hair cells. We then observed the restoration of hair cell numbers, suggesting a remarkable capacity for the sensory epithelium to maintain homeostasis. The recovery of hair cell numbers in Atoh1-crispant basilar papilla (BP) to wild-type BP hair cell numbers indicates a homeostatic mechanism. This homeostatic mechanism in supporting cells involves Wnt and Notch signaling and their crosstalk to determine the required hair cell number for functional physiology. The study highlights the complex interplay between Wnt and Notch signaling pathways in regulating hair cell fate and regeneration.

The implications of our study extend to the development of gene therapy approaches aimed at restoring hair cell function and treating hearing loss. The observed restoration of hair cells following Atoh1 depletion, a process potentially mimicking regeneration, suggests the involvement of similar molecular mechanisms. In both restoration and regeneration, the pseudostratified morphology of supporting cells with progenitor-like potential enables them to contribute to hair cell recovery through transdifferentiation or mitotic division.

The ability to genetically ablate genes and observe the effects on hair cells within the basilar papilla provides a model for studying the molecular mechanisms underlying hair cell formation and function. Using this genome-editing model, we can examine various cell

signaling pathways and their phenotypes in detail, as demonstrated with key genes such as Vangl2[218] and Actin4 (Data not shown here), which play crucial roles in hair cell orientation and cytoskeletal integrity, respectively. This research provides the groundwork for developing gene therapies to restore hearing. While the chick model offers valuable insights, translating these findings to humans necessitates further investigation.

5.7 Limitation of the study

While the study demonstrates remarkable hair cell (HC) number restoration in the chick basilar papilla (BP) following mosaic Atoh1 deletion, several key areas require further investigation to fully understand the phenomenon's potential for HC regeneration. One crucial aspect is functional recovery. Although the study reports restored HC numbers, the limited timeframe (observation at E12) restricts our understanding of the long-term stability of restored HCs. It's vital to investigate whether these cells persist over time and if there are any delayed effects. Long-term studies are essential to assess the if these restored HCs exhibit normal electrical properties and contribute to functional hearing. Another critical question remains unanswered: the cellular origin of the newly generated HCs. The study proposes two possibilities: (1) a yet-to-be-identified pool of progenitor cells within the BP, or (2) existing supporting cells undergoing transdifferentiation. Lineage tracing experiments and single-cell RNA sequencing could provide valuable insights into this process.

The study utilizes CRISPR-Cas9 for targeted mosaic Atoh1 deletion. While aiming for specificity, off-target effects are a possibility, potentially influencing the results. Future studies could employ additional controls to mitigate this concern. The study demonstrates the influence of Wnt signaling modulation on HC restoration. However, a deeper understanding of the intricate interplay between Wnt and Notch pathways, both crucial for hair cell development and regeneration, is lacking. These pathways don't function in isolation but engage in complex crosstalk, influencing each other's activity. Future studies should explore this interplay in more detail. Furthermore, the study observes that inhibiting Wnt signaling with XAV-939 blocks HC restoration, but the underlying molecular mechanisms remain unclear. Does Wnt inhibition directly affect HC differentiation gene expression, or does it alter the balance of Notch signaling, indirectly impacting HC regeneration? Elucidating these mechanisms is essential for a more comprehensive understanding. Isolating signalling pathway manipulation risks unintended consequences. Wnt activation for HC regeneration

could disrupt supporting cell fate or cochlear development if Notch signaling is not well-regulated.

The chick model, while valuable, has limitations in its generalizability to mammals. Although some hair cell regeneration mechanisms might be conserved in the mammalian organ of Corti, the greater heterogeneity of supporting cell types in mammals compared to non-mammalian organisms makes direct translation to the human hearing system challenging. Future research could enhance translational relevance by exploring similar in utero electroporation approaches in mammalian models, such as mice, targeting Atoh1 deletion in the otocyst at embryonic stages using CRISPR.

5.8 Future Directions

Building upon the foundation established in this study, future research can delve deeper into the observed hair cell (HC) restoration process and address the limitations of the study.

5.8.1 Live-Cell Imaging and Reporter Assays

To elucidate the real-time dynamics of supporting cell conversion into HCs, future studies could employ live-cell imaging techniques. This would allow visualization of morphological changes in supporting cells, such as shape and size alterations, during transdifferentiation. Additionally, utilizing reporters for Wnt and Notch signaling pathways will enable researchers to capture the dynamic nature of this process. Analyzing the expression patterns of key components (ligands, receptors, target genes) of these pathways through live-cell imaging could provide valuable insights into their temporal and spatial activity during HC restoration.

5.8.2 Dissecting Wnt/Notch Crosstalk

While this study demonstrates the independent upregulation of Wnt signaling following HC deletion, it leaves unanswered questions regarding the detailed mechanisms of Wnt signaling and its interaction with the Notch pathway. Future investigations could explore whether manipulating Wnt signaling influences Notch activity during hair cell regeneration. This could involve using specific Wnt agonists (like CHIR99021) and antagonists (like XAV939) to observe their impact on Notch reporter activity. Furthermore, employing more specific agonists and antagonists can dissect the individual contributions of different Wnt and Notch signaling pathways. Investigating the role of ß-catenin stabilization in maintaining progenitor

cell fate within the basilar papilla (BP) through Wnt signaling, and the potential role of GSK-3β in facilitating NICD (Notch Intracellular Domain) phosphorylation in the inner ear, would provide valuable insights into the complex interplay between these pathways during cochlear regeneration. Unveiling these interactions could illuminate potential avenues for future therapeutic interventions.

5.8.3 Computational Modeling and Functional Assays

While this study focuses on experimental data, incorporating computational modeling with quantitative analysis of cell contact changes and simulations could offer a deeper understanding of the dynamic interplay between cellular rearrangements, signaling pathways, and HC differentiation. Additionally, expanding the scope beyond HC number restoration to include functional assays, such as electrophysiology or auditory brainstem response measurements, would provide a more comprehensive understanding of the restored hair cells' functional capacity.

5.9 Conclusion

This study demonstrates a model using CRISPR-Cas9 mediated targeted gene deletion in the somatic otocyst of embryonic chicks to investigate hair cell (HC) differentiation, development, and regeneration regulators. It reveals a homeostatic mechanism for regulating HC restoration in the chick basilar papilla. Mosaic deletion of Atoh1 depletes HC numbers at E9, but they are restored by E12, suggesting a homeostatic mechanism that regulates HC numbers. The study sheds light on how the basilar papilla might sense HC absence, activate quiescent progenitors, and replace HCs through a series of not yet defined signaling steps. Pharmacological inhibitor studies in explant culture indicate a role for Wnt/Notch crosstalk in HC restoration in basilar papilla. Notch signaling maintains quiescent progenitor status, while canonical Wnt signaling promotes activation, suggesting a potential interplay between Wnt and Notch signaling in HC restoration. This exploration opens new avenues for future research aimed at harnessing the regenerative potential of the inner ear to combat hearing loss. While many questions remain unanswered.

Chapter 6: References

1. Davis A. Hearing in Adults: The Prevalence and Distribution of Hearing Impairment and Reported Hearing Disability in the MRC Institute of Hearing Research's National Study of Hearing. Reprinted. Whurr; 1998.

2. World Health Organization. Hearing Loss Due to Recreational Exposure to Loud Sounds: A Review. World Health Organization; 2015. Accessed July 21, 2024. https://iris.who.int/handle/10665/154589

3. Coleman JW. Hair cell loss as a function of age in the normal cochlea of the guinea pig. Acta Otolaryngol. 1976;82(1-2):33-40. doi:10.3109/00016487609120860

4. McGill TJ, Schuknecht HF. Human cochlear changes in noise induced hearing loss. Laryngoscope. 1976;86(9):1293-1302. doi:10.1288/00005537-197609000-00001

5. Hirokawa N. Cytoskeletal architecture of the chicken hair cells revealed with the quick-freeze, deep-etch technique. Hear Res. 1986;22:41-54. doi:10.1016/0378-5955(86)90076-6

6. Fritzsch B, Pan N, Jahan I, et al. Evolution and development of the tetrapod auditory system: an organ of Corti-centric perspective. Evolution and Development. 2013;15(1):63-79. doi:10.1111/ede.12015

7. Fritzsch B, Kersigo J, Rejent K, et al. Hair cell morphological patterns and polarity organization in the sea lamprey vestibular cristae. Anat Rec (Hoboken). 2023;306(8):2170-2184. doi:10.1002/ar.25164

8. Ladich F, Schulz-Mirbach T. Diversity in Fish Auditory Systems: One of the Riddles of Sensory Biology. Front Ecol Evol. 2016;4. doi:10.3389/fevo.2016.00028

9. Tanaka K, Smith CA. Structure of the chicken's inner ear: SEM and TEM study. Am J Anat. 1978;153(2):251-271. doi:10.1002/aja.1001530206

10. Smith CA, Konishi M, Schuff N. Structure of the barn owl's (Tyto alba) inner ear. Hear Res. 1985;17(3):237-247. doi:10.1016/0378-5955(85)90068-1

11. Manley GA. The Hearing Organs of Lizards. In: Dooling RJ, Fay RR, Popper AN, eds. Comparative Hearing: Birds and Reptiles. Vol 13. Springer Handbook of Auditory Research. Springer New York; 2000:139-196. doi:10.1007/978-1-4612-1182-2_4

12. Basch ML, Brown RM, Jen HI, et al. Fine-tuning of Notch signaling sets the boundary of the organ of Corti and establishes sensory cell fates. Elife. 2016;5:e19921. doi:10.7554/eLife.19921

13. Chang W, ten Dijke P, Wu DK. BMP pathways are involved in otic capsule formation and epithelial-mesenchymal signaling in the developing chicken inner ear. Dev Biol. 2002;251(2):380-394. doi:10.1006/dbio.2002.0822

14. D'Amico-Martel A, Noden DM. Contributions of placodal and neural crest cells to avian cranial peripheral ganglia. Am J Anat. 1983;166(4):445-468. doi:10.1002/aja.1001660406

15. Fritzsch B, Jahan I, Pan N, Kersigo J, Duncan J, Kopecky B. Dissecting the molecular basis of organ of Corti development: Where are we now? Hear Res. 2011;276(1-2):16-26. doi:10.1016/j.heares.2011.01.007

16. Ekker M, Akimenko MA, Bremiller R, Westerfield M. Regional expression of three homeobox transcripts in the inner ear of zebrafish embryos. Neuron. 1992;9(1):27-35. doi:10.1016/0896-6273(92)90217-2

17. Groves AK, Bronner-Fraser M. Competence, specification and commitment in otic placode induction. Development. 2000;127(16):3489-3499. doi:10.1242/dev.127.16.3489

18. Solomon KS, Fritz A. Concerted action of two dlx paralogs in sensory placode formation. Development. 2002;129(13):3127-3136. doi:10.1242/dev.129.13.3127

19. Liu D, Chu H, Maves L, et al. Fgf3 and Fgf8 dependent and independent transcription factors are required for otic placode specification. Development. 2003;130(10):2213-2224. doi:10.1242/dev.00445

20. Bissonnette JP, Fekete DM. Standard atlas of the gross anatomy of the developing inner ear of the chicken. Journal of Comparative Neurology. 1996;368(4):620-630. doi:10.1002/(SICI)1096-9861(19960513)368:4<620::AID-CNE12>3.0.CO;2-L

21. Sanchez-Calderon H, Milo M, Leon Y, Varela-Nieto I. A network of growth and transcription factors controls neuronal differentation and survival in the developing ear. Int J Dev Biol. 2007;51(6-7):557-570. doi:10.1387/ijdb.072373hs

22. Daudet N, Ariza-McNaughton L, Lewis J. Notch signalling is needed to maintain, but not to initiate, the formation of prosensory patches in the chick inner ear. Development. 2007;134(12):2369-2378. doi:10.1242/dev.001842

23. Li H, Corrales CE, Wang Z, et al. BMP4 signaling is involved in the generation of inner ear sensory epithelia. BMC Dev Biol. 2005;5:16. doi:10.1186/1471-213X-5-16

24. Pujades C, Kamaid A, Alsina B, Giraldez F. BMP-signaling regulates the generation of hair-cells. Dev Biol. 2006;292(1):55-67. doi:10.1016/j.ydbio.2006.01.001

25. Morrison A, Hodgetts C, Gossler A, Hrabé de Angelis M, Lewis J. Expression of Delta1 and Serrate1 (Jagged1) in the mouse inner ear. Mech Dev. 1999;84(1-2):169-172. doi:10.1016/s0925-4773(99)00066-0

26. Cole LK, Le Roux I, Nunes F, Laufer E, Lewis J, Wu DK. Sensory organ generation in the chicken inner ear: contributions of bone morphogenetic protein 4, serrate1, and lunatic fringe. J Comp Neurol. 2000;424(3):509-520. doi:10.1002/1096-9861(20000828)424:3<509::aid-cne8>3.0.co;2-q

27. Kiernan AE, Pelling AL, Leung KKH, et al. Sox2 is required for sensory organ development in the mammalian inner ear. Nature. 2005;434(7036):1031-1035. doi:10.1038/nature03487

28. Adam J, Myat A, Le Roux I, et al. Cell fate choices and the expression of Notch, Delta and Serrate homologues in the chick inner ear: parallels with Drosophila sense-organ development. Development. 1998;125(23):4645-4654. doi:10.1242/dev.125.23.4645

29. Daudet N, Lewis J. Two contrasting roles for Notch activity in chick inner ear development: specification of prosensory patches and lateral inhibition of hair-cell differentiation. Development. 2005;132(3):541-551. doi:10.1242/dev.01589

30. Jeon SJ, Fujioka M, Kim SC, Edge ASB. Notch signaling alters sensory or neuronal cell fate specification of inner ear stem cells. J Neurosci. 2011;31(23):8351-8358. doi:10.1523/JNEUROSCI.6366-10.2011

31. Wegner M, Stolt CC. From stem cells to neurons and glia: a Soxist's view of neural development. Trends Neurosci. 2005;28(11):583-588. doi:10.1016/j.tins.2005.08.008

32. Takahashi K, Yamanaka S. Induction of pluripotent stem cells from mouse embryonic and adult fibroblast cultures by defined factors. Cell. 2006;126(4):663-676. doi:10.1016/j.cell.2006.07.024

33. Oh SH, Johnson R, Wu DK. Differential expression of bone morphogenetic proteins in the developing vestibular and auditory sensory organs. J Neurosci. 1996;16(20):6463-6475. doi:10.1523/JNEUROSCI.16-20-06463.1996

34. Wu DK, Oh SH. Sensory organ generation in the chick inner ear. J Neurosci. 1996;16(20):6454-6462. doi:10.1523/JNEUROSCI.16-20-06454.1996

35. Ladher RK, Anakwe KU, Gurney AL, Schoenwolf GC, Francis-West PH. Identification of synergistic signals initiating inner ear development. Science. 2000;290(5498):1965-1967. doi:10.1126/science.290.5498.1965

36. Freter S, Muta Y, Mak SS, Rinkwitz S, Ladher RK. Progressive restriction of otic fate: the role of FGF and Wnt in resolving inner ear potential. Development. 2008;135(20):3415-3424. doi:10.1242/dev.026674

37. Pirvola U, Ylikoski J, Trokovic R, Hébert JM, McConnell SK, Partanen J. FGFR1 is required for the development of the auditory sensory epithelium. Neuron. 2002;35(4):671-680. doi:10.1016/s0896-6273(02)00824-3

38. Millimaki BB, Sweet EM, Dhason MS, Riley BB. Zebrafish atoh1 genes: classic proneural activity in the inner ear and regulation by Fgf and Notch. Development. 2007;134(2):295-305. doi:10.1242/dev.02734

39. Nicholl AJ, Kneebone A, Davies D, et al. Differentiation of an auditory neuronal cell line suitable for cell transplantation. Eur J Neurosci. 2005;22(2):343-353. doi:10.1111/j.1460-9568.2005.04213.x

40. Driver EC, Kelley MW. Specification of cell fate in the mammalian cochlea. Birth Defects Res C Embryo Today. 2009;87(3):212-221. doi:10.1002/bdrc.20154

41. Bermingham NA, Hassan BA, Price SD, et al. Math1: an essential gene for the generation of inner ear hair cells. Science. 1999;284(5421):1837-1841. doi:10.1126/science.284.5421.1837

42. Lanford PJ, Shailam R, Norton CR, Gridley T, Kelley MW. Expression of Math1 and HES5 in the cochleae of wildtype and Jag2 mutant mice. J Assoc Res Otolaryngol. 2000;1(2):161-171. doi:10.1007/s101620010023

43. Chen P, Johnson JE, Zoghbi HY, Segil N. The role of Math1 in inner ear development: Uncoupling the establishment of the sensory primordium from hair cell fate determination. Development. 2002;129(10):2495-2505. doi:10.1242/dev.129.10.2495

44. Zheng JL, Gao WQ. Overexpression of Math1 induces robust production of extra hair cells in postnatal rat inner ears. Nat Neurosci. 2000;3(6):580-586. doi:10.1038/75753

45. Kawamoto K, Ishimoto SI, Minoda R, Brough DE, Raphael Y. Math1 gene transfer generates new cochlear hair cells in mature guinea pigs in vivo. J Neurosci. 2003;23(11):4395-4400. doi:10.1523/JNEUROSCI.23-11-04395.2003

46. Woods C, Montcouquiol M, Kelley MW. Math1 regulates development of the sensory epithelium in the mammalian cochlea. Nat Neurosci. 2004;7(12):1310-1318. doi:10.1038/nn1349

47. Jones JM. Inhibitors of Differentiation and DNA Binding (Ids) Regulate Math1 and Hair Cell Formation during the Development of the Organ of Corti. Journal of Neuroscience. 2006;26(2):550-558. doi:10.1523/JNEUROSCI.3859-05.2006

48. Lanford PJ, Lan Y, Jiang R, et al. Notch signalling pathway mediates hair cell development in mammalian cochlea. Nat Genet. 1999;21(3):289-292. doi:10.1038/6804

49. Hartman BH, Hayashi T, Nelson BR, Bermingham-McDonogh O, Reh TA. Dll3 is expressed in developing hair cells in the mammalian cochlea. Dev Dyn. 2007;236(10):2875-2883. doi:10.1002/dvdy.21307

50. Zheng JL, Shou J, Guillemot F, Kageyama R, Gao WQ. Hes1 is a negative regulator of inner ear hair cell differentiation. Development. 2000;127(21):4551-4560. doi:10.1242/dev.127.21.4551

51. Zine A, Aubert A, Qiu J, et al. Hes1 and Hes5 activities are required for the normal development of the hair cells in the mammalian inner ear. J Neurosci. 2001;21(13):4712-4720. doi:10.1523/JNEUROSCI.21-13-04712.2001

52. Murata J, Tokunaga A, Okano H, Kubo T. Mapping of notch activation during cochlear development in mice: implications for determination of prosensory domain and cell fate diversification. J Comp Neurol. 2006;497(3):502-518. doi:10.1002/cne.20997

53. Hayashi T, Kokubo H, Hartman BH, Ray CA, Reh TA, Bermingham-McDonogh O. Hesr1 and Hesr2 may act as early effectors of Notch signaling in the developing cochlea. Dev Biol. 2008;316(1):87-99. doi:10.1016/j.ydbio.2008.01.006

54. Li K, Li Y, Wu W, et al. Modulation of Notch signaling by antibodies specific for the extracellular negative regulatory region of NOTCH3. J Biol Chem. 2008;283(12):8046-8054. doi:10.1074/jbc.M800170200

55. Doetzlhofer A, Basch ML, Ohyama T, Gessler M, Groves AK, Segil N. Hey2 regulation by FGF provides a Notch-independent mechanism for maintaining pillar cell fate in the organ of Corti. Dev Cell. 2009;16(1):58-69. doi:10.1016/j.devcel.2008.11.008

56. Schlosser G. A Short History of Nearly Every Sense-The Evolutionary History of Vertebrate Sensory Cell Types. Integr Comp Biol. 2018;58(2):301-316. doi:10.1093/icb/icy024

57. Tilney LG, Tilney MS, Saunders JS, DeRosier DJ. Actin filaments, stereocilia, and hair cells of the bird cochlea. III. The development and differentiation of hair cells and stereocilia. Dev Biol. 1986;116(1):100-118. doi:10.1016/0012-1606(86)90047-3

58. Katayama A, Corwin JT. Cell production in the chicken cochlea. J Comp Neurol. 1989;281(1):129-135. doi:10.1002/cne.902810110

59. Goodyear RJ, Kros CJ, Richardson GP. The Development of Hair Cells in the Inner Ear. In: Eatock RA, Fay RR, Popper AN, eds. Vertebrate Hair Cells. Vol 27. Springer

Handbook of Auditory Research. Springer-Verlag; 2006:20-94. doi:10.1007/0-387-31706-6_2

60. McGrath J, Roy P, Perrin BJ. Stereocilia morphogenesis and maintenance through regulation of actin stability. Semin Cell Dev Biol. 2017;65:88-95. doi:10.1016/j.semcdb.2016.08.017

61. Cid E, Santos-Ledo A, Parrilla-Monge M, et al. Prox1 expression in rod precursors and Müller cells. Exp Eye Res. 2010;90(2):267-276. doi:10.1016/j.exer.2009.10.015

62. Wight PA, Duchala CS, Readhead C, Macklin WB. A myelin proteolipid protein-LacZ fusion protein is developmentally regulated and targeted to the myelin membrane in transgenic mice. The Journal of cell biology. 1993;123(2):443-454. doi:10.1083/jcb.123.2.443

63. Storck T, Schulte S, Hofmann K, Stoffel W. Structure, expression, and functional analysis of a Na(+)-dependent glutamate/aspartate transporter from rat brain. Proc Natl Acad Sci USA. 1992;89(22):10955-10959. doi:10.1073/pnas.89.22.10955

64. Choi BH, Kim RC. Expression of Glial Fibrillary Acidic Protein in Immature Oligodendroglia. Science. 1984;223(4634):407-409. doi:10.1126/science.6197755

65. Katsura H, Obata K, Miyoshi K, et al. Transforming growth factor-activated kinase 1 induced in spinal astrocytes contributes to mechanical hypersensitivity after nerve injury. Glia. 2008;56(7):723-733. doi:10.1002/glia.20648

66. Nielsen S, Nagelhus EA, Amiry-Moghaddam M, Bourque C, Agre P, Ottersen OP. Specialized membrane domains for water transport in glial cells: high-resolution immunogold cytochemistry of aquaporin-4 in rat brain. J Neurosci. 1997;17(1):171-180. doi:10.1523/JNEUROSCI.17-01-00171.1997

67. Mata M, Alessi D, Fink DJ. S100 is preferentially distributed in myelin-forming Schwann cells. J Neurocytol. 1990;19(3):432-442. doi:10.1007/BF01188409

68. Jarman AP, Grau Y, Jan LY, Jan YN. atonal is a proneural gene that directs chordotonal organ formation in the Drosophila peripheral nervous system. Cell. 1993;73(7):1307-1321. doi:10.1016/0092-8674(93)90358-w

69. Jarman AP, Grell EH, Ackerman L, Jan LY, Jan YN. Atonal is the proneural gene for Drosophila photoreceptors. Nature. 1994;369(6479):398-400. doi:10.1038/369398a0

70. Aguado-Llera D, Goormaghtigh E, De Geest N, et al. The basic helix-loop-helix region of human neurogenin 1 is a monomeric natively unfolded protein which forms a “fuzzy” complex upon DNA binding. Biochemistry. 2010;49(8):1577-1589. doi:10.1021/bi901616z

71. Helms AW, Johnson JE. Progenitors of dorsal commissural interneurons are defined by MATH1 expression. Development. 1998;125(5):919-928. doi:10.1242/dev.125.5.919

72. Helms AW, Abney AL, Ben-Arie N, Zoghbi HY, Johnson JE. Autoregulation and multiple enhancers control Math1 expression in the developing nervous system. Development. 2000;127(6):1185-1196. doi:10.1242/dev.127.6.1185

73. Gómez-Dorado M, Daudet N, Gale JE, Dawson SJ. Differential regulation of mammalian and avian ATOH1 by E2F1 and its implication for hair cell regeneration in the inner ear. Sci Rep. 2021;11(1):19368. doi:10.1038/s41598-021-98816-w

74. Akazawa C, Ishibashi M, Shimizu C, Nakanishi S, Kageyama R. A mammalian helix-loop-helix factor structurally related to the product of Drosophila proneural gene atonal is a positive transcriptional regulator expressed in the developing nervous system. J Biol Chem. 1995;270(15):8730-8738. doi:10.1074/jbc.270.15.8730

75. Seipel K, Yanze N, Schmid V. Developmental and evolutionary aspects of the basic helix-loop-helix transcription factors Atonal-like 1 and Achaete-scute homolog 2 in the jellyfish. Dev Biol. 2004;269(2):331-345. doi:10.1016/j.ydbio.2004.01.035

76. Wang VY, Hassan BA, Bellen HJ, Zoghbi HY. Drosophila atonal fully rescues the phenotype of Math1 null mice: new functions evolve in new cellular contexts. Curr Biol. 2002;12(18):1611-1616. doi:10.1016/s0960-9822(02)01144-2

77. Butts T, Green MJ, Wingate RJT. Development of the cerebellum: simple steps to make a “little brain.” Development. 2014;141(21):4031-4041. doi:10.1242/dev.106559

78. Maricich SM, Wellnitz SA, Nelson AM, et al. Merkel cells are essential for light-touch responses. Science. 2009;324(5934):1580-1582. doi:10.1126/science.1172890

79. Whitear M. Merkel cells in lower vertebrates. Arch Histol Cytol. 1989;52(Suppl):415-422. doi:10.1679/aohc.52.Suppl_415

80. Graziadei PP, Levine RR, Monti Graziadei GA. Plasticity of connections of the olfactory sensory neuron: regeneration into the forebrain following bulbectomy in the neonatal mouse. Neuroscience. 1979;4(6):713-727. doi:10.1016/0306-4522(79)90002-2

81. Jørgensen JM, Mathiesen C. The avian inner ear. Continuous production of hair cells in vestibular sensory organs, but not in the auditory papilla. Naturwissenschaften. 1988;75(6):319-320. doi:10.1007/BF00367330

82. Roberson DF, Weisleder P, Bohrer PS, Rubel EW. Ongoing production of sensory cells in the vestibular epithelium of the chick. Hear Res. 1992;57(2):166-174. doi:10.1016/0378-5955(92)90149-h

83. Johns PR, Easter SS. Growth of the adult goldfish eye. II. Increase in retinal cell number. J Comp Neurol. 1977;176(3):331-341. doi:10.1002/cne.901760303

84. Raymond PA, Rivlin PK. Germinal cells in the goldfish retina that produce rod photoreceptors. Dev Biol. 1987;122(1):120-138. doi:10.1016/0012-1606(87)90338-1

85. Fernald RD. Teleost vision: seeing while growing. J Exp Zool Suppl. 1990;5:167-180. doi:10.1002/jez.1402560521

86. Schwob JE. Neural regeneration and the peripheral olfactory system. Anat Rec. 2002;269(1):33-49. doi:10.1002/ar.10047

87. Stone LS. The development of lateral-line sense organs in amphibians observed in living and vital-stained preparations. J of Comparative Neurology. 1933;57(3):507-540. doi:10.1002/cne.900570307

88. Stone LS. Further experimental studies of the development of lateral-line sense organs in amphibians observed in living preparations. J of Comparative Neurology. 1937;68(1):83-115. doi:10.1002/cne.900680105

89. Speidel CC. Correlated studies of sense organs and nerves of the lateral-line in living frog tadpoles. J Comp Neurol. 1947;87(1):29-55. doi:10.1002/cne.900870104

90. Wright MR. Regeneration and degeneration experiments on lateral line nerves and sense organs in anurans. J Exp Zool. 1947;105(2):221-257. doi:10.1002/jez.1401050206

91. Jones JE, Corwin JT. Regeneration of sensory cells after laser ablation in the lateral line system: hair cell lineage and macrophage behavior revealed by time-lapse video microscopy. J Neurosci. 1996;16(2):649-662. doi:10.1523/JNEUROSCI.16-02-00649.1996

92. Capranica RR. Sound communication and auditory physiology in anurans. The Journal of the Acoustical Society of America. 1978;64(S1):S2-S2. doi:10.1121/1.2004143

93. Corwin JT, Cotanche DA. Regeneration of sensory hair cells after acoustic trauma. Science. 1988;240(4860):1772-1774. doi:10.1126/science.3381100

94. Ryals BM, Rubel EW. Hair cell regeneration after acoustic trauma in adult Coturnix quail. Science. 1988;240(4860):1774-1776. doi:10.1126/science.3381101

95. Pickles JO, Comis SD, Osborne MP. Cross-links between stereocilia in the guinea pig organ of Corti, and their possible relation to sensory transduction. Hear Res. 1984;15(2):103-112. doi:10.1016/0378-5955(84)90041-8

96. Clark JA, Pickles JO. The effects of moderate and low levels of acoustic overstimulation on stereocilia and their tip links in the guinea pig. Hear Res. 1996;99(1-2):119-128. doi:10.1016/s0378-5955(96)00092-5

97. Husbands JM, Steinberg SA, Kurian R, Saunders JC. Tip-link integrity on chick tall hair cell stereocilia following intense sound exposure. Hear Res. 1999;135(1-2):135-145. doi:10.1016/s0378-5955(99)00101-x

98. Zheng JL, Keller G, Gao WQ. Immunocytochemical and morphological evidence for intracellular self-repair as an important contributor to mammalian hair cell recovery. J Neurosci. 1999;19(6):2161-2170. doi:10.1523/JNEUROSCI.19-06-02161.1999

99. Gale JE, Meyers JR, Periasamy A, Corwin JT. Survival of bundleless hair cells and subsequent bundle replacement in the bullfrog's saccule. J Neurobiol. 2002;50(2):81-92. doi:10.1002/neu.10002

100. Cotanche DA. Structural recovery from sound and aminoglycoside damage in the avian cochlea. Audiol Neurootol. 1999;4(6):271-285. doi:10.1159/000013852

101. Henderson D, McFadden SL, Liu CC, Hight N, Zheng XY. The role of antioxidants in protection from impulse noise. Ann N Y Acad Sci. 1999;884:368-380. doi:10.1111/j.1749-6632.1999.tb08655.x

102. Ohlemiller KK, Wright JS, Dugan LL. Early elevation of cochlear reactive oxygen species following noise exposure. Audiol Neurootol. 1999;4(5):229-236. doi:10.1159/000013846

103. Yamashita D, Jiang HY, Schacht J, Miller JM. Delayed production of free radicals following noise exposure. Brain Res. 2004;1019(1-2):201-209. doi:10.1016/j.brainres.2004.05.104

104. Evans P, Halliwell B. Free radicals and hearing. Cause, consequence, and criteria. Ann N Y Acad Sci. 1999;884:19-40. doi:10.1111/j.1749-6632.1999.tb08633.x

105. Warchol ME, Corwin JT. Regenerative proliferation in organ cultures of the avian cochlea: identification of the initial progenitors and determination of the latency of the proliferative response. J Neurosci. 1996;16(17):5466-5477. doi:10.1523/JNEUROSCI.16-17-05466.1996

106. Corwin JT, Jones JE, Katayama A, Kelley MW, Warchol ME. Hair cell regeneration: the identities of progenitor cells, potential triggers and instructive cues. Ciba Found Symp. 1991;160:103-120; discussion 120-130. doi:10.1002/9780470514122.ch6

107. Jones JE, Corwin JT. Replacement of lateral line sensory organs during tail regeneration in salamanders: identification of progenitor cells and analysis of leukocyte activity. J Neurosci. 1993;13(3):1022-1034. doi:10.1523/JNEUROSCI.13-03-01022.1993

108. Warchol ME. Macrophage activity in organ cultures of the avian cochlea: demonstration of a resident population and recruitment to sites of hair cell lesions. J Neurobiol. 1997;33(6):724-734.

109. Warchol ME. Immune cytokines and dexamethasone influence sensory regeneration in the avian vestibular periphery. J Neurocytol. 1999;28(10-11):889-900. doi:10.1023/a:1007026306730

110. Bhave SA, Oesterle EC, Coltrera MD. Macrophage and microglia-like cells in the avian inner ear. J Comp Neurol. 1998;398(2):241-256. doi:10.1002/(sici)1096-9861(19980824)398:2<241::aid-cne6>3.0.co;2-0

111. Warchol ME. Supporting cells in isolated sensory epithelia of avian utricles proliferate in serum-free culture. Neuroreport. 1995;6(7):981-984. doi:10.1097/00001756-199505090-00008

112. Warchol ME. Cell density and N-cadherin interactions regulate cell proliferation in the sensory epithelia of the inner ear. J Neurosci. 2002;22(7):2607-2616. doi:10.1523/JNEUROSCI.22-07-02607.2002

113. Witte MC, Montcouquiol M, Corwin JT. Regeneration in avian hair cell epithelia: identification of intracellular signals required for S-phase entry. Eur J Neurosci. 2001;14(5):829-838. doi:10.1046/j.0953-816x.2001.01695.x

114. Forge A. Outer hair cell loss and supporting cell expansion following chronic gentamicin treatment. Hear Res. 1985;19(2):171-182. doi:10.1016/0378-5955(85)90121-2

115. Cotanche DA, Saunders JC, Tilney LG. Hair cell damage produced by acoustic trauma in the chick cochlea. Hear Res. 1987;25(2-3):267-286. doi:10.1016/0378-5955(87)90098-0

116. Cotanche DA, Dopyera CE. Hair cell and supporting cell response to acoustic trauma in the chick cochlea. Hear Res. 1990;46(1-2):29-40. doi:10.1016/0378-5955(90)90137-e

117. Marsh RR, Xu LR, Moy JP, Saunders JC. Recovery of the basilar papilla following intense sound exposure in the chick. Hear Res. 1990;46(3):229-237. doi:10.1016/0378-5955(90)90004-9

118. Li L, Nevill G, Forge A. Two modes of hair cell loss from the vestibular sensory epithelia of the guinea pig inner ear. J Comp Neurol. 1995;355(3):405-417. doi:10.1002/cne.903550307

119. Katayama A, Corwin JT. Cochlear cytogenesis visualized through pulse labeling of chick embryos in culture. J Comp Neurol. 1993;333(1):28-40. doi:10.1002/cne.903330103

120. Oesterle EC, Rubel EW. Postnatal production of supporting cells in the chick cochlea. Hear Res. 1993;66(2):213-224. doi:10.1016/0378-5955(93)90141-m

121. Cotanche DA. Regeneration of hair cell stereociliary bundles in the chick cochlea following severe acoustic trauma. Hear Res. 1987;30(2-3):181-195. doi:10.1016/0378-5955(87)90135-3

122. Cruz RM, Lambert PR, Rubel EW. Light microscopic evidence of hair cell regeneration after gentamicin toxicity in chick cochlea. Arch Otolaryngol Head Neck Surg. 1987;113(10):1058-1062. doi:10.1001/archotol.1987.01860100036017

123. Stone JS, Cotanche DA. Identification of the timing of S phase and the patterns of cell proliferation during hair cell regeneration in the chick cochlea. J Comp Neurol. 1994;341(1):50-67. doi:10.1002/cne.903410106

124. Kil J, Warchol ME, Corwin JT. Cell death, cell proliferation, and estimates of hair cell life spans in the vestibular organs of chicks. Hear Res. 1997;114(1-2):117-126. doi:10.1016/s0378-5955(97)00166-4

125. Williams JA, Holder N. Cell turnover in neuromasts of zebrafish larvae. Hear Res. 2000;143(1-2):171-181. doi:10.1016/s0378-5955(00)00039-3

126. Matsui JI, Ogilvie JM, Warchol ME. Inhibition of caspases prevents ototoxic and ongoing hair cell death. J Neurosci. 2002;22(4):1218-1227. doi:10.1523/JNEUROSCI.22-04-01218.2002

127. Matsunaga M, Kita T, Yamamoto R, et al. Initiation of Supporting Cell Activation for Hair Cell Regeneration in the Avian Auditory Epithelium: An Explant Culture Model. Front Cell Neurosci. 2020;14:583994. doi:10.3389/fncel.2020.583994

128. Cafaro J, Lee GS, Stone JS. Atoh1 expression defines activated progenitors and differentiating hair cells during avian hair cell regeneration. Dev Dyn. 2007;236(1):156-170. doi:10.1002/dvdy.21023

129. Hashino E, Tanaka Y, Salvi RJ, Sokabe M. Hair cell regeneration in the adult budgerigar after kanamycin ototoxicity. Hear Res. 1992;59(1):46-58. doi:10.1016/0378-5955(92)90101-r

130. Hashino E, Shero M. Endocytosis of aminoglycoside antibiotics in sensory hair cells. Brain Res. 1995;704(1):135-140. doi:10.1016/0006-8993(95)01198-6

131. Roberson DW, Alosi JA, Cotanche DA. Direct transdifferentiation gives rise to the earliest new hair cells in regenerating avian auditory epithelium. J Neurosci Res. 2004;78(4):461-471. doi:10.1002/jnr.20271

132. Warchol ME, Lambert PR, Goldstein BJ, Forge A, Corwin JT. Regenerative proliferation in inner ear sensory epithelia from adult guinea pigs and humans. Science. 1993;259(5101):1619-1622. doi:10.1126/science.8456285

133. Forge A, Li L, Nevill G. Hair cell recovery in the vestibular sensory epithelia of mature guinea pigs. J Comp Neurol. 1998;397(1):69-88.

134. Berggren D, Liu W, Frenz D, Van De Water T. Spontaneous hair-cell renewal following gentamicin exposure in postnatal rat utricular explants. Hear Res. 2003;180(1-2):114-125. doi:10.1016/s0378-5955(03)00112-6

135. Adler HJ, Raphael Y. New hair cells arise from supporting cell conversion in the acoustically damaged chick inner ear. Neurosci Lett. 1996;205(1):17-20. doi:10.1016/0304-3940(96)12367-3

136. Baird RA, Burton MD, Lysakowski A, Fashena DS, Naeger RA. Hair cell recovery in mitotically blocked cultures of the bullfrog saccule. Proc Natl Acad Sci U S A. 2000;97(22):11722-11729. doi:10.1073/pnas.97.22.11722

137. Baird RA, Torres MA, Schuff NR. Hair cell regeneration in the bullfrog vestibular otolith organs following aminoglycoside toxicity. Hear Res. 1993;65(1-2):164-174. doi:10.1016/0378-5955(93)90211-i

138. Li L, Forge A. Morphological evidence for supporting cell to hair cell conversion in the mammalian utricular macula. Int J Dev Neurosci. 1997;15(4-5):433-446. doi:10.1016/s0736-5748(96)00102-5

139. Matsui JI, Haque A, Huss D, et al. Caspase inhibitors promote vestibular hair cell survival and function after aminoglycoside treatment in vivo. J Neurosci. 2003;23(14):6111-6122. doi:10.1523/JNEUROSCI.23-14-06111.2003

140. Fekete DM, Muthukumar S, Karagogeos D. Hair cells and supporting cells share a common progenitor in the avian inner ear. J Neurosci. 1998;18(19):7811-7821. doi:10.1523/JNEUROSCI.18-19-07811.1998

141. Presson JC, Lanford PJ, Popper AN. Hair cell precursors are ultrastructurally indistinguishable from mature support cells in the ear of a postembryonic fish. Hear Res. 1996;100(1-2):10-20. doi:10.1016/0378-5955(96)00109-8

142. Stone JS, Leaño SG, Baker LP, Rubel EW. Hair cell differentiation in chick cochlear epithelium after aminoglycoside toxicity: in vivo and in vitro observations. J Neurosci. 1996;16(19):6157-6174. doi:10.1523/JNEUROSCI.16-19-06157.1996

143. Kruger RP, Goodyear RJ, Legan PK, et al. The supporting-cell antigen: a receptor-like protein tyrosine phosphatase expressed in the sensory epithelia of the avian inner ear. J Neurosci. 1999;19(12):4815-4827. doi:10.1523/JNEUROSCI.19-12-04815.1999

144. Goodyear RJ, Richardson GP. Extracellular matrices associated with the apical surfaces of sensory epithelia in the inner ear: molecular and structural diversity. J Neurobiol. 2002;53(2):212-227. doi:10.1002/neu.10097

145. Stone JS, Shang JL, Tomarev S. cProx1 immunoreactivity distinguishes progenitor cells and predicts hair cell fate during avian hair cell regeneration. Dev Dyn. 2004;230(4):597-614. doi:10.1002/dvdy.20087

146. Bhave SA, Stone JS, Rubel EW, Coltrera MD. Cell cycle progression in gentamicin-damaged avian cochleas. J Neurosci. 1995;15(6):4618-4628. doi:10.1523/JNEUROSCI.15-06-04618.1995

147. Lewis J. Rules for the production of sensory cells. Ciba Found Symp. 1991;160:25-39; discussion 40-53.

148. Duckert LG, Rubel EW. Ultrastructural observations on regenerating hair cells in the chick basilar papilla. Hear Res. 1990;48(1-2):161-182. doi:10.1016/0378-5955(90)90206-5

149. Stone JS, Rubel EW. Cellular studies of auditory hair cell regeneration in birds. Proc Natl Acad Sci U S A. 2000;97(22):11714-11721. doi:10.1073/pnas.97.22.11714

150. Stone JS, Choi YS, Woolley SM, Yamashita H, Rubel EW. Progenitor cell cycling during hair cell regeneration in the vestibular and auditory epithelia of the chick. J Neurocytol. 1999;28(10-11):863-876. doi:10.1023/a:1007022205821

151. Duckert LG, Rubel EW. Morphological correlates of functional recovery in the chicken inner ear after gentamycin treatment. J Comp Neurol. 1993;331(1):75-96. doi:10.1002/cne.903310105

152. Ryals BM, Westbrook EW. TEM analysis of neural terminals on autoradiographically identified regenerated hair cells. Hear Res. 1994;72(1-2):81-88. doi:10.1016/0378-5955(94)90208-9

153. Ruben RJ. Development of the inner ear of the mouse: a radioautographic study of terminal mitoses. Acta Otolaryngol. Published online 1967:Suppl 220:1-44.

154. Roberson DW, Rubel EW. Cell division in the gerbil cochlea after acoustic trauma. Am J Otol. 1994;15(1):28-34.

155. Chardin S, Romand R. Regeneration and mammalian auditory hair cells. Science. 1995;267(5198):707-711. doi:10.1126/science.7839151

156. Burns JC, Kelly MC, Hoa M, Morell RJ, Kelley MW. Single-cell RNA-Seq resolves cellular complexity in sensory organs from the neonatal inner ear. Nat Commun. 2015;6:8557. doi:10.1038/ncomms9557

157. Kolla L, Kelly MC, Mann ZF, et al. Characterization of the development of the mouse cochlear epithelium at the single cell level. Nat Commun. 2020;11(1):2389. doi:10.1038/s41467-020-16113-y

158. Kubota M, Scheibinger M, Jan TA, Heller S. Greater epithelial ridge cells are the principal organoid-forming progenitors of the mouse cochlea. Cell Rep. 2021;34(3):108646. doi:10.1016/j.celrep.2020.108646

159. McGovern MM, Randle MR, Cuppini CL, Graves KA, Cox BC. Multiple supporting cell subtypes are capable of spontaneous hair cell regeneration in the neonatal mouse cochlea. Development. 2019;146(4):dev171009. doi:10.1242/dev.171009

160. Waldhaus J, Durruthy-Durruthy R, Heller S. Quantitative High-Resolution Cellular Map of the Organ of Corti. Cell Rep. 2015;11(9):1385-1399. doi:10.1016/j.celrep.2015.04.062

161. Chen P, Segil N. p27(Kip1) links cell proliferation to morphogenesis in the developing organ of Corti. Development. 1999;126(8):1581-1590. doi:10.1242/dev.126.8.1581

162. Chen P, Zindy F, Abdala C, et al. Progressive hearing loss in mice lacking the cyclin-dependent kinase inhibitor Ink4d. Nat Cell Biol. 2003;5(5):422-426. doi:10.1038/ncb976

163. Kelley MW, Xu XM, Wagner MA, Warchol ME, Corwin JT. The developing organ of Corti contains retinoic acid and forms supernumerary hair cells in response to exogenous retinoic acid in culture. Development. 1993;119(4):1041-1053. doi:10.1242/dev.119.4.1041

164. Lenoir M, Vago P. Does the organ of Corti attempt to differentiate new hair cells after antibiotic intoxication in rat pups? Int J Dev Neurosci. 1997;15(4-5):487-495. doi:10.1016/s0736-5748(96)00105-0

165. Daudet N, Vago P, Ripoll C, Humbert G, Pujol R, Lenoir M. Characterization of atypical cells in the juvenile rat organ of corti after aminoglycoside ototoxicity. J Comp Neurol. 1998;401(2):145-162.

166. Daudet N, Lebart MC. Transient expression of the t-isoform of plastins/fimbrin in the stereocilia of developing auditory hair cells. Cell Motil Cytoskeleton. 2002;53(4):326-336. doi:10.1002/cm.10092

167. Li W, Wu J, Yang J, et al. Notch inhibition induces mitotically generated hair cells in mammalian cochleae via activating the Wnt pathway. Proc Natl Acad Sci U S A. 2015;112(1):166-171. doi:10.1073/pnas.1415901112

168. Munnamalai V, Fekete DM. Notch-Wnt-Bmp crosstalk regulates radial patterning in the mouse cochlea in a spatiotemporal manner. Development. 2016;143(21):4003-4015. doi:10.1242/dev.139469

169. Bramhall NF, Shi F, Arnold K, Hochedlinger K, Edge ASB. Lgr5-positive supporting cells generate new hair cells in the postnatal cochlea. Stem Cell Reports. 2014;2(3):311-322. doi:10.1016/j.stemcr.2014.01.008

170. Jayasena CS, Ohyama T, Segil N, Groves AK. Notch signaling augments the canonical Wnt pathway to specify the size of the otic placode. Development. 2008;135(13):2251-2261. doi:10.1242/dev.017905

171. Agathocleous M, Iordanova I, Willardsen MI, et al. A directional Wnt/beta-catenin-Sox2-proneural pathway regulates the transition from proliferation to differentiation in the Xenopus retina. Development. 2009;136(19):3289-3299. doi:10.1242/dev.040451

172. Logan CY, Nusse R. The Wnt signaling pathway in development and disease. Annu Rev Cell Dev Biol. 2004;20:781-810. doi:10.1146/annurev.cellbio.20.010403.113126

173. Habas R, Dawid IB. Dishevelled and Wnt signaling: is the nucleus the final frontier? J Biol. 2005;4(1):2. doi:10.1186/jbiol22

174. Clevers H. Wnt/beta-catenin signaling in development and disease. Cell. 2006;127(3):469-480. doi:10.1016/j.cell.2006.10.018

175. Jin T, George Fantus I, Sun J. Wnt and beyond Wnt: multiple mechanisms control the transcriptional property of beta-catenin. Cell Signal. 2008;20(10):1697-1704. doi:10.1016/j.cellsig.2008.04.014

176. Jacques BE, Puligilla C, Weichert RM, et al. A dual function for canonical Wnt/β-catenin signaling in the developing mammalian cochlea. Development. 2012;139(23):4395-4404. doi:10.1242/dev.080358

177. Shi F, Hu L, Jacques BE, Mulvaney JF, Dabdoub A, Edge ASB. β-Catenin is required for hair-cell differentiation in the cochlea. J Neurosci. 2014;34(19):6470-6479. doi:10.1523/JNEUROSCI.4305-13.2014

178. Jansson L, Kim GS, Cheng AG. Making sense of Wnt signaling-linking hair cell regeneration to development. Front Cell Neurosci. 2015;9:66. doi:10.3389/fncel.2015.00066

179. de Lau W, Barker N, Low TY, et al. Lgr5 homologues associate with Wnt receptors and mediate R-spondin signalling. Nature. 2011;476(7360):293-297. doi:10.1038/nature10337

180. de Lau WBM, Snel B, Clevers HC. The R-spondin protein family. Genome Biol. 2012;13(3):242. doi:10.1186/gb-2012-13-3-242

181. Chai R, Xia A, Wang T, et al. Dynamic expression of Lgr5, a Wnt target gene, in the developing and mature mouse cochlea. J Assoc Res Otolaryngol. 2011;12(4):455-469. doi:10.1007/s10162-011-0267-2

182. Zhang Y, Chen Y, Ni W, et al. Dynamic expression of Lgr6 in the developing and mature mouse cochlea. Front Cell Neurosci. 2015;9:165. doi:10.3389/fncel.2015.00165

183. Chai R, Kuo B, Wang T, et al. Wnt signaling induces proliferation of sensory precursors in the postnatal mouse cochlea. Proc Natl Acad Sci U S A. 2012;109(21):8167-8172. doi:10.1073/pnas.1202774109

184. Cox BC, Chai R, Lenoir A, et al. Spontaneous hair cell regeneration in the neonatal mouse cochlea in vivo. Development. 2014;141(4):816-829. doi:10.1242/dev.103036

185. Wang T, Chai R, Kim GS, et al. Lgr5+ cells regenerate hair cells via proliferation and direct transdifferentiation in damaged neonatal mouse utricle. Nat Commun. 2015;6:6613. doi:10.1038/ncomms7613

186. Eddison M, Le Roux I, Lewis J. Notch signaling in the development of the inner ear: lessons from Drosophila. Proc Natl Acad Sci U S A. 2000;97(22):11692-11699. doi:10.1073/pnas.97.22.11692

187. Kelley MW. Exposing the roots of hair cell regeneration in the ear. Nat Med. 2003;9(10):1257-1259. doi:10.1038/nm1003-1257

188. Hartenstein V, Posakony JW. A dual function of the Notch gene in Drosophila sensillum development. Dev Biol. 1990;142(1):13-30. doi:10.1016/0012-1606(90)90147-b

189. Yang Z, Strickland DK, Bornstein P. Extracellular matrix metalloproteinase 2 levels are regulated by the low density lipoprotein-related scavenger receptor and thrombospondin 2. J Biol Chem. 2001;276(11):8403-8408. doi:10.1074/jbc.M008925200

190. Radtke F, Wilson A, Mancini SJC, MacDonald HR. Notch regulation of lymphocyte development and function. Nat Immunol. 2004;5(3):247-253. doi:10.1038/ni1045

191. Fehon RG, Kooh PJ, Rebay I, et al. Molecular interactions between the protein products of the neurogenic loci Notch and Delta, two EGF-homologous genes in Drosophila. Cell. 1990;61(3):523-534. doi:10.1016/0092-8674(90)90534-l

192. Artavanis-Tsakonas S, Simpson P. Choosing a cell fate: a view from the Notch locus. Trends Genet. 1991;7(11-12):403-408. doi:10.1016/0168-9525(91)90264-q

193. Iso T, Kedes L, Hamamori Y. HES and HERP families: multiple effectors of the Notch signaling pathway. J Cell Physiol. 2003;194(3):237-255. doi:10.1002/jcp.10208

194. Kageyama R, Ohtsuka T, Hatakeyama J, Ohsawa R. Roles of bHLH genes in neural stem cell differentiation. Exp Cell Res. 2005;306(2):343-348. doi:10.1016/j.yexcr.2005.03.015

195. Murata J, Ikeda K, Okano H. Notch signaling and the developing inner ear. Adv Exp Med Biol. 2012;727:161-173. doi:10.1007/978-1-4614-0899-4_12

196. Estrach S, Ambler CA, Lo Celso C, Hozumi K, Watt FM. Jagged 1 is a beta-catenin target gene required for ectopic hair follicle formation in adult epidermis. Development. 2006;133(22):4427-4438. doi:10.1242/dev.02644

197. Ambler CA, Watt FM. Expression of Notch pathway genes in mammalian epidermis and modulation by beta-catenin. Dev Dyn. 2007;236(6):1595-1601. doi:10.1002/dvdy.21151

198. Raft S, Groves AK. Segregating neural and mechanosensory fates in the developing ear: patterning, signaling, and transcriptional control. Cell Tissue Res. 2015;359(1):315-332. doi:10.1007/s00441-014-1917-6

199. Raft S, Nowotschin S, Liao J, Morrow BE. Suppression of neural fate and control of inner ear morphogenesis by Tbx1. Development. 2004;131(8):1801-1812. doi:10.1242/dev.01067

200. Raft S, Koundakjian EJ, Quinones H, et al. Cross-regulation of Ngn1 and Math1 coordinates the production of neurons and sensory hair cells during inner ear development. Development. 2007;134(24):4405-4415. doi:10.1242/dev.009118

201. Morsli H, Choo D, Ryan A, Johnson R, Wu DK. Development of the mouse inner ear and origin of its sensory organs. J Neurosci. 1998;18(9):3327-3335. doi:10.1523/JNEUROSCI.18-09-03327.1998

202. Haddon C, Jiang YJ, Smithers L, Lewis J. Delta-Notch signalling and the patterning of sensory cell differentiation in the zebrafish ear: evidence from the mind bomb mutant. Development. 1998;125(23):4637-4644. doi:10.1242/dev.125.23.4637

203. Oesterle EC, Campbell S, Taylor RR, Forge A, Hume CR. Sox2 and JAGGED1 expression in normal and drug-damaged adult mouse inner ear. J Assoc Res Otolaryngol. 2008;9(1):65-89. doi:10.1007/s10162-007-0106-7

204. Neves J, Abelló G, Petrovic J, Giraldez F. Patterning and cell fate in the inner ear: a case for Notch in the chicken embryo. Dev Growth Differ. 2013;55(1):96-112. doi:10.1111/dgd.12016

205. Kiernan AE, Xu J, Gridley T. The Notch ligand JAG1 is required for sensory progenitor development in the mammalian inner ear. PLoS Genet. 2006;2(1):e4. doi:10.1371/journal.pgen.0020004

206. Brooker R, Hozumi K, Lewis J. Notch ligands with contrasting functions: Jagged1 and Delta1 in the mouse inner ear. Development. 2006;133(7):1277-1286. doi:10.1242/dev.02284

207. Neves J, Parada C, Chamizo M, Giráldez F. Jagged 1 regulates the restriction of Sox2 expression in the developing chicken inner ear: a mechanism for sensory organ specification. Development. 2011;138(4):735-744. doi:10.1242/dev.060657

208. Liu Z, Owen T, Fang J, Zuo J. Overactivation of Notch1 signaling induces ectopic hair cells in the mouse inner ear in an age-dependent manner. PLoS One. 2012;7(3):e34123. doi:10.1371/journal.pone.0034123

209. Daudet N, Gibson R, Shang J, Bernard A, Lewis J, Stone J. Notch regulation of progenitor cell behavior in quiescent and regenerating auditory epithelium of mature birds. Dev Biol. 2009;326(1):86-100. doi:10.1016/j.ydbio.2008.10.033

210. Shailam R, Lanford PJ, Dolinsky CM, Norton CR, Gridley T, Kelley MW. Expression of proneural and neurogenic genes in the embryonic mammalian vestibular system. J Neurocytol. 1999;28(10-11):809-819. doi:10.1023/a:1007009803095

211. Katoh M, Katoh M. Notch ligand, JAG1, is evolutionarily conserved target of canonical WNT signaling pathway in progenitor cells. Int J Mol Med. 2006;17(4):681-685.

212. Romero-Carvajal A, Navajas Acedo J, Jiang L, et al. Regeneration of Sensory Hair Cells Requires Localized Interactions between the Notch and Wnt Pathways. Dev Cell. 2015;34(3):267-282. doi:10.1016/j.devcel.2015.05.025

213. Singh N, Prakash A, Chakravarthy SR, Kaushik R, Ladher RK. In Ovo and Ex Ovo Methods to Study Avian Inner Ear Development. J Vis Exp. 2022;(184). doi:10.3791/64172

214. Concordet JP, Haeussler M. CRISPOR: intuitive guide selection for CRISPR/Cas9 genome editing experiments and screens. Nucleic Acids Res. 2018;46(W1):W242-W245. doi:10.1093/nar/gky354

215. Gandhi S, Piacentino ML, Vieceli FM, Bronner ME. Optimization of CRISPR/Cas9 genome editing for loss-of-function in the early chick embryo. Developmental Biology. 2017;432(1):86-97. doi:10.1016/j.ydbio.2017.08.036

216. Aigouy B, Prud'homme B. Segmentation and Quantitative Analysis of Epithelial Tissues. In: Dahmann C, ed. Drosophila. Vol 2540. Methods in Molecular Biology. Springer US; 2022:387-399. doi:10.1007/978-1-0716-2541-5_20

217. Goodyear R, Richardson G. Pattern formation in the basilar papilla: evidence for cell rearrangement. J Neurosci. 1997;17(16):6289-6301. doi:10.1523/JNEUROSCI.17-16-06289.1997

218. Prakash A, Weninger J, Singh N, et al. Junctional Force Patterning drives both Positional and Orientational Order in Auditory Epithelia. Published online March 3, 2023. doi:10.21203/rs.3.rs-2508957/v1

219. Chen Y, Gu Y, Li Y, et al. Generation of mature and functional hair cells by co-expression of Gfi1, Pou4f3, and Atoh1 in the postnatal mouse cochlea. Cell Rep. 2021;35(3):109016. doi:10.1016/j.celrep.2021.109016

220. Stone JS, Cotanche DA. Hair cell regeneration in the avian auditory epithelium. Int J Dev Biol. 2007;51(6-7):633-647. doi:10.1387/ijdb.072408js

221. Shang J, Cafaro J, Nehmer R, Stone J. Supporting cell division is not required for regeneration of auditory hair cells after ototoxic injury in vitro. J Assoc Res Otolaryngol. 2010;11(2):203-222. doi:10.1007/s10162-009-0206-7

222. Huang SMA, Mishina YM, Liu S, et al. Tankyrase inhibition stabilizes axin and antagonizes Wnt signalling. Nature. 2009;461(7264):614-620. doi:10.1038/nature08356

223. Selkoe D, Kopan R. Notch and Presenilin: regulated intramembrane proteolysis links development and degeneration. Annu Rev Neurosci. 2003;26:565-597. doi:10.1146/annurev.neuro.26.041002.131334

224. Zine A, Van De Water TR, de Ribaupierre F. Notch signaling regulates the pattern of auditory hair cell differentiation in mammals. Development. 2000;127(15):3373-3383. doi:10.1242/dev.127.15.3373

225. Mizutari K, Fujioka M, Hosoya M, et al. Notch inhibition induces cochlear hair cell regeneration and recovery of hearing after acoustic trauma. Neuron. 2013;77(1):58-69. doi:10.1016/j.neuron.2012.10.032

226. Jiang L, Romero-Carvajal A, Haug JS, Seidel CW, Piotrowski T. Gene-expression analysis of hair cell regeneration in the zebrafish lateral line. Proc Natl Acad Sci U S A. 2014;111(14):E1383-1392. doi:10.1073/pnas.1402898111

227. Chrysostomou E, Gale JE, Daudet N. Delta-like 1 and lateral inhibition during hair cell formation in the chicken inner ear: evidence against cis-inhibition. Development. 2012;139(20):3764-3774. doi:10.1242/dev.074476

228. Steiner AB, Kim T, Cabot V, Hudspeth AJ. Dynamic gene expression by putative hair-cell progenitors during regeneration in the zebrafish lateral line. Proc Natl Acad Sci U S A. 2014;111(14):E1393-1401. doi:10.1073/pnas.1318692111

229. Raphael Y, Altschuler RA. Structure and innervation of the cochlea. Brain Research Bulletin. 2003;60(5-6):397-422. doi:10.1016/S0361-9230(03)00047-9

230. Goutman JD, Elgoyhen AB, Gómez-Casati ME. Cochlear hair cells: The sound-sensing machines. FEBS Letters. 2015;589(22):3354-3361. doi:10.1016/j.febslet.2015.08.030

231. Alvarado DM, Hawkins RD, Bashiardes S, et al. An RNA interference-based screen of transcription factor genes identifies pathways necessary for sensory regeneration in the avian inner ear. J Neurosci. 2011;31(12):4535-4543. doi:10.1523/JNEUROSCI.5456-10.2011

232. Singh N, Kaushik R, Prakash A, et al. Mosaic Atoh1 Deletion in the Chick Auditory Epithelium Reveals a Second Period of Differentiation to Restore Hair Cell Number. Published online 2024. doi:10.2139/ssrn.4814834

233. Foltz DR, Santiago MC, Berechid BE, Nye JS. Glycogen synthase kinase-3beta modulates notch signaling and stability. Curr Biol. 2002;12(12):1006-1011. doi:10.1016/s0960-9822(02)00888-6

234. Morton CC. Genetics, genomics and gene discovery in the auditory system. Hum Mol Genet. 2002;11(10):1229-1240. doi:10.1093/hmg/11.10.1229

235. Atar O, Avraham KB. Therapeutics of hearing loss: expectations vs reality. Drug Discov Today. 2005;10(19):1323-1330. doi:10.1016/S1359-6446(05)03618-4

236. Steel KP, Kros CJ. A genetic approach to understanding auditory function. Nat Genet. 2001;27(2):143-149. doi:10.1038/84758

237. Kurima K, Peters LM, Yang Y, et al. Dominant and recessive deafness caused by mutations of a novel gene, TMC1, required for cochlear hair-cell function. Nat Genet. 2002;30(3):277-284. doi:10.1038/ng842

238. Kudo T, Kure S, Ikeda K, et al. Transgenic expression of a dominant-negative connexin26 causes degeneration of the organ of Corti and non-syndromic deafness. Hum Mol Genet. 2003;12(9):995-1004. doi:10.1093/hmg/ddg116

239. Rozengurt N, Lopez I, Chiu CS, Kofuji P, Lester HA, Neusch C. Time course of inner ear degeneration and deafness in mice lacking the Kir4.1 potassium channel subunit. Hear Res. 2003;177(1-2):71-80. doi:10.1016/s0378-5955(02)00799-2